VANESSA MENDES HENRIQUES

Characterization of TRIB2-mediated resistance to pharmacological inhibition of MEK

UAlg
UNIVERSIDADE DO ALGARVE
DEPARTAMENTO DE CIÊNCIAS BIOMÉDICAS E MEDICINA

Oncobiology Master Thesis

Faro, 2017

VANESSA MENDES HENRIQUES

Characterization of TRIB2-mediated resistance to pharmacological inhibition of MEK

Supervisors: Dr. Wolfgang Link

Dr. Bibiana Ferreira

Oncobiology Master Thesis

Faro, 2017

Título: **“Characterization of TRIB2-mediated resistance to pharmacological inhibition of MEK”**

Declaração de autoria do trabalho

Declaro ser a autora deste trabalho, que é original e inédito. Autores e trabalhos consultados estão devidamente citados no texto e constam da listagem de referências incluída.

_____

Acknowledgements

First, I would like to thank the greatest opportunity given by professor doctor Wolfgang Link to accepting me into his team, contributing to my scientific and personal progress. Thank You for all Your knowledge and help across the year.

A special thanks to Bibiana Ferreira who stayed by me all year and trained me. Thank You for all you taught me, thank you for all your patience and time and all the support. Thank you for all the great times that You provided me. It was an amazing experience to learn and work with You, which made me grow as a scientist and also as a person. Thank You for everything.

To the other members of my team Susana Machado and Pedro Charlito, for their help and support all the time and for the good moments in the lab.

To João Santos who I promised a special thanks. Thank You for all the help and support in the lab, thank You for all the conversations in the TCU and for being my friend.

To all the Professors of Oncobiology Master at Algarve's University for the knowledge transmitted and for all the support.

To my brother and also best friend Tiago Henriques, who has been one of the most important persons of my life. Thank You for all the kindness and support across the years. Thank You for being always there for me.

To my father António Henriques and mother Carmo Mendes who made everything possible, to provide me this amazing opportunity and for all the support. To my godmother Carla Silva who has been a second mother to me. Thanks for every happy moment by Your side, for all the laughs and mainly for being always there when I need.

To my friends of a life-time: Alexandra Borges, Tiago Dias, Lara Neves e Carolina Roque for all the good moments, the support during this year and to make me who I am. I hope to have You at my side for the eternity.

To my friends specially to Elisabete Silva, who has revealed one of my best friends in the past few years, to Marisa Flook, Cátia Salvador. Thank You for all the conversations and confidences, for all the nights out, for all the laughs and all the support.

To my friends that I had the pleasure to meet during my master and who also revealed to be incredible friends: Cristina Fernandes, Gabriela Carrasqueiro and Rita Bastos. Thank you Cristina for being there in the good and in the bad moments, you're an example of strength and

a person who I certainly admire. Thank You Gabriela, “THE friend”, for all the support and kindness, for all the advices and the conversations, for the right words on the right moments, for all the good moments You provided and for being there when I most needed. Thank You Rita, one of the weirdest and amazing persons that I had the pleasure to meet, thanks for all the conversations, support and good moments. I will miss You.

Abstract

Chemoresistance and metastasis are the main reasons for treatment failure in melanoma patients. MAPK pathway is often hyperactivated in melanoma due to BRAF mutations. BRAF and MEK inhibitors revolutionized the standard-care of patients with advanced melanoma. Yet, patients develop resistance to these drugs very fast.

Previous studies showed that Tribbles homolog 2 (TRIB2) is overexpressed in melanoma and confers resistance to chemotherapeutic and targeted drugs such as darcarbazin, PI3K and mTOR inhibitors. Furthermore, TRIB2 protein contains a MEK1 binding site. Taking this into account, we hypothesize that TRIB2 might confer resistance to MEK inhibition.

In order to test our hypothesis, we generated isogenic melanoma cell lines with TRIB2 knockdown, using shRNA, and cells with TRIB2 depletion using CRISPR technique.

Since the members of the Tribbles protein family might be functionally redundant and compensate for TRIB2 depletion, we decided to determine mRNA and protein levels of TRIB1, TRIB2 and TRIB3 using q-PCR and Western-Blot techniques, respectively, on a panel of melanoma and non-melanoma cell lines. We treated these isogenic cell lines with the MEK inhibitor Refametinib for 72h. The resistance was evaluated through cell death analysis, using cell counting based on trypan-blue and annexin V/ Propidium iodide staining.

The isogenic cell lines were successfully established and determined that compensation of TRIB2 through TRIB1 or TRIB3 only plays a minor role. Importantly Refametinib treatment of melanoma cell lines with different levels of TRIB2 showed that cell death correlated with TRIB2 expression level suggesting that TRIB2 confers resistance to MEK inhibitors.

Understanding the resistance mechanisms to the therapeutic agents can improve the outcomes of current therapies and contribute to the development of new therapeutic approaches.

Resumo

Melanoma é uma das formas mais agressivas do cancro da pele, sendo responsável por 80% das mortes para este tipo de cancro. Trata-se de um cancro é potencialmente metastático altamente resistente à terapia, levando a uma baixa taxa de sobrevivência. Existem duas vias de sinalização que estão comummente mutadas ou hiperactivas neste cancro, que contribuem para a proliferação celular e para a resistência a algumas terapias que atuam segundo as vias de sinalização PI3K e MAPK.

A via-de-sinalização MAPK está frequentemente hiperactiva devido a mutação numa das serinas/treoninas kinases que compõem a via, BRAF. Vemurafenib foi o primeiro fármaco "alvo" aprovado pela FDA no melanoma, e sem dúvida revolucionou a terapia no melanoma. Trata-se de um inibidor do RAF, específico para a mutação V600E. Contudo, o melanoma é um cancro altamente heterogéneo e os pacientes eventualmente adquirem resistência a esta terapia. Por isso, têm se apostado no desenvolvimento de inibidores de MEK, que se localiza jusante de BRAF na via de sinalização. No entanto, os mecanismos de resistência continuam a ser das maiores preocupações, e das principais causas de morte nestes pacientes. Recentemente o nosso grupo identificou um novo mecanismo de resistência aos inibidores de PI3K/ mTOR, BEZ235, a inibidores de PI3K, BAY236, BAY439, inibidores do mTOR, Rapamycin e até mesmo a fármacos citotóxicos utilizados na quimioterapia (DTIC, gemcitabine and 5-fluorouracil) mediado por TRIB2. TRIB2 é uma pseudokinase que pertence à família de proteínas Tribbles, constituída por três elementos: TRIB1, TRIB2 e TRIB3, altamente conservados e homólogos. Na sua estrutura, TRIB2 possui um domínio pseudokinase, um domínio COP1 e um domínio de ligação às proteínas MAPK. Este estudo em que foi identificado um mecanismo de resistência mediado por TRIB2, demonstrou que TRIB2 se liga ao AKT via domínio COP1 ativando o AKT através da fosforilação da serina 473. Uma vez fosforilado e ativo, o AKT fosforila MDM2, que regula a atividade de p53, sendo considerado um oncogene. Quando MDM2 está fosforilado, fosforila o p53 enviando-o para degradação, bloqueando assim os mecanismos apoptóticos mediados por p53. Os autores demonstraram ainda que o AKT, uma vez ativado, fosforila também FOXO3a, um gene supressor de tumores, enviando o para degradação. Estudos anteriores demonstraram que a proteína TRIB2 é sobreexpressa em linhas celulares de melanoma e também em pacientes com melanoma. Considerando estas três principais observações: (a) TRIB2 na sua estrutura tem um domínio de ligação MAPK, (b) TRIB2 está sobreexpressa em Melanoma e (c) TRIB2 confere resistência

aos inibidores de PI3K e mTOR, levantamos a hipótese de que TRIB2 confere também resistência a inibidores de MEK.

TRIB2 pertence à família de proteínas tribbles que são altamente conservados entre espécies e apresentam alta homologia, podendo ter funções redundantes. Deste modo, antes de testarmos a nossa hipótese, decidimos averiguar os níveis de mRNA, através de q-PCR, e de proteína, através de um western blot, dos diferentes tribbles em linhas celulares de melanoma (G361, SK-Mel-28 e A375), osteossarcoma e HEK293T. Os resultados mostram que os níveis de mRNA de TRIB1 e TRIB2 são maiores em linhas celulares de melanoma comparativamente às linhas HEK293T e osteossarcoma, enquanto os de TRIB3 são mais elevados na linha celular HEK293T em relação às linhas celulares de melanoma e a de osteossarcoma. Os resultados de expressão de proteína mostram que todas os membros da família Tribbles são mais expressos nas linhas celulares de melanoma comparativamente às linhas celulares de Osteossarcoma e HEK293T.

Para testar a nossa hipótese criámos dois sistemas diferentes em linhas celulares de melanoma: uma linha celular com níveis de expressão de TRIB2 mais reduzidos (knockdown) através de shRNA; outro onde eliminamos a expressão de TRIB2 utilizando a técnica CRISPR-Cas9. Para obtenção de knockdowns para TRIB2 transfetámos um plasmídeo que codifica com shRNA que codifica para TRIB2que é depois processado a small interference (si)RNA, e liga-se ao mRNA específico promovendo a sua degradação. O knockdown foi conseguido na linha celular G361. Nas restantes (SK-Mel-28 e A375) o controlo da técnica, shGFP interferiu também com a expressão de TRIB2. A técnica de CRISPR Cas9 baseia-se o sistema imune de *E. coli:* este sistema é constituído por single-guide RNA (sgRNA) e pela Cas9, uma nuclease que reconhece a sequência especifica e causa quebras duplas no DNA, que são depois corrigidas pelo sistema de reparação de material genético NHEJ levando a pequenas inserções ou deleções, culminando na perda de função do gene alvo. As células foram transfetadas com um plasmídeo que codifica para sgRNA e também para a Cas9. Foram testados vários clones para a obtenção de TRIB2 knockouts (KO), apenas uma parte está representada neste trabalho. Optámos por utilizar um KO de SK-Mel-28 (#8) e um de G361 (#14). Estas duas técnicas já tinham sido previamente validadas no nosso laboratório.

O processo de obtenção de linhas celulares é bastante moroso, por isso decidimos otimizar algumas condições para depois testarmos a nossa hipótese de que TRIB2 confere resistência à inibição de MEK. Testámos duas concentrações para o inibidor de MEK (Refametinib) 100nM e 1µM onde é possível observar que ambas as concentrações inibem a via de sinalização e

induzem morte celular. Optámos por usar as duas concentrações visto que utilizamos diferentes linhas celulares que se comportam de maneira distinta. Testámos também períodos curtos e longos de exposição ao fármaco, e verificámos que após 72 horas a via ainda está inibida. Deste modo, optámos por este período de incubação pois facilita a análise da morte celular. Testámos também plaquear diferentes números de células, para ter a certeza que estas não morriam por falta de espaço, mas sim devido ao inibidor, e observámos que o número de células plaqueadas não exerce influência na morte celular. Decidimos também averiguar qual o melhor tempo de incubação do controlo positivo para morte celular (etoposide) onde verificámos que 48horas de incubação causa mais morte celular.

Após a obtenção das linhas celulares, as células foram submetidas ao tratamento com um inibidor de MEK, Refametinib, durante 72 horas. A morte celular foi avaliada através de contagem de células com trypan blue (células mortas surgem com citoplasma azul), através da técnica Annexin V / Propidium Iodide (PI), um método para identificar as células em apoptose que se baseia na integridade da membrana celular (as células em apoptose apresentam mudanças na morfologia da membrana celular que permite a estes componentes se ligarem aos alvos e emitir fluorescência) e apenas com PI. As técnicas Annexin V/PI e apenas marcação com PI foram analizadas no aparelho FACs Calibur utilizando o programa CellQuestPro. Todos os dados foram tratados/ analisados utilizando GraphPad Prism6. Os nossos resultados mostram que a morte celular se correlaciona com os níveis de expressão de TRIB2: nos vários sistemas utilizados, as células com reduzida ou sem expressão de TRIB2 morreram mais que as que tinham TRIB2, sugerindo que esta proteína pode, de algum modo, conferir resistência à inibição do MEK.

Em suma, este trabalho mostra evidencias que sugerem que TRIB2 confere resistência à inibição do MEK tornando TRIB2 um alvo importante na terapia do melanoma. Estudos anteriores sugerem TRIB2 como um biomarcador no Melanoma, uma vez que este prediz a resposta clinica a uma dada terapia. Neste estudo demonstramos evidências que TRIB2 confere também resistência à inibição do MEK e que poderá ser útil no futuro, para diferenciar os doentes que poderão beneficiar da terapia. Um estudo aprofundado dos mecanismos de resistência aos fármacos contribui para o desenvolvimento e melhoria das terapias, aumento a esperança de vida dos doentes oncológicos.

Contents

Figures Index

Tables Index

Abbreviations

A

ABC proteins -ATP – Binding Cassette (ABC) proteins

AJCC - American Joint Committee on Cancer (AJCC)

AML- Acute myelogenous leukemia

ANOVA- Analysis of Variance

APS- Ammonium Persulfate

ATCC – American Type Culture Collection

ATP – Adenosine Triphosphate

B

BRAF - B-type Raf kinase

BSA – Bovine serum albumin

C

Cas9 – *Clustered Regularly Interspaced Short Palindromic Repeats* associated protein

CO_2 - Carbon Dioxide

cDNA - Complementary DNA

C/EBPs - CCAAT/ enhancer binding proteins

CRISPR - *Clustered Regularly Interspaced Short Palindromic Repeats*

D

DMEM - Dulbecco's Modified Eagle's Medium

DMSO - Dimethyl-sulfoxide

DNA - Deoxyribonucleic acid

DOC- Sodium deoxycholate

dsbreaks - Double strand breaks

DTIC- Dacarbazine

E

ECL - Enchanced chemiluminescente solution

E.coli – Escherichia coli

EGFR - Epidermal Growth Factor Receptor

EMT- Epithelial-mesenchymal-transition

ERK - Extracellular signal-regulated kinases

F

FACS - Fluorescent Activated Cell Scanning

FDA - Food and Drug Administration

FBS - Fetal Bovine Serum

FOXO - Forkhead transcription factor

G

GRB2 - Growth factor receptor-bound protein 2

GST - Glutathione – S- Transferase

GTP - Guanosine-5'-triphosphate

H

HCl - Hydrochloric acid

HDR- Homology directed repair

HEK - Human Embryonic Kidney – HEK

HGF - Hepatocyte growth factor

HR - Homologous recombination

HRP - Horseradish peroxidase

I

IARC - International Agency for Research on Cancer

IC50 - half maximal inhibitory concentration

IL-2 – Interleukine -2

J

JNK - c-Jun N-terminal kinases

K

KD- Knockdown

kDa – Kilo daltons

KI- Knock-in

KO- Knockout

M

MAPK – Mitogen-activated protein kinases

MAPKK - Mitogen-activated protein kinase kinase

MDM2 - Double minute 2 homologue

MMR - DNA-mismatch repair

MMP2 - Metalloprotease 2

MEK – Mitogen-activated protein kinase kinase

MRP - Multidrug resistance protein

mTOR - Mechanistic target of rapamycin

N

NER - Nucleotide Excision Repair

NF-ƙb - Nuclear factor kappa B

NHEJ - Non-Homologous End Joing

NP40 - Nonidet P 40

O

OVO4 - Sodium Orthovanadate

P

PAM - Protospacer adjacent motif (PAM)

PARP - oly(ADP-ribose) polymerase

PBS - Phosphate buffered saline

PCR- Polymerase Chain Reaction

pH – Potential of hydrogen

PI - Propidium Iodite

PIC- Protein Inhibitors Cocktail

PI3K - Phosphatidylinositol 3 kinase

Pgp - P- glycoprotein

PS - Phosphatidylserine

PTEN - Phosphatase and tensin homolog

Q

q- PCR - quantitative Polymerase Chain Reaction

R

RNA - Ribonucleic acid

rpm - Revolutions per minute

RTKs - Receptor Tyrosine Kinases

S

SD - Standard Deviation

SDS - Sodium dodecyl sulfate

sgRNA - Single guide RNA

shGFP – Short hairpin against Green Fluorescent Protein

shRNA - Short hairpin RNA

siRNA - Small interference RNA

shTRIB2 - Short hairpin against Tribbles homolog 2

SNL - Sentinel lymph node

SOS - Son of Sevenless (SOS)

T

TBS – T - tris-*buffered* saline with tween

TEMED - Tetramethylethylenediamine

TMZ - Temozolomide

TNF- Tumor necrosis factor

TRIB1 - Tribbles homolog 1

TRIB2 - Tribbles homolog 2

TRIB3 - Tribbles homolog 3

TSC2 - *Tuberous Sclerosis Complex 2*

TSG – Tumor suppressor gene

U

UV- Ultraviolet radiation

V

VEGF - Vascular endothelial growth factor

VEGFR - Vascular endothelial growth factor

VLS- Vascular leak syndrome

W

WB – Western Blot

WHO - World Health Organization

1. Introduction

1.1 Cancer

Cancer is among the leading causes of death worldwide. In 2013 there were 14.9 million of new cancer cases and 8.2 million deaths worldwide. Cancer incidence has been increasing in most countries since 1990. By 2030 it is expected 21.7 million new cases and 13 million cancer deaths (1, 2). Genetic differences and environmental factors, including infectious agents, lifestyle and culture, such as smoking, dietary patterns, sun exposure, physical inactivity and reproductive behaviors have been known to be the major risk factors for cancer (3-5).

Cancer is usually viewed as an evolutionary process that results from the accumulation of mutations (usually somatic mutations) or epigenetic events (which do not alter DNA sequence, conferring a selective growth advantage and ultimately uncontrolled proliferation (6). There are two major types of mutations: the hereditary that arise on a germ cell (7, 8) and somatic mutations that occur in any non-germ cell. The latter include base pair substitutions, small insertions or deletions, chromosomal rearrangements and gain or losses of gene copy number. Tumorigenesis is a multi-step process that can arise from the alteration in three main types of genes: **oncogenes** with dominant gain of function: genes that stimulate cell division, inhibit cell differentiation and halt cell death; **tumor suppressor genes** loss-of-function: genes that inhibit cell proliferation and regulate apoptosis; and **DNA repair genes** (9, 10). Traditionally, the accumulation of genetic mutations has been considered the major cause of cancer progression. However, this paradigm has changed and is currently accepted that epigenetic changes also play an important role in cancer development (11).

After centuries of research it is now established that cancer is a very complex group of diseases. In 2001 Hanahan and Weinberg described for the first time “rules that govern the transformation of normal cells into malignant cancers”, known as the “hallmarks of cancer”. These hallmarks can be defined as a small number of molecular, biochemical and cellular characteristics shared by most of all human cancer (12, 13). The first six hallmarks of cancer described were (figure1.1): self-sufficiency in growth signals, insensitivity to anti-growth signals, limitless replicative potential, sustained angiogenesis, evading apoptosis and tissue invasion and metastasis (12). In 2011, Hanahan and Weinberg purposed two new hallmarks essential for malignant transformation: genomic instability which confers tumor heterogeneity and

inflammation which is believed to foment multiple hallmarks functions. There are two more capabilities emerging: a reprograming metabolism and avoid immune destruction (13).

Figure 1.1. The hallmarks of Cancer. Almost every cancer has acquired some capabilities during its development. The first 6 hallmarks of cancer suggested in 2000 were: sustaining proliferative signaling, reducing their dependence on growth factors from normal tissue microenvironment, evading growth suppressors, resisting cell death, allowing cells to proliferate out of control, angiogenesis in order to obtain oxygen and nutrients, immortality and invasion & metastasis mainly due to morphological cell changes and activation of metalloproteases. In 2011, the same authors suggested 2 new hallmarks of cancer involved in cancer pathogeny: genomic instability that allows cancer cells with driver mutations to proliferate and gives rise to tumor heterogeneity and tumor promoting inflammation that can support and enhance the other capabilities. New capabilities are emerging: one of them involves the ability of cancer cells to reprogram its metabolism in order to sustain neoplasic proliferation and the other involves the ability to avoid immune system mediated destruction. Adapted from *Hanahan D. and Weisenberg R., Cell 2011.*

1.2 Melanoma

Melanoma is the most dangerous form of skin cancer and represents less than 5% of all skin cancers, yet is responsible for 80% of skin cancer deaths (14). Metastatic melanoma has a poor clinical outcome, about 5% after six months. The World Health Organization (WHO) estimates that each year are diagnosed 132,000 of new cases of melanoma. The International Agency for Research on Cancer (IARC) estimates that in Europe there is 100,000 new cases and 22,000 deaths each year (15-17).

Melanoma is a cancer that arises from melanocytes, which are specialized pigmented cells (figure 1.2), derived from the neural crest and are found predominantly in the skin and hair follicles. A major risk associated with melanoma is the ultraviolet radiation (UV), along with the family history, fair skin and immunosupression. Melanoma has a high somatic mutation rate, among the highest of any cancer type, largely attributed to UV radiation (18). In response to UV radiation, keratinocytes, which are cells that secrete the major structural components of the epidermal barrier, synthesize factors that regulate melanocyte survival, differentiation, proliferation and motility. In this way, keratinocytes stimulate melanocytes to produce melanin resulting in the tanning response. When exposed to UV radiation, melanocytes are activated and secrete melanin and protect the neighboring cells from further damage (15, 18-21). Increased survival features of melanocytes depend not only on themselves, but also on paracrine stimulation from fibroblasts and keratinocytes. Melanocytes can escape their regulation by keratinocytes through disrupted intracellular signaling due to mutations in growth regulatory genes, production of autocrine growth signals and loss of adhesion receptors. Therefore, melanocytes can proliferate and spread, leading to the formation of a naevus (a pre-malignant lesion) (15, 21).

Melanoma is highly metastatic, and highly resistant to treatment (22-24). As mentioned before, melanocytes derived from neural crest cells. These cells undergo epithelial-mesenchymal-transition (EMT) in order to migrate and exit from the neural tube. In a similar way, melanoma cells are able to undergo EMT in the initial events of metastasis to dissociate from surrounding keranocytes (22). In fact, metastasis are the main cause of the death in melanoma patients (25).

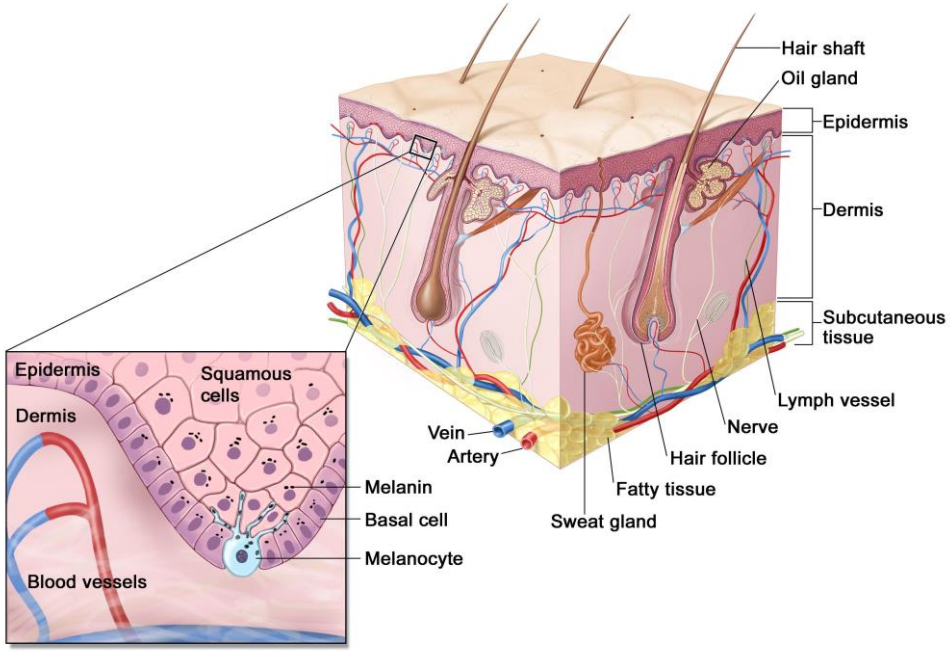

Figure 1.2. Anatomy of the normal skin. Melanocytes are specialized pigmented cells that produce melanin and reside in the basal layer of human skin. Adapted from *National Cancer Institute, 2017.*

1.2.1 Melanoma Classification

Melanoma can be categorized into five different stages according to their tumor thickness, number of metastatic nods and distant metastasis (figure 1.3). The first stage, stage 0 is the less aggressive one, when cell proliferations is limited to the epidermis and has not reached the underlying dermis. In these stage the treatment applied is surgical resection. Melanomas in stage I and II differ on tumor thickness and ulceration and are treated by surgical resection followed by drug or radiation treatment. When melanoma spreads to the lymph nodes is classified as stage III. In this case surgical removal of the lymph nodes is required. Stage IV refers to a cancer that has spread into distant organs, and it is treated with chemotherapy. According to American Joint Committee on Cancer (AJCC), Melanoma can be clinically categorized in 5 different subtypes including: superficial spreading melanoma, amelanotic melanoma, nodular melanoma, acral lentiginous melanoma, and uveal melanoma (table 1.1) (15, 18, 21, 26-29).

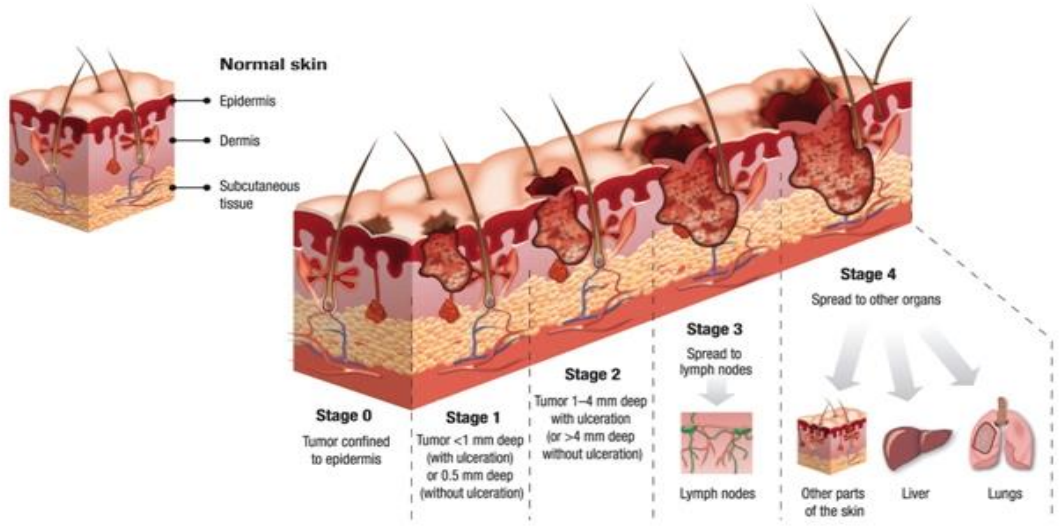

Figure 1.3. The four stages of Melanoma. Melanoma is staged depending on tumor thickness, number of metastatic nodes and distant metastasis. Stage 0-II is confined to the epidermis, stage III includes lesions spread to the lymph nodes and on stage IV the lesions spread to other organs. Adapted from *Colegio Oficial de Enfermeros de Badajoz, 2017*.

Table 1.1- Clinical Classification of Melanoma. Adapted from *Chudnovsky Y. et al, JCI 2005*.

Subtype	*Description*	*Frequency*	*Common Site*
Superficial Spreading Melanoma	Form of melanoma in which cancer cells tend to stay within the tissue of origin: epidermis.	70 %	Trunk of men Legs of Women
Amelanotic Melanoma	Type of skin cancer in which the cells do not produce melanin, they have lack of pigment.	2-8 %	Glabrous skin (skin that is normally devoid of hair)
Nodular melanoma	Melanoma cells proliferate downwards through the skin (vertical growth).	10-25%	Trunk of men Legs of Women
Acral Lentiginous Melanoma	Form of melanoma characterized by its site of origin: palm, sole, or beneath the nail.	5%	Palms Soles Nails
Uveal Melanoma	Melanoma of the eye.	3-5%	Iris, ciliary body or choroid

1.2.2 Melanoma Genetics

The MAPK signaling cascade plays a key role in melanoma, making it an important therapeutic target. In normal cells, the MAPK pathway (figure 1.4) is activated by mitogens or hormones and extracellular growth factors. This signaling pathway controls fundamental cellular processes such as growth, proliferation, differentiation, migration and apoptosis (30, 31). The MAPK pathway includes a small G protein (RAS) and three serine/threonine protein kinases: B- type RAF kinase (RAF), Mitogen-activated protein kinase kinase (MEK) and Extracellular signal-regulated kinase(ERK). The binding of mitogens, hormones, cytokines or neurotransmitters to tyrosine kinase receptors causes its dimerization, which triggers the activation of RAS. Mechanistically, the phosphorylated SH2 (Src Homology 2) of GRB2 (Growth factor receptor-bound protein 2), an adaptor protein, brings Son of Sevenless (SOS) into close proximity to GDP-Ras and converts it into Guanosine-5'-triphosphate (GTP) -Ras (activated form) by catalyzing the GDP to GTP (32). This guanine nucleotide exchange leads to the activation of RAS signaling. Once activated, RAS attracts and binds RAF, which usually is found in cytosol, via effector loop. Therefore, RAF becomes attached to the membrane via RAS. In this way, RAF becomes activated and is able to activate a second kinase, MEK, by phosphorylating its serine / threonine domains (33). MEK is considered a “dual specificity kinase”, which means that it is able to phosphorylate serine/ threonine residues as well as tyrosine residues. By phosphorylation, MEK activates ERK1 and ERK2 that, once activated, each of these ERKs phosphorylates downstream substrates regulating several cellular processes (33). The activation of MAPK signaling potentiates PI3K signaling. These pathways can interact at different levels creating a complex network. The resulting signaling cascade culminates with translocation of ERK to the nucleus where it activates transcription factors, resulting in gene expression (15, 17, 32, 34, 35). Some transcription factors activated by ERK are cdc25 (phosphatase), MSK1/2 (stress activated kinases) and CREB. Once activated, these transcription factors regulate cell proliferation and survival (36, 37). Most cancer lesions that lead to constitutive activation of ERK signaling occur during the early steps of tumorigenesis. The constitutive activation of ERK signaling can result from the overexpression of receptor tyrosine kinases (RTKs), activating mutations in receptor tyrosine kinases, sustained autocrine production of activating ligands, RAS mutations and BRAF mutations (38).

MAPK and PI3K pathways are key regulators of cell proliferation in melanoma. The most common mutation found in melanoma is in *BRAF* (~50%) (39, 40), followed by *Phosphatase and tensin homolog (PTEN)* (30-50%) (41) and *NRAS* mutations (10-20%),

figure 1.4 (39, 42). AKT3 is activated in ~60% of melanomas, due to its overexpression or alterations in upstream regulators such as PTEN (43). *BRAF* and *NRAS* mutations can result in hyperactivated ERK, which is present in up to 90% of human melanomas (26).

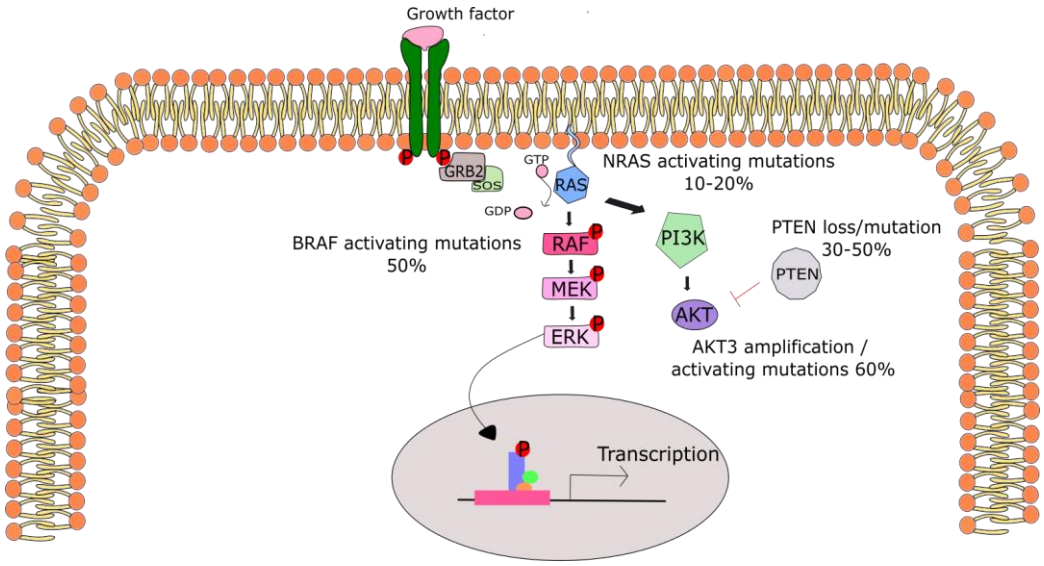

Figure 1.4. The MAPK signaling pathway. Growth factors bind to the tyrosine kinase receptor, which brings SOS into close proximity. GDP-RAS is converted into GTP-RAS and phosphorylates RAF. RAF phosphorylates MEK, and MEK phosphorylates ERK. ERK translocates into the nucleus and stimulates transcription of target genes. Mutations in *NRAS* are found in ~20% of melanoma patients. MAPK pathway is frequently activated by mutations on *BRAF* (~50%). The PI3K pathway can be activated due to *PTEN* mutations (30-50%) or *AKT* mutations (~30% in *AKT3*).

1.2.3 Melanoma Treatment

Until 2010 the standard care for metastatic melanoma included surgical resection, chemotherapy and high interleukine 2 (IL-2) doses (figure 1.5) (17). When detected early, melanoma can be treated by surgical resection, which has over 95% success rate at stages I/II (44). If detected in advanced stages, melanoma is difficult to treat since currently there is no effective treatment. Melanoma lesions can be asymptomatic for long periods, or be detected at stage IV without a clearly identified primary lesion. The main drugs used in melanoma patients are chemotherapy, immunotherapy and targeted therapies (table 1.2). Despite all the efforts, melanoma is still one of the most aggressive cancers, with extremely poor prognosis (21, 44, 45).

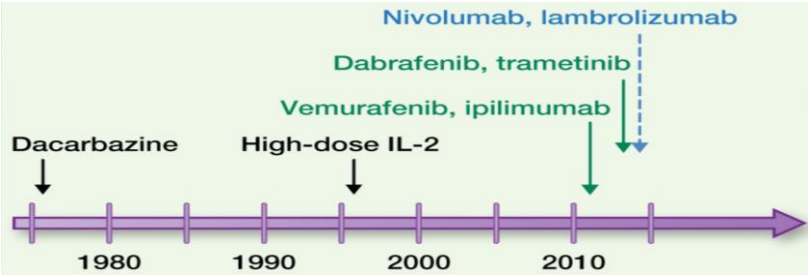

Figure 1.5. Treatment applied in metastatic melanoma. Dacarbazine was the first chemotherapeutic drug used, followed by high doses of Interleukine 2 (IL-2). After 2010 new therapeutic strategies became available such as immunotherapies (exp. Ipilimumab, Nivolumab) and targeted therapies (examples: Vemurafenib and Trametinib). Adapted from *Sullivan EJ et al, CCR 2013.*

Surgical Resection

Surgical resection is still the first treatment choice for patients with early stages melanoma having huge success rate in stage I/II. In cases of metastatic melanoma, surgical resection has a minimal impact in treatment (44, 46). The treatment choice for melanoma patients in stage I-III is surgery. An important prognostic indicator, which provides information about disease progression independently of the treatment, is the analysis of sentinel lymph node (SNL), the first node draining the primary melanoma in the lymphatic system (47). The first rout of metastasis in melanoma is the lymphatic system, making the study of SNL an important toll because it allows the detection of locoregional dissemination (46, 47). If melanoma is spread to the SLN it is performed a complete lymphadenectomy as a gold standard treatment in order to remove metastatic cells present in the lymphatic drainage (48).

Table 1.2. Drugs used in melanoma.

	Drug Group	Drug Class	Examples	Effects
CHEMOTHERAPY	**Alkylating Agentes**	Nitrosaureas	Fotemustine/ Carmustine	SsDNA breaks
		Nitrogen Mustards	Cyclophosphamide	DNA crosslinking
		Triazenes	Dacarbazine/ Temolozomide	Inhibition of nucleic acid and protein synthesis
	Antibiotics	Anthracyclines	Doxorubicin (adriamycin)	SsDNA breaks DNA crosslinking Inhibition of DNA and RNA replication
	Plant-derived products	Vinca Alkaloids	Vincristine	Altered cell division, motility
	Taxanes		Taxol	Altered cell division, motility
	Hormonal Analogs	Antiestrogen	Tamoxifen	Altered estrogen signaling
	Platinium Drugs		Cisplatin	SsDNA and dsDNA breaks
IMMUNOTHERAPY	**Cytokines**		IL-2	Growth and activation of T-cells and natural killers, promoting tumor regression
	Checkpoint inhibitors		Ipilimumab (antibody against CTLA-4)	Promotes T-cell activation and proliferation ; amplifies T cell immunity
			Nivolumab / Pembrolizumab (antibodies against PD-1)	Promotes T cell activation, IL-2 production and mediates immune toxicity
TARGETED THERAPIES	**BRAF inhibitors**		Vemurafenib (against V600E mutation)	Anti- proliferative effects
	MEK inihibitors		Trametinib	Induces cell cycle arrest and reduces tumor growth

Chemotherapy

Cytotoxic chemotherapy has been used for the treatment of metastatic melanoma for the last decades. Chemotherapy is based on the inhibition of the division of rapidly growing cells, which is a characteristic of cancerous cells, but it is also a characteristic of normal cells with fast proliferation rates, such as the bone marrow, skin cells, gastrointestinal tract cells and hair follicles cells. The fact that chemotherapeutic agents non-specifically target cells that are dividing rapidly is the major reason for their toxicity (49-52). The first chemotherapeutic agent used to treat advanced melanoma was dacarbazine (DTIC), an alkylating agent (figure 1.5). The alkylating agents are the most widely used anti-cancer drugs and have the ability to covalently bind an alkyl group to the DNA bases (commonly to the N7 guanine) forming an adduct, thereby preventing multiplication of rapidly growing cells. DTIC has an overall response rate ranging between 10-20% and only allow a complete remission on 5% of patients (21, 53, 54). Temozolomide (TMZ) is another alkylating agent widely used in melanoma that has some advantages over many alkylating agents because of its unique chemical structure and pharmacokinetic properties. In particular, its small weight allows the compound to cross the blood brain barrier. This drug has shown efficacy in the treatment of malignant brain tumors and metastatic melanoma in the brain (55, 56). Other cytotoxic chemotherapeutic drugs have been tested such as nitrosaureas (Carmustine), vinka alcaloides (Vincristine), taxanos (Taxol) and platinium compounds (Cisplatin) (table 1.2) but they had no better results than DTIC (21, 53, 54). Another nitrosourea used is Fotemustine, which was proven to be efficient, mainly in brain metastasis giving its high lipophilicity (57). Other conventional chemotherapeutic drugs have also been used to treat melanoma, such as plant-derived products, antibiotics and hormonal analogs (table 2). Alkylating agents, along with most other cytotoxic agents, are not “magic bullets” envisioned by Paul Erhlich: *drugs that go straight to their intended cell-structural targets.* The resistance to conventional chemotherapeutic agents in melanoma leads to an extremely poor prognosis (21, 53, 54, 58-63).

The scientific progress during the last decades, allowed for a deeper study of molecular mechanisms driving melanoma progression, leading to an improvement in melanoma treatment. Since the last decade two new therapeutic approaches improved the standard care for melanoma patients: Immunotherapies and targeted therapies (17, 64).

Immunotherapy

Melanoma is a highly immunogenic type of cancer, and melanocytes have the ability to induce adaptive immune responses. The primary effector cells of the adaptive immune response against cancer are the T lymphocytes that include helper T cells and cytotoxic T lymphocytes (65, 66). The ability of melanoma cells to induce adaptive immune responses was associated with the fact that melanoma has a high mutation load that leads to the presentation of immune stimulatory neoantigens. Neoantigens are antigenic proteins that have new epitopes that have not been previously exposed / recognized by the immune system, leading to an immune response (67-69). The statement that melanoma is highly immunogenic is supported on several observations: (a) spontaneous remissions occur; (b) in about 5% of the melanomas the primary tumor is not found; (c) it was found that primary tumor and metastasis have infiltrated lymphocytes; (d) studies demonstrated that tumor infiltrating T lymphocytes can recognize some melanoma antigens; (e) melanomas respond to immunotherapy. In cases of immunosuppression the risk of developing melanoma is higher (70). Immunotherapy is defined as the use of the immune system to treat cancer (71, 72). Immunotherapy, including cytokine and vaccine treatments are an alternative to conventional chemotherapeutic drugs (73). One of the first "immunotherapeutic tools" used was IL-2, started in the 90's. Initial studies revealed that IL-2 is able to induce tumor regression in melanoma and other malignancies (65). Yet, IL-2 has shown some degree of toxicity mainly associated to vascular leak syndrome (VLS) (65). VLS is a phenomenon characterized by an increased vascular permeability along with protein and fluid extravasation, resulting in interstitial edema and organ failure (74). Recently, three new immunotherapeutic drugs have been approved by the FDA to treat melanoma: Ipilimumab, an antagonist monoclonal antibody to CTLA-4 (approved in 2011), (figure 1.6) Pembrolizumab and Nivolumab. Pembrolizumab and Nivolumab are both antagonist monoclonal antibodies to PD-1 and were approved in 2014 (65, 73, 75). Immune checkpoints are negative regulators of the immune system, important to maintain self-tolerance and avoid an auto-immune response. Melanoma cells can take advantage of this mechanism and block an immune response against them. The anti-CTLA-4 antibody binds to CTLA-4 receptor blocking CTLA-4 signaling. This blockade contributes to T cell activation and proliferation, amplifying T cell mediated immunity against melanoma cells (76). Similar to CTLA-4, PD-1 is also a checkpoint inhibitor, playing a key role in immune tolerance. In cancer cells, PD-1 interaction with its ligand promotes T cell apoptosis limiting T cell proliferation and inhibiting IL-2 production. The PD-1 pathway blockade induces T cell activation and proliferation, enhancing anti-tumoral activity (70, 77). However, these therapies have an extremely high cost, and do not benefit the majority of the

patients. In fact, the immunotherapy is only beneficial to 15- 50% of melanoma patients. Some patients have intrinsic resistance in tumor cells that have genetic or non-genetic changes that contributes to natural cell survival. One example is that tumors can express proteins with few molecular exchanges, making the immune system unable to recognize these antigens as foreign. It is also possible that, with tumor development, cancer cells lose a proportion of its non-silent mutations, producing lower ratio of antigenic epitopes leading to a phenomenon called the immunoadaption of tumors. Moreover, cancer cells have developed mechanisms to escape the immune system resulting in a less efficient therapy (14, 64, 70-72, 74). Another promising strategy is the use of this dual inhibition combined with immunotherapy including IL-2, interferon, anti-CTLA4, anti-PD1 (78, 79). The future of immunotherapies includes the understanding of resistance mechanisms and the development / improvement of biomarkers in order to provide information about the patient response to the treatment. Hopefully, the ability to distinguish patients that may benefit from these treatments may improve the clinical outcome of melanoma patients (37). In the past few years much attention has been focused on the development of targeted therapies (17, 64).

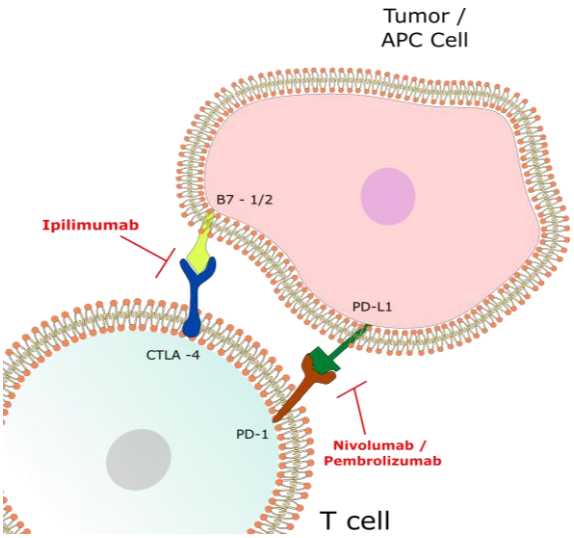

Figure 1.6. Immune checkpoint blockade in Melanoma. Ipilimumab (against CTLA-4) blocks the immunosuppression induced by the interaction between the B7 family and CTLA-4 proteins. Nivolumab or Pembrolizumab (against PD-1) blocks the interaction of PD-L1 ligand to its receptor. The inhibition of these immune checkpoints allows the immune system to target cancer cells.

Targeted Therapies

Over the past years a new generation of cancer treatment arose, such as targeted therapies. Targeted therapies interfere with disease-specific proteins involved in tumorigenesis (49, 50, 80). Target-based therapies are considered to be the future of cancer treatment and much attention has been focused on developing inhibitors for MAPK signaling pathway. MAPK pathway is often hyperactivated in melanoma due to *BRAF* and *NRAF* mutations (two thirds of melanomas) (15, 18, 38).

Deregulation of the MAPK pathway, described in section 1.2.2, is frequent in melanoma leading to increased cell proliferation, invasion, metastasis and angiogenesis, making this pathway an important target in melanoma treatment. Despite recent therapeutic advances in the treatment of advanced melanoma, targeting *RAS* has not been so successful. *NRAS* mutations are commonly found in codon 12, 13 and 61 and have been associated and aggressive clinical which is easy to understand since active RAS can activate both MAPK and PI3K pathways leading to tumor progression and cancer cell survival. Although much effort has been made to target *NRAS*, to date no effective anti- RAS therapies have been successfully developed. Previous strategies were focused mainly in posttranslational modifications of *NRAS* using farnesyltransferase inhibitors. Nowadays the efforts are focused on targeting *NRAS* with small molecules or siRNA and mainly on downstream effectors of *NRAS* (81-83). BRAF, one of the downstream effector of *NRAS*, is one of the three human RAF genes (together with A-RAF and C-RAF) and it is one of the most common mutated genes in melanoma ~50%. The most common mutation leads to a substitution of a glutamic acid for a valine at position 600 (V600E). The mutant V600E BRAF protein results in increased kinase activity (10 fold more activity) which induces hyperactivity of MAPK pathway, stimulating proliferation, survival and neo-angiogenesis by stimulating autocrine vascular endothelial growth factor (VEGF), contributing to the development of nevi. Some studies have shown that V600E BRAF regulates expression of IL-8 a pro-inflammatory chemokine to promote tumor growth and angiogenesis. This mutant form also induces metastasis by triggering invasive cellular behavior and by promoting IL-8 mediated anchoring of melanoma cells to the vascular endothelium, which helps cell extravasation and the development of lung metastasis. As mentioned before, the most common gene mutated in melanoma is BRAF. Patients with BRAF mutations were associated with a poor prognosis. (15, 32, 38, 84). Sorafenib is a nonselective inhibitor of tyrosine kinases (like BRAF) and RTKs such as vascular endothelial growth factor receptor (VEGFR) and was the first BRAF inhibitor investigated in clinical trials in melanoma (38). Clinical trials using

sorafenib as a monotherapy failed to demonstrate anti-tumor activity (85). Studies using sorafenib along with other therapeutic agents such as DTIC, carboplatin and paclitaxel in patients with metastatic melanoma were also clinically ineffective. (85-88). The limited activity of sorafenib in tumors with BRAF mutations contributed to the development of new inhibitors with greater selectivity such as Vemurafenib. This inhibitor was the first molecularly targeted therapy approved by the FDA in 2011 for the treatment of advanced melanoma (89). This drug has shown potent anti-proliferative effects in several preclinical models, including the ones harboring the V600E mutation. The mechanism of action involves selective inhibition of the mutated BRAF V600E kinase, which leads to reduced MAPK signaling activity. A phase III clinical trial comparing Vemurafenib and DTIC as first line therapy showed that Vemurafenib improved overall and progression-free survival compared to DTIC group. However, were detected some adverse effects associated with Vemurafenib such as arthralgia, rash, fatigue, alopecia, photosensitivity, nausea and diarrhea. In fact, there are some cutaneous adverse effects described in 92-95% of melanoma patients treated with BRAF inhibitors. There are also some benign and malignant lesions associated with Vemurafenib treatment, being the most commons squamous cell carcinoma and keratocanthoma (73, 84, 89, 90). The mechanism behind the neoplasia development points to MAPK re-activation in skin with mutated RAS. BRAF inhibitors activate C-RAF in wildtype cells, that can induce ERK signaling, leading to squamous cell carcinoma development. Some of the patients treated with Vemurafenib also developed basal cell carcinoma (84, 91). The major problem / concern using Vemurafenib (and also other inhibitors) is that patients eventually develop resistance to therapy, leading to a poor prognosis. Actually, there are already some resistance mechanisms associated with BRAF inhibitors such as re-activation of MAPK signaling, changes in ERK1/2 regulated cell cycle events, activation of alternative signaling pathways and chromatin-regulating events (92). Re-activation of MAPK signaling can emerge due to mutations on *RAS*, which promotes C-RAF dimerization and activation and due to ERK mutations. In fact, a study has demonstrated that elevated expression of C-RAF was associated with a mutant BRAF melanoma cell resistance to AZ628, a RAF inhibitor (92-94). Herkert B. *et al.*, also showed that ~40% of melanoma patients with BRAF mutations have concomitant loss of PTEN, contributing to the hyperactivation of PI3K pathway and consequently to cancer cell survival (95-97) .

Vemurafenib revolutionized the standard care of melanoma patients. Yet, a big part of melanoma patients dies from resistance once drugs stop having a clinical effect. An intrinsic mechanism of resistance to Vemurafenib is the expression of Hepatocyte growth factor (HGF),

which leads to increased cell proliferation (98). Acquired resistance mechanisms were also described such as upstream mutations on *NRAS*, downstream mutations of MEK and BRAF splice variants. Considering these complications, an alternative strategy is the development of inhibitors for downstream effectors of BRAF, such as MEK (99-103).

Nowadays, selective MEK inhibitors represent a promising new therapeutic option in *BRAF* and *NRAS* mutated melanomas. Some studies demonstrate that preclinical models with *BRAF* mutations are sensitive to MEK inhibitors. Patients harboring *NRAS* mutations were found to be partially sensitive to MEK inhibitors (104, 105). In *BRAF* mutated melanoma murine xenografs, MEK inhibitors contributed to tumor regression through increased apoptosis and reduced angiogenesis and proliferation (104, 106) The first MEK inhibitor, PD098059, was described in 1995 (104, 107, 108). Until now, about thirteen MEK inhibitors have been tested in the clinic. The first MEK inhibitor approved by FDA in 2013 was Trametinib (GSK1120212), a selective inhibitor of MEK1 and MEK2 (100, 104, 108). MEK inhibitors can be classified in two major classes: Adenosine Triphosphate (ATP) competitive or non-ATP competitive inhibitors (108). The ATP competitive inhibitors bind to the ATP binding site of MEK, preventing MEK to be phosphorylated. E6201 is an ATP-competitive MEK inhibitor that proved to be effective against Vemurafenib resistance melanoma harboring a MEK1 mutation in a preclinical model (109). However, the sensitivity to E6201 was correlated to wildtype PTEN suggesting that parallel signaling of PI3K pathway may play a role in resistance to this inhibitor (110). Most of MEK inhibitors are non-ATP competitive, which means that they bind to an allosteric binding site close to the ATP binding site preventing MEK activation. MEK 1 and 2 are very similar and consists in a N-terminal sequence, a kinase domain and a C-terminal sequence. In the N-terminal sequence MEK1/2 contains an inhibitory/allosteric segment, which is only present in MEK1/2 and not in the other MAPKK. This allosteric segment present in MEK1/2 is relatively unique making the ATP non- competitive MEK inhibitors highly specific (108, 111). Trametinib is an orally available, small molecule, non-ATP competitive MEK inhibitor that induces cell cycle arrest, reducing tumor grow. It was proven to be clinically effective in the presence of BRAF and NRAS mutations. Therefore, it was accepted by the FDA as a single agent for the treatment of patients with V600E BRAF and in combination with dabrafenib (104, 112). Refamatinib is a non-ATP competitive MEK inhibitor very similar to Trametinib, which is still in clinical trials (108). Another MEK inhibitor approved by FDA in 2015 for the treatment of advanced melanoma is Cobimetinib in combination with Vermurafenib. Cobimetinib is also an ATP non-competitive MEK 1/2

inhibitor (113, 114). Although all the efforts in developing an effective treatment, resistance to therapy is still the most difficult issue to be overcome. Patients develop resistance to almost all drugs, including to MEK inhibitors, such as the mutation MEK1 P124L (the substitution of a leucine by a proline), resulting in a gain-of-function mutation. Mutations on ERK were also associated with MEK inhibitors resistance leading to MAPK hyperactivation (94, 115-117). Another resistance mechanism is the activation of PI3K pathway. It was already shown that PI3K and MAPK pathways interact in order to regulate several cellular processes like cell proliferation and apoptosis. The MAPK pathway cross-activates PI3K signaling through regulation of PI3K, *Tuberous Sclerosis Complex 2* (TSC2) and mTORC1. GTP-RAS can bind and activate directly PI3K kinase. When *RAS* or *PTEN* are mutated, even in the presence of a MEK inhibitor, the PI3K pathway remains active contributing to tumor growth. Taking this into account, the inhibition of both PI3K and MAPK pathways might be used to more efficiently treat melanoma patients. Nowadays, there are several fair options for melanoma treatment. Yet, there are still significant obstacles to be overcome, like resistance mechanisms, that should be treated as a priority in melanoma care (32, 118, 119).

1.2.4 Resistance mechanisms

Understanding the mechanisms underlying the resistance associated with different therapeutic agents can improve the outcome of current therapies and contribute to the development of new therapeutic approaches. As mentioned before, one of the biggest concerns in melanoma is the development of resistance to treatment. Resistance can be **intrinsic**, meaning that it exists before the treatment or **acquired** when the resistance occurs after the treatment, which means that the tumor was initially sensitive to the treatment. There are some acquired resistance mechanisms already described, such as mutation on drug target / pathway, drug inactivation, drug efflux pumps, DNA damage repair, activation of alternative pathways, tumor heterogeneity and one of the most commons, defects in cell death control (figure 1.7) (120-122).

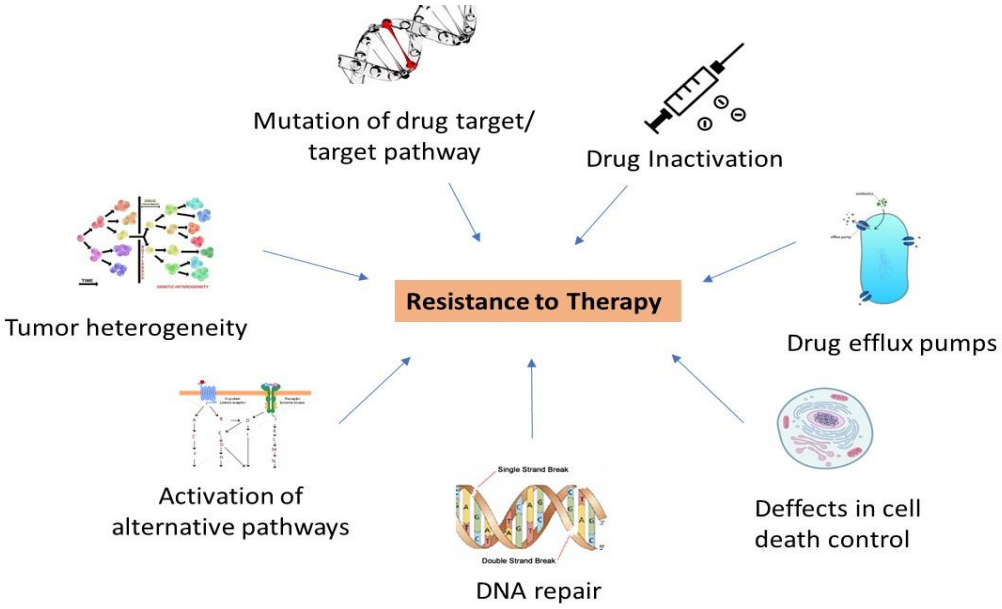

Figure 1.7. Mechanisms of acquired resistance to cancer therapy. The main resistance mechanisms to cancer therapy involve changes in drug metabolism, like drug inactivation, mutation of drug target or target pathway, and drug efflux pumps that decreases the amount of drug that has an effect on cancer cells. The crosstalk between oncogenic pathways is also an important resistance mechanism. Some cancer cells are also able to increase DNA repair allowing mutated cells to survive. Tumor heterogeneity plays also a crucial role in therapy resistance: not all cells are sensitive to treatment, and resistant cells can proliferate and contribute to tumor growth. One of the main resistance mechanisms is dysregulated cell death control which leads to cancer cell survival, and consequently, to cell proliferation and tumor grow.

Most of the anti-cancer drugs must undergo metabolic activation in order to have a clinical effect. The toxicity to the normal tissues is a limiting factor to the amount of drug that can be administered. The amount of drug that reaches the tumor mass is also limited by the drug pharmacokinetics (absorption, distribution, metabolism and elimination) (121). Cancer cells can develop resistance to the treatments due to a decreased drug activation or drug inactivation. This phenomenon can occur, for example, due to Glutathione – S- Transferase (GST) superfamily, a group of detoxifying enzymes that protect cellular macromolecules from attack by reactive electrophiles. GST play an important role in the regulation of MAPK pathway via protein- protein interactions (122-124). Some studies show an increased expression of GST in cancer allowing the detoxification of the anticancer drugs, which culminates in less efficient cytotoxic damage of cells (122, 123, 125). Glutathione transferase levels were found to be

higher in melanoma cells compared to normal melanocytes, which allows cancer cells to protect themselves against oxidative stress (126, 127). This increased expression of GST has also been associated with resistance to apoptosis (122, 123, 125).

A drug's efficacy is influenced by the drug target or mutations in the drug target pathway. Many anticancer drugs target topoisomerase II (example Etoposide) which is a nuclear enzyme essential for DNA replication, chromosome condensation and chromosome segregation. This enzyme forms a complex with DNA that is normally transient. When a topoisomerase II inhibitor is present, the complex stabilizes leading to DNA damaged and later results in cell death. Some cancer cells acquire mutations in topoisomerase II gene, conferring resistance to this type of anticancer drugs (122, 128, 129). A study shows that melanoma cells exposed to etoposide (which induces DNA damage) have tenfold reduced topoisomerase II activity corresponding to an increased drug resistance (126, 130, 131). Another example is the mutation of cellular receptors such as Epidermal Growth Factor Receptor (EGFR) or in one of its downstream targets (122, 128, 129).

The efficacy of a drug depends also in the real amount of drug able to reach the tumor. One of the most resistance mechanisms studied is the drug efflux that results in a reduced drug accumulation. Several cell membrane transport proteins, such as the ATP – Binding Cassette (ABC) proteins have been associated with drug resistance by promoting drug efflux (121, 122). The ABC superfamily proteins function as ATP-dependent efflux transports, mediating drug efflux resulting in lower drug accumulation (126, 132). P- glycoprotein (Pgp) and multidrug resistance protein (MRP) belongs to ABC transports superfamily and are thought to contribute to treatment failure (133). Melanoma cells express MRP, yet a study shows that its expression did not increase after chemotherapy (134).

The response to anticancer drugs culminates direct or indirectly in DNA damage, leading to cell death. An increased repair of drug-induced DNA damage is an important mechanism of chemo-resistance. The DNA damage response can occur through the nucleotide excision repair (NER), or homologous recombination (HR). This mechanism can reverse the effect induced by anticancer drugs, such as cisplatin, that causes DNA crosslinks leading to apoptosis. There are some studies showing that some drug resistant melanoma cell lines present an increased NER of DNA damage (126, 135). Furthermore, DNA-mismatch repair (MMR) deficiency results in drug-resistance by changing the ability of cancer cells to repair DNA damage (136).

The crosstalk between signaling pathways in cancer is also a mechanism that can contribute to drug resistance (137). Connections between signaling pathways give the cell the ability to deal with perturbations of homeostasis. In this way, cancer cells are able to activate a similar

mechanism through the activation of an alternative pathway which will compensate the drug effect on one pathway. It has been shown that the crosstalk between MAPK and PI3K/AKT signaling pathways contributes to resistance in melanoma (137, 138). RAS is a small G protein located upstream of this two pathways. Upon MAPK inhibition, cancer cells display a strong PI3K activation leading to cell survival and melanoma progression (64, 138).

The deregulation of the apoptotic pathway is probably one of the most important mechanisms of resistance in melanoma cells. Apoptosis, often called programmed cell death, involves two different pathways: an intrinsic and an extrinsic pathway. The extrinsic pathway is triggered by binding of Fas ligand to death receptors that belong to the Tumor Necrosis Factor (TNF) superfamily. These are extracellular membrane receptors, which activates caspase 8 an important component of the apoptotic pathway. Caspases are enzymes that cleave after aspartic acid and become activated upon cleavage by other caspases (proteolytic cascade). The intrinsic pathway can be triggered by different stimuli, including death receptor signaling and intracellular signals like the absence of growth factor, hormones or cytokines (negative stimuli) and radiation, toxins, hypoxia and free radicals (positive stimuli). Once activated, the intrinsic pathway leads to the release of mitochondrial cytochrome-c, which in combination with Apaf-1 results in caspase 9 activation. The intrinsic pathway is mainly controlled by Bcl2 proteins, which include proteins with pro- and anti- apoptotic activity. The two pathways converge with the activation of caspase 3 and 7 that cleave proteins responsible for nuclear membrane and cytoskeletal structure, replication systems and DNA repair (126, 139). Dysregulated cell death control can be associated with three main molecular changes: enhanced survival signals, activation of anti-apoptotic factors and inactivation of pro-apoptotic effectors(21, 126, 140).

Tumor heterogeneity also plays a crucial role in anticancer drug resistance. Tumor heterogeneity can be defined as the differences between tumors of the same type in different patients and between cancer cells within the same tumor mass (141, 142). Resistance can develop from a clone with a specific characteristic that allows it to survive to a certain drug, that proliferates originating a resistant cell subpopulation. Recent studies have demonstrated that a fraction of cells that compose part of the heterogeneous tumor mass have stem cell properties and are usually drug resistance. The cancer treatment affects the sensitive cells, but not the resistant cells that survive and can expand contributing to the disease relapse (122, 141).

1.2.5 The Role of TRIB2 in resistance to anti-melanoma drugs

Recently, the Link lab has discovered a novel resistance mechanism to anti-cancer drugs currently in clinical trials, namely to BEZ235, a PI3K/mTOR inhibitor, BAY236 and BAY1082439, both PI3K inhibitors and Rapamycin, a mTOR inhibitor and also to conventional cytotoxic drugs DTIC, gemcitabine and 5-fluorouracil, mediated by Tribbles homolog 2 (TRIB2) (143). TRIB2 is a protein that belongs to the Tribbles family of proteins, enhanced cell resistance to these drugs (143) . Furthermore, TRIB2 protein levels were correlated with AKT activation. TRIB2 was able to inhibit Forkhead BoxO (FOXO), a tumor suppressor gene, contributing to the malignant phenotype of melanoma cells. These findings suggest that TRIB2 is conferring resistance by reducing cell death induced by PI3K/mTOR inhibitors (143, 144). In fact, previous studies from this group proved that TRIB2 is overexpressed in melanoma cell lines and in melanoma patients. TRIB2 expression correlates with disease stage and clinical progression, suggestingTRIB2 as a potential biomarker for diagnosis and prognosis of melanoma (14, 144).

The Link lab found that TRIB2 is a repressor of FOXO through a screening for FOXO repressors (144). FOXO suppresses cell survival and proliferation through regulation of the expression of apoptotic proteins and cell cycle regulators. Some studies have shown that hyperactivation of MAPK pathway leads to FOXO inactivation (37, 145). Since FOXO functions as a tumor suppressor gene inactivated in many human cancers inhibiting its repressor proteins might represent an attractive therapeutic strategy to reactivate them. ERK and p38 are known to phosphorylate FOXO1 at various sites, suggesting that MAPK signaling cascade may play a key role in FOXO regulation (37, 119, 146). FOXO regulation is receiving increasing attention in cancer research since FOXO family members were found to be associated with cancer initiation, progression and resistance (36). FOXO proteins represent a subfamily of transcription factors that belong to the forkhead family (145, 147). In mammals there are 4 *FOXO* genes: *FOXO1, FOXO3, FOXO4*, and *FOXO6* involved in crucial cellular processes like regulation of stress resistance, metabolism, cell cycle arrest and apoptosis (146-148). FOXOs activity is regulated at three different levels: subcellular localization, stability and transcriptional activity (144). This regulation is mediated by different processes such as phosphorylation, acetylation and ubiquitination FOXO proteins regulate biological processes involved in cell proliferation, cell cycle progression, cell differentiation, tissue homeostasis, angiogenesis and apoptosis through apoptotic genes such as cyclin-dependent kinase inhibitor

p27, BIM, Fas ligand and Bcl-6 (36, 37, 146, 147, 149). As result, it is not surprising that deregulation of FOXO proteins may be involved in some pathological processes such as cancer. It was shown that the activation of PI3K or MAPK pathways leads to the repression of FOXO-mediated growth arrest and apoptosis (37). FOXO transcription factors are tumor suppressors that are inactivated in some human cancers (36, 150). It was shown that FOXO overexpression inhibits tumor growth in vitro and tumor size in vitro in breast cancer, correlating FOXO cytoplasmic localization of FOXO with a poor prognosis. Contrarily, when FOXO has a nuclear localization cell cycle stops, angiogenesis is reduced and apoptosis is induced, contributing to tumor regression. The tumor suppressor role of FOXO was also described in leukemia, prostate cancer, and glioblastoma (150-154). Most importantly, recent studies, have revealed that the cytostatic and cytotoxic effects of many chemotherapeutic agents, including paclitaxel, doxorubicin, lapatinib, gefitinib, imatinib, cisplatin and tamoxifen are mediated by FOXO activity (36). Therefore, FOXO can be determinant to the sensitivity to chemotherapeutic drugs. It has been established that AKT phosphorylates FOXO proteins, promoting cell survival, since FOXO regulates pro-apoptotic proteins including TRAIL and BIM. FOXO phosphorylation by AKT induces its translocation to cell cytoplasm and posterior degradation, in particular FOXO3a, which is also regulated by MAPK pathway. FOXO can be inactivated, also by the crosstalk between PI3K and MAPK pathways (36, 155). Thus, FOXO is considered a very important target to melanoma treatment. An interesting approach would be the reactivation of FOXO to take advantage of its tumor suppressor properties. Importantly Zanella F. *et al.*, discovered, TRIB2 as a novel FOXO-repressor, that might be useful as a target to reactivate FOXO factors(144).

Tribbles

TRIB2 belongs to the tribble family of genes, first described in 2000 as a *Drosophila* protein that coordinates morphogenesis by inhibiting mitosis. Tribble family members were identified in a genetic screen that aimed at identifying mutations that control cell division and cell migration during embryonic *Drosophila* development. The name originates from the fictional small animal that vexed the crew of the Enterprise in the “Trouble with Tribbles” episode from Star Trek television series (156, 157). Tribbles encodes an evolutionarily conserved protein family that influences cell proliferation, motility and metabolism (158). Tribbles homologs are characterized by the presence of a N-terminal portion, a central serine/threonine kinase like domain and a C-terminal that contains a COP-1 binding site for E3 ubiquitin ligases and a

MEK1 binding site which mediates interactions with multiple Mitogen-activated protein kinase kinases (MAPKKs) (figure 1.8). These proteins are considered catalytically inactive since they lack conserved residues from the characteristic ATP binding site. Thus, are considered pseudokinases (156-159). However, recent data shows that human TRIB2 has the ability to bind and hydrolyze ATP showing a weak kinase activity(160-162).

Figure 1.8. Structure of the Tribble protein family. Tribble proteins have 3 main domains: a central serine/ threonine pseudokinase domain, MEK1 binding domains, which mediates interaction with MAPK and COP-1 binding site.

The mechanism of action of Tribble proteins is still not fully understood, though some investigators hypothesized that Tribble proteins function as scaffold proteins that contributes to balance signaling pathways, and in several contexts they facilitate ubiquitin-dependent degradation of their target protein (156, 163). There are three mammalian Tribble homologs proteins: TRIB1, TRIB2 and TRIB3. Its structure includes a pseudokinase domain, a MEK1 and a COP-1 binding site in the C-terminal (158, 161). TRIB1 is highly expressed in the bone marrow, peripheral blood leukocytes, thyroid gland and pancreas (158, 164). TRIB2 is highly expressed in peripheral blood leukocytes, thymus, heart, brain, kidney, lung, skin and white adipose tissue while TRIB3 is more expressed in human liver (158, 164). Tribbles family members coordinate a number of critical cellular processes including glucose and lipid metabolism, inflammation, cellular stress, survival, apoptosis and tumorigenesis (158). Tribble s proteins regulate AKT and MAPK signaling pathways via regulating the activity of MAPK and PI3K pathways. TRIB2 was described as a dosage dependent suppressor of FOXO, mainly as modulator of cytoplasmic location of FOXO3a (157, 161). Aberrant regulation of pseudokinases has been implicated in the progression of cancer (157). Recent studies have shown that Tribble pseudokinases play an important role dysregulating signaling in malignant hematopoiesis. In fact, TRIB1 and TRIB2 appear to function as oncogenes in acute myelogenous leukemia (AML) (164-166). TRIB1 and TRIB2 induce efficient degradation of one of the members of CCAAT/ enhancer binding proteins (C/EBPs), C/EBP α. C/EBPs are

transcription factors that regulate several processes like cell cycle, inflammation, metabolism, differentiation a proliferation. The C/EBP α function is better characterized in the hematopoietic system: controls maturation of myeloid lineage (167, 168). The C/EBP α has two main isoforms: p42 that function as a tumor suppressor gene and p30, an N–terminally truncated form that function as an oncogene. TRIB2 is highly expressed in patients with AML. It was shown that TRIB2 leads to the degradation of C/EBP α p42 via E3 ligase COP1 domain, leaving p30 isoform intact, which leads to uncontrolled proliferation.

In vitro and *in vivo* data shows that TRIB2 transcript levels are elevated in melanoma cell lines and in patients with malignant melanoma (144). These high levels TRIB2 were shown to facilitate the growth and survival of melanomas by downregulation of FOXO activity (14). Published work from the Link laboratory has shown that TRIB2 knockdown increases the activity of FOXO in melanoma and reverts the malignant phenotype of malignant melanoma cells where TRIB2 is overexpressed (144). More recently, Hill *et al*., showed that TRIB2 could be used as a biomarker for diagnosis and progression of melanoma (14, 144). A biomarker can be defined as a biological characteristic that can be objectively measured and evaluated as an indicator of a determined process or disease. In these way, a biomarker is a powerful tool that provides information about the disease progression (169, 170). In oncology, a biomarker provides information about differential diagnosis, prognosis, prediction of response to the treatment and they are essential to monitor disease progression. Biomarkers can be classified as predictive, prognostic or diagnostic biomarkers. A predictive biomarker helps to predict a response to a specific treatment regarding a specific characteristic such as the presence/absence of a protein. A prognostic biomarker gives information about the disease progression, recurrence or death independently of the treatment received. A diagnostic biomarker is used in order to detect/ confirm the presence of a specific disease or a specific condition that allows the classification of a subtype of disease (170-172). Hill *et al.*, found that TRIB2 expression correlated with disease stage and prognosis. They demonstrated, with a statistical significant transcription difference, that TRIB2 expression was elevated in metastatic melanoma samples compared to normal skin (14). This group also proved that TRIB2 protein levels correlates with AKT activation: TRIB2 interacts with AKT activating it via COP-1 domain. Through this experiments they were able to show that TRIB2 confers resistance to inhibitors such as PI3K inhibitors (BAY236 and BAY1082439) , mTOR (a serine/threonine kinase that belongs to PI3K pathway) inhibitors (Rapamycin), PI3K/MTOR inhibitors (BEZ235) and also to conventional cytotoxic drugs (DTIC, gemcitabine and 5-fluorouracil) (143). In this study, they created stable isogenic TRIB2 cell lines and submitted them to BEZ235, a PI3K/mTOR inhibitor. Through

the analysis of SubG1 cell population and reduced caspase 3 activation, they proved that the high levels of TRIB2 correlated with cell resistance to this drug (143). The same happened when cell lines were treated with BAY236 and BAY439, both PI3K inhibitors: TRIB2 reduced cell death induced by these drugs. When exposed to Rapamycin, an mTOR inhibitor, the isogenic cell lines with higher levels of TRIB2 displayed resistance to this compound (143). A deeper investigation demonstrated that cell lines with higher TRIB2 protein levels correlated with AKT activation through its phosphorylation on serine 473 and also with increased total AKT. In melanoma cells with TRIB2 depletion the levels of AKT pSer473 and total AKT were lower (143). Surprisingly, TRIB2 overexpression contributed to increased levels of AKT pSer473 and total AKT before and after the treatment with PI3K and mTOR inhibitors which suggests that drugs targeting PI3K and mTOR may not be clinically efficient in tumors where TRIB2 is overexpressed, like in melanoma. Moreover, they proved that TRIB2- mediated resistance was AKT-dependent via FOXO3a (143). AKT1 phosphorylates FOXO3a (tumor suppressor gene) for proteasome degradation, and also activates E3 ubiquitin ligase mouse double minute 2 homologue (MDM2) with consequent apoptosis inhibition mediated by p53. MDM2 is considered and oncogene once it regulates p53 activity (173). MDM2 function as a E3 ligase that ubiquitinates p53 for degradation blocking its transcriptional activity directly (174-176). The authors showed that TRIB2 and AKT interacts and form a complex, promoting AKT activation and consequent inhibition of P53 mediated apoptosis. Concomitant to reduced p53 protein levels, they also found that P53 target genes were downregulated, including*: p21, MDM2, Bax and Puma*. TRIB2 COP1 binding site was shown to be essential for AKT activation. In this way, through several experiments, our group showed that TRIB2 is able to activate AKT leading to P53 and FOXO3a inactivation and confers resistance to PI3K inhibitors (143). *In vivo* experiments confirmed that TRIB2 confers resistance to PI3K inhibitors. The authors created isogenic 293T subcutaneous tumors in the flanks of NOD/Scid mice. Tumor growth revealed to be independent of TRIB2 status. When treated daily with BEZ235, a PI3K/mTOR inhibitor, the 293T-GFP xenograft tumors reduced significantly while 293T-TRIB2 tumors were highly resistant to treatment showing that the high levels of TRIB2 reduced the efficacy of BEZ235 *in vivo* (143). To compare to a clinical situation, they analyzed tumor tissue samples from melanoma, pancreatic and colon cancer were analyzed, they found that the levels of TRIB2 transcription and proteins were elevated in tumor tissues compared to the normal tissue samples. Similar to in vitro models, they proved that in tumor samples the levels of TRIB2 the levels of AKT pSer473 and pSer253-FOXO3a protein levels were significantly higher, confirming their experiments. Also, they demonstrated that the transcripts and proteins

of FOXO dependent gene such as *BIM*, *FasLG* and *TRAIL* were significantly lower in melanoma samples compared to the normal control tissue samples (143). In summary, Hill *et al.*, discovered a new mechanism: TRIB2 binds to AKT via COP1 domain promoting the activation of AKT via Ser473 phosphorylation, which in turn phosphorylated MDM2, increasing its activity inhibiting p53 mediated apoptosis (figure 1.9). AKT also leads to FOXO3a phosphorylation via Ser235 sending it to degradation. This study was extremely important once it revealed a novel resistance mechanism of TRIB2 mediated resistance to PI3K inhibitors, meaning that patients with TRIB2 overexpression are predicted to respond poorly to these treatments, rendering TRIB2 as a biomarker predicting the treatment outcome (143). Taking into account that: (a) TRIB2 has a MEK1 binding site (figure 1.8) (157, 158, 177); (b) TRIB2 is highly expressed in melanoma cell lines and in patients with melanoma (144) and (c) TRIB2 confers resistance to PI3K and mTOR inhibitors (143) we hypothesize that TRIB2 might also be conferring resistance to MEK inhibition as well, through a similar or unrelated mechanism.

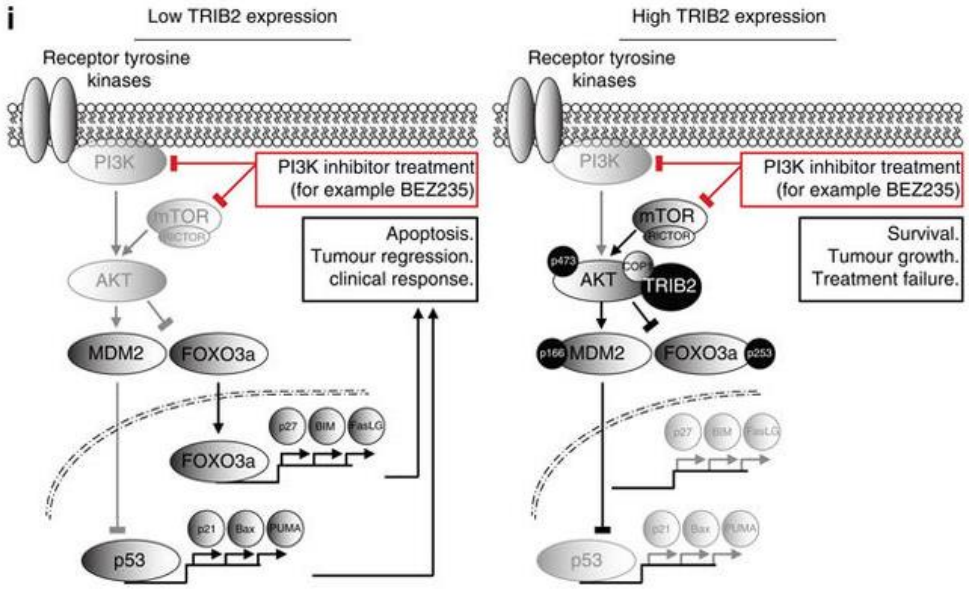

Figure 1.9. Proposed model of TRIB2 mediated drug-resistance. In the left, with low levels of TRIB2 pathway is inhibited leading to apoptosis and tumor regression and consequently a good clinical response. In the right, with high levels of TRIB2, TRIB2 binds to AKT via COP1 domain causing its activation via p-Ser473AKT. Activated AKT causes MDM2 phosphorylation via Ser166 which and turn phosphorylates P53 sending it to degradation. AKT also phosphorylates FOXO3a via Ser235 sending it also to degradation, culminating with cell survival, tumor growth and finally, treatment failure. Adapted from *Hill et all, Nat Comm, 2017(143).*

2. Methods

2.1 Cell culture

Cell culture is one of the most important tools used in molecular biology, providing systems to study the majority of diseases. The cell lines used are described in section 2.2. The cells were cultivated in Dulbecco's Modified Eagle's Medium (DMEM) with Ultraglutamine 1 and 4,5g/L Glucose (Lonza, Verviers, Belgium) supplemented with 10% Fetal Bovine Serum (FBS) (Biowest, South America) and 5ml of Penicilin / Streptamicin (Amresco, Ohio). All cell lines were routinely cultured in 100mm plates (SLP life science, Korea) or 60mm plates (SLP life science, Korea) and maintained in an incubator (Thermo electron corporation 311, Canada) at 37ºC and 5% carbon dioxide (CO_2). Culture medium was changed every 2 or 3 days. When cells reached 70-80% confluency, cells were washed twice with 1X Phosphate Bovine Serum (PBS) (Sigma Aldrich, USA) and coated with 1.5X Trypsin (Sigma Aldrich, USA), diluted in PBS. Trypsin is used to detach cells from the plates and maintain a subculture.

For long term storage, we trypsinized and centrifuged cells (VWR 881117, Taiwan) at 1100 revolutions per minute (rpm) for 4 minutes, we removed the supernatant and ressuspended the cells in fresh media supplemented with 10% FBS and 10% Dimethyl-sulfoxide (DMSO) (VWR, France) that functions as a cryopreserving agent. Cells were stored in cryovials (VWR, China) at -80ºC and then, transferred to -150ºC.

For thawing, we placed the cryovials for a couple of seconds at 37ºC water bath (Clifton, Great Britain) and the solution transferred to 15ml falcon tubes (Labbox, Spain), and then centrifuged at 1100 rpm for 4minutes. We discarded the supernatant, containing DMSO in order to avoid cell damage, and cells were ressuspended in 1ml media and plated in 100mm plates.

We performed cell counting using a Neubauer chamber (Blau brand, Germany). Briefly, we collected 10µL of cell suspension and mixed with 10µL Trypan Blue (Sigma Aldrich, UK) in an Eppendorf tube (Eppendorf, Germany). We transferred 10µl to the Neubauer chamber and the four external corners were counted. Cell concentration was obtained according to this equation: $(X_1+ X_2 + X_3+ X_4)/4 \times 2 \times 10^4$ cells /mL (figure 2.1).

All the procedures were performed under sterile conditions using a laminar flow chamber (Microflow, advanced biosafety cabinet class II, UK).

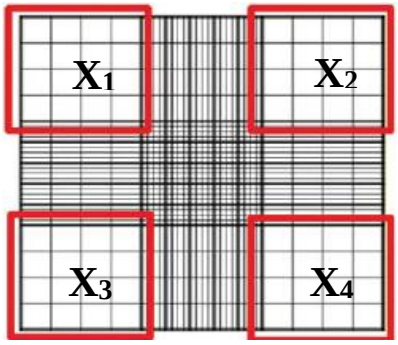

Figure 2.1. Scheme of a Neubauer Chamber. The total number of cells results from the average number of cells from the four external corners, X_1, X_2, X_3 and X_4 multiplied by the factor of dilution (in our case 2) and by 10^4: $(X_1+ X_2 + X_3+ X_4)/4 \times 2 \times 10^4$ cells /mL. Adapted from *Ansair N. et al, Methods Cell Biol, 2013.*

2.2 Cell lines characterization

For our study we used the following melanoma cell lines: G361, SK-Mel-28 and A375 and the non-melanoma cell lines: U2OS (osteosarcoma) and Human Embryonic Kidney (HEK) 293T cells. All of them provided by American Type Culture Collection (ATCC). Melanoma cell lines are characterized in table 2.1

Table 2.1. Genetic characterization of the melanoma cell lines used.

	BRAF	NRAS	P53
G361	Wt* / Mutant	Wt	Wt
SK-Mel-28	Mutant	Wt	R273H
A375	Mutant	ND**	ND

*Wt – Wild Type; **ND – non-descriminated

Since Tribbles family members are highly conserved and might be functionally redundant, we decided to analyze the mRNA and protein levels of all three proteins. We evaluated mRNA and protein levels using quantitative polymerase chain reaction (q-PCR) and Western Blot (WB) techniques, respectively.

2.3 q-PCR

The q-PCR is a sensitive method that allows the detection and quantification of minute amounts of nucleic acids. First, RNA is transcribed into a complementary DNA (cDNA) by reverse transcriptase from mRNA. Then, cDNA is used as a template for the qPCR reaction. The reaction is detected by the use of fluorescent reporters that permits the detection after hybridization of the probe with its complementary sequence, allowing to follow the procedure at the time that it happens and the quantification of the product accumulation (178).

RNA extraction

In order to perform the RNA extraction, we used E.Z.N.A.® Total RNA Kit (Omega) protocol, describe in annex A, from cell pellets collected from each cell line.

CDNA synthesis

For the cDNA synthesis we used NZY first-strand cDNA synthesis kit (Nzytech, Lisbon) thermal cycler (TC-48, BioRad) protocol in Annex B. The resulting cDNA was divided, one part was diluted 1:10 to the PCR and the remaining was frozen at –80ºC.

PCR

PCR is composed of 3 different steps: **Denaturation** in which the high temperature allows the separation of the DNA into 2 single strands; **Annealing** when the temperature is lowered allowing the primers to attach to the DNA strand; the final step is the **Extension** in which the temperature is raised again and a new complementary strand of DNA is formed by Taq polymerase (179). For qPCR we used LuminoCt Syber Green qPCR ReadyMix L6544 (Sigma Aldrich, USA). The protocol included 20 seconds at 94ºC plus 3 seconds at 94ºC for denaturation, 20 seconds at 56ºC for annealing/extension and then at 4ºC. We performed three technical replicates. The primers used are described in table 2.2. Results were analyzed using Bio-Rad CFX Manager 3.1 software.

Table 2.2. Primers used in q-PCR.

Gene	Oligo Name	Sequence	Supplier
TRIB1	hTRIB1_RTPCR_FOR_I	ATCGCCGACTACCTGCTG	NZYTech
	hTRIB1_RTPCR_REV_I	GTAATGTTGCTGTGCGATGG	NZYTech
TRIB2	hTRIB2_RTPCR_FOR_I	GACTCCGAACTTGTCGCATT	NZYTech
	hTRIB2_RTPCR_REV_I	ATGAGCAGACAGGCAAAAGC	NZYTech
TRIB3	hTRIB3_RTPCR_FOR_I	TGCCCTACAGGCACTGAGTA	NZYTech
	hTRIB3_RTPCR_REV_I	GTCCGAGTGAAAAAGGCGTA	NZYTech
GAPDH	GAPDH FOR RT-PCR	CAATGACCCCTTCATTGACC	NZYTech
	GAPDH REV RT-PCR	TTGATTTTGGAGGGATCTCG	NZYTech

2.4 Western Blot

The protein levels were assessed using the WB technique, commonly used to separate and identify proteins. Briefly, the proteins are separated according to their molecular weight in a sodium dodecyl sulfate polyacrylamide gel electrophoresis (SDS-PAGE). The percentage of SDS gel should be according to the size of the proteins of interest. The separated proteins are then transferred to a nitrocellulose membrane. Next, the membrane is blocked, usually in 5% milk diluted in 1X tris-*buffered* saline tween (TBS-T), to prevent the antibodies from binding to the membrane nonspecifically. After blocking, the proteins of interest are detected using specific primary antibodies and the revelation solution (180).

Once the cell plates (60mm) were confluent, we performed two washes with 1X PBS and trypsinized the cells. Next, we centrifuged cells at 1100 rpm for 4m and discarded the supernatant. We ressuspended the cell pellet in 1X PBS and centrifuged for brief seconds. We removed the supernatant and froze the cell pellet at -20ºC.

Protein Extraction

The protein extraction is the first step of WB. Protein extraction was performed in ice, using RIPA buffer (0,1% sodium dodecyl sulfate (SDS) (Applichem, Germany), 0,5 % Sodium deoxycholate (DOC) (Sigma Aldrich, New Zeeland), 1% Nonidet P (NP) 40 (Sigma Aldrich, USA), 50mM Tris Hydrochloric acid (HCl) pH 8(Sigma Aldrich, USA), 150 mM NaCl (Merck, Germany), 0,05M NaF (VWR, EC), 1 mM sodium orthovanadate (OVO4) (Sigma Aldrich,

USA), 0,0001µg/µL Calyculin (Santa Cruz, Dallas), 0,01 0,0001µg/µL Protease Inhibitors Cocktail (PIC) (Sigma Aldrich, USA)) that effectively lyses and extracts membrane, cytoplasmic and nuclear proteins while avoiding protein degradation. We add the proper amount of RIPA to the cell pellet and homogenized the samples by repetitive pipetting followed by a 20-minute incubation on an orbital shaker (Labnet, New Jersey) at 4ºC. Next, we centrifuged the samples at 15000 rpm (VWR, Japan) for 20 minutes at 4ºC. Once centrifuged, we transferred the supernatant (protein fraction) to a new Eppendorf tube.

Protein Quantification

Next, we normalized all samples to the same final protein concentration using the Bradford (NZTech, Portugal) assay accomplished by measurement of absorbance at 590 nm. It is a colorimetric protein assay based on an absorbance shift of Comassie Brilliant Blue, being a rapid and sensitive method. This method relies in the fact that the concentration of an unknown sample is based on a protein standard/ reference with similar properties to the sample being analyzed, like Bovine Serum Albumin (BSA) 2mg/mL (ThermoFisher Scientific, USA) with serial dilutions (181, 182). The Bradford assay involves the binding of Comassie Blue dye to proteins. This dye can present three different colors: cationic (red), neutral (green) and anionic (blue). In the presence of proteins, the dye is converted to a stable blue form, detected at 595nm using a microplate reader. For calculation of protein concentration, we used a linear standard curve, obtained from BSA solutions with different concentrations: 0µg/mL, 150 µg/mL, 300 µg/mL, 600µg/mL 800 µg/mL,1000 µg/mL and 2000 µg/mL. We diluted our samples with 10 of dilution factor. From this dilution, we loaded 5µL to a microplate (in duplicated) and added 250µL of Bradford to each well. The absorbance was measured on a microplate reader (Tecan Life Sciences, Austria) using I-control software. Using the absorbance and our linear standard curve ("y = mx + b" where y = absorbance at 595 nm and x = protein concentration) we calculated our protein concentration and calibrated our samples at the same concentration. Our laemli 6x stock solution contains 0,2M TrisHCl (Sigma Aldrich, USA) pH6.8, 40% of glycerol (Sigma Aldrich, USA), 0,04% Blue Bromophenol (Santa Cruz, Dallas), 0,3 M of SDS (Applichem, Germany) and 20% of β-Mercaptoethanol (Sigma Aldrich, Steinheim). Laemmli buffer allows to see the sample during loading and the run (blue bromophenol), increases the density of the sample (glycerol). The SDS present in laemmli buffer denatures proteins and gives negative charge so they can be separated by size. The β-Mercaptoethanol reduces disulfide bonds. We heated the samples at 95º in a sample mixer/ heater (thermo shaker, EU)

for 5 minutes. This step will allow denaturation of the proteins and migration through an electric field. Samples were immediately loaded on a gel or kept at -20º C for long-term storage.

SDS-PAGE

Proteins were separated according to their molecular weight on a 10% SDS-PAGE gel (0,4M Tris (Sigma Aldrich, USA) pH 8.8, 10% acrylamide (Fisher BioReagents, USA), 0,1% SDS (Applichem, Germany), 0,1% Ammonium Persulfate (APS) (Sigma Aldrich, USA), 0,15% Tetramethylethylenediamine (TEMED) (Santa Cruz Biotechnologies, Dallas). The stacking gel was prepared with 0,1 M Tris (Sigma Aldrich, USA) pH 6.5, 3,8% acrylamide, 0.08% SDS 0,1% APS, 0,1% TEMED. The electrophoresis was performed in SDS-Page running buffer (0,02M Tris (Sigma Aldrich, USA), 0,025M Glycine (Sigma Aldrich, Belgium), and 0,003MSDS (Applichem, Germany)) using the BIO-RAD WB power source initially at 75V until proteins reach the running gel and then at 140V.

Protein Transference and detection

We performed a wet transfer on a nitrocellulose membrane (Amersham, UK). The SDS-PAGE Transfer Buffer used contained 20% methanol (VWR, France), 0,05M TRIS (Sigma Aldrich, USA) and 0,05M Glycine (Sigma Aldrich, Belgium)). Following, we blocked the membrane in 5% milk (Nestlé, Portugal) for one hour, and incubated with the primary antibody (see antibodies and dilutions in annex C) overnight at 4ºC using an roller mixer (Stuart, UK) (see primary antibodies references in annex C). Next day, the membranes were washed three times for five minutes with TBS-Tween (0,075M Tris (Sigma Aldrich, USA), 0,15M NaCl (Merck Millipore, Germany) and 0.1% Tween 20 (Merck Millipore, EC) followed by one-hour incubation at room temperature with the proper secondary antibody (see annex C). All membranes were washed three times for five 5 minutes. Later, all membranes were incubated for 5 minutes in a home-made enhanced chemiluminescente (ECL) (1,25mM Luminol (Sigma Aldrich, USA) diluted in DMSO, 0,2 mM p-coumaric acid (Sigma Aldrich, UK) diluted in DMSO, 0,1M TRIS pH 8,5, 0,01% H_2O_2 (VWR, EC) and signal was developed using the Chemidoc (BioRad, USA). Briefly, in the presence of horseradish peroxidase (HRP), coupled to the antibodies, and peroxide, luminol oxidizes producing an excited state product that emits light. Light emission signal was captured using ImageLab (Bio-Rad) software.

2.5 Cell lines generation

In order to test our hypothesis, that TRIB2 confers resistance to MEK inhibition, and taking into account the protein expression of the three Tribbles in melanoma cell lines, we generated TRIB2 knockdown using shRNA, and TRIB2 knockout (KO) using Clustered Regularly Interspaced Short Palindromic Repeats (CRISPR). This dual approach allows us to have, on one hand a system with lower expression of TRIB2 and on the other hand a system where we abrogated TRIB2 expression (figure 2.2). With these tools we will be able to evaluate the effect of TRIB2 expression after MEK inhibition. At the same time, we also generated TRIB2-FLAG knock-in (KI) for future experiments.

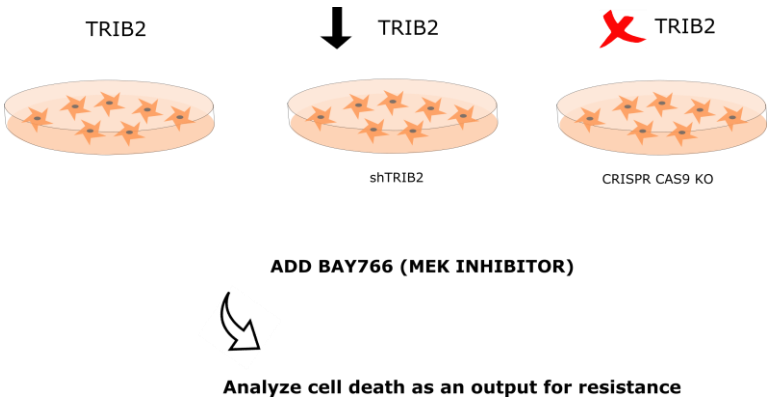

Figure 2.2. Different cell systems to test if TRIB2 confers resistance to MEK inhibition. We created a system with lower expression of TRIB2 using a short hairpin technique and a system in which we abrogated TRIB2 expression using the CRISPR-Cas9 technique. In this way, we originated 2 different systems to test our hypothesis that TRIB2 confers resistance to MEK inhibition.

2.5.1 shTRIB2

Interference RNA (RNAi) is a powerful tool to study gene function through gene silencing. The silence mechanisms can lead to the degradation of the target mRNA and can be induced by double stranded siRNA or vector based short hairpin RNA (shRNA). We used shRNA against TRIB2 (see the construct maps on Annex D). The mechanism for protein knockdown consists in the introduction of a bacterial vector encoding for a shRNA of interest. The vector is incorporated in cell nucleus and shRNA is synthetized in the nucleus of transfected cells. The shRNA, an oligonucleotide sequence that contains a loop structure, is processed to small

interference RNA (siRNA) by DICER (ribonuclease III enzyme). The siRNA is then loaded onto the RISC complex where the process of target mRNA recognition and degradation takes course (183, 184). The siRNA binds to the target mRNA in a sequence specific manner leading to its cleavage (183, 184). These tools have been previously generated and validated in our lab. We plated the cells the day before transfection. Next day, we changed the media before and transfected 2µg of the plasmid coding for the shGFP (technical control) and the shTRIB2 (see Annex D) using lipofectamin 2000 (Thermo Scientific, Scotland). The day after we replace the plates with fresh media, and 48 hours after transfection we added puromycin (Amresco, Ohio) selection.

2.5.2 TRIB2 KO – CRISPR

For TRIB2 abrogation we used CRISPR-Cas9 technique. CRISPR-CasCas9 allows genome editing being considered highly specific and efficient. This technique is based on a small guide RNA that defines the target location and the Cas9, a nuclease that induces double strand breaks (dsbreaks) at specific genome loci. Protospacer adjacent motif (PAM) is a 2-6bp immediately adjacent to DNA sequence targeted by Cas9, which is crucial for the Cas9 to recognize, bind and cleave the target (185). Using this method small non sense mutations are introduced into the reading frame of a target gene via NHEJ a repair mechanism that joins the 2 broken ends together leading to insertions/ deletions. The CRISPR-Cas9 machinery can be introduced into cells through lentivirus or DNA vector transfection (186).

The CRISPR-CasCas9 system targeting TRIB2 was previously designed and validated in our laboratory. Similar to what previously described, we plated the cells the day before transfection in 6-well plates. We transfected 2µg of the plasmid coding for guide RNA and Cas9 (px459, addgene, pSpCas9(BB)-2A-Puro (PX459)). We changed the media the following day and added puromycin two days after for 48h to select the cells that contained the plasmid. In order to get individual clones, we trypsinized the cells and performed 4-5 serial dilutions to allow single clones to grow individually. The different clones are selected by washing the cells twice with 1X PBS and individually trypsinized and plated them in a 24 well plate. When confluent, we trypsinized the cells and plated them in two 60mm plates, one plate was used to extract protein and test by WB and the second plate was used to keep a frozen stock.

2.5.3 TRIB2-FLAG KI – CRISPR

If our hypothesis of TRIB2 overexpression being responsible for conferring resistance to MEK inhibitors is confirmed, we will proceed to characterize underlying the mechanism through the analysis of protein-protein interaction and protein-localization assays. To this end, we simultaneously generated a TRIB2-FLAG Knock-In (KI) also using the CRISPR-Cas9 system. The CRISPR-Cas9 system can be used to generate a knock-In, an insertion of exogenous DNA sequence to a specific locus in mammalian cells. This occurs when dsbreaks induced by CRISPR-Cas9 are repaired by homology directed repair (HDR) in the presence of a specific template (187). FLAG is a tag. A tag is composed of a small DNA sequence, which is fused with the protein of interest using DNA recombinant technology. The specific tag, along with the respective antibody, allows protein detection in a very specific and sensitive manner. Tags are also used for protein purification and identification of protein-protein interactions (188, 189).

The protocol was similar to the one described in TRIB2 KO -CRISPR (section 2.5.2), with the difference that during the transfection we added an oligo (NZY Tech, sequence: CTC GCC AGC GAC TCA TCT CTC CAG CGG GTT TTT TTT) that is used as a template for HDR. Clones were validated by WB.

2.6 Experimental Conditions Optimization

2.6.1 Drug concentration and time-points

To confirm that our drug, Refametinib (Bay 86-9766, or as in several figures referred to as BAY766; MEK inhibitor, kindly provided by Bayer AG, Germany), induced cell death and in which concentrations and time-points it was mostly effective, we performed a pilot experiment. In this experiment we tested two different drug concentrations, 100nM and 1µM and six different time-points: 4, 8, 12, 24, 48 and 72 hours, based on previous studies (143, 144). We plated the cells the day before and added the drug after changing the media. Cells were then trypsinized, centrifuged and ressuspended in fresh media.

To confirm that Refametinib inhibits MAPK pathway we performed a Western Blot to evaluate the phosphorylation status of a downstream effector of MEK, ERK using a phosphor specific antibody against p-ERK (annex C).

Our main goal is to investigate if TRIB2 confers resistance to MEK inhibition. We analyzed cell death as a readout for resistance. In this way, was important to confirm that our MEK inhibitor, Refametinib (BAY766) induces cell death in our melanoma cell lines.

Cell death was analyzed using Annexin V / Propidium Iodite Protocol.

Annexin V / Propidium Iodite (PI) Protocol

We performed Annexin V/PI protocol to analyze cell death after 72 hours treatment. Apoptosis is a cell death program. Annexin V / PI protocol is widely used to determine if cells are viable, apoptotic, or necrotic by analyzing the differences in the plasma membrane integrity and permeability (190).

PI is a nuclear stain, and it is economic, stable and a good indicator of cell viability making it a better choice, compared to other nuclear stains. PI staining is dependent on plasma membrane integrity. Cells undergoing late apoptosis or necrosis have changes in plasma and nuclear membranes. In this way, PI enters in the cell, passes the disrupted nuclear membrane and intercalates with nucleic acids, and display a red fluorescence. (190-192).

Annexins are a family of calcium-dependent phospholipid-binding proteins. Annexins bind to phosphatidylserine (PS) to identify apoptotic cells. In normal viable cells, PS is located on the cytoplasmic surface of the cell membrane. During apoptosis, PS is translocated from the inner to the outer of cell membrane. PS is exposed to the external cellular environment, making it accessible to annexin. Annexin V binds to PS and displays a highly fluorescent signal (191, 193). Annexin V/PI protocol was done according to Annexin V/PI protocol sc- 4252 SK (Santa Cruz biotechnology), annex E. Etoposide (Sigma Aldrich, USA) was used as a positive control since it induces cell death. Results were obtained with Fluorescent Activated Cell Scanning (FACS) Calibur (BD Biosciences, Ireland) using CellQuestPro software and treated in GraphPad Prism6.

2.7 MEK inhibition Experiments

In order to understand if TRIB2 was conferring resistance to MEK inhibitors we used the tools that he have generated: cell lines with TRIB2 KD and KO and added Refametinib, also known as **BAY 86-9766,** MEK inhibitor, to evaluate cell death as a readout for drug resistance.
We plated the cells the day before, changed the media and add Refametinib at 100nM and 1µM for 72 hours and then analyzed cell death. The details of the experiments are described in table 2.3 (Annex F).

Table 2.3. Details of MEK inhibitor Refametinib (BAY766) experiments in different cell lines.

	A375 TRIB2 knockdown	*G361 TRIB2 Knockdown*	*G361 TRIB2 Knockout*	*SK-Mel-28 TRIB2 Knockout*
Number of cells plated	100000	200000	125000	125000
Time of Treatment	72hours	72hours	72hours	72hours
Positive control for cell death	Etoposide 50µM for 48h	Etoposide 50µM for 48h	Etoposide 50µM for 48h	Etoposide 50µM for 48h
Cell death analysis	Trypan blue cell death counting	Trypan blue cell death counting	Trypan blue cell death counting	Trypan blue cell death counting / Propidium Iodite Protocol

The experiment with SK-Mel-28 KO (#8) cell line was performed twice. Results were analyzed using GraphPad Prism 6. Statistical analysis was performed using two-way Analysis of Variance (ANOVA) and Bonferroni's correction test in GraphPad Prism 6.

3. Results

Tribbles are pseudokinases that play important roles in immune function, lipoprotein metabolism, cellular differentiation and proliferation being crucial in eukaryotic signaling (194-197). Tribbles proteins are highly conserved, have a MEK1 binding domain and regulate the MAPK signaling pathway (177, 198, 199). The Link lab discovered TRIB2 as a FOXO repressor protein by conducting a screening for FOXO suppressors (144). It was shown that TRIB2 is overexpressed in melanoma cell lines and patients (144), and it confers resistance to PI3K and mTOR inhibitors (143). The aim of this master project was to investigate if TRIB2 confers resistance to MEK inhibitors.

3.1. Characterization of Cell Lines

3.1.1. TRIB1 and TRIB2 mRNA levels are higher in melanoma cell lines.

Considering that Tribbles are highly homologs and conserved (200) they can have redundant functions. We decided to create isogenic cell lines for TRIB2 to test our hypothesis that TRIB2 confers resistance to MEK inhibition. Since Tribbles members are highly conserved and homolog we decided to investigate the mRNA and protein levels of all three tribbles in melanoma and non-melanoma cell lines. If Tribbles have redundant function it means that other Tribbles members can compensate TRIB2 depletion. We characterized a panel of melanoma and non-melanoma cell lines (listed in section 2.2). We investigated the mRNA levels, using q-PCR technique, of all three Tribble members considering that their levels are not described yet in melanoma and non-melanoma cell lines. The results were normalized to the non-melanoma U2OS cell line (osteosarcoma cells) since this cell line did not show visible TRIB2 protein expression by western blot (143). Data was analyzed using Bio Rad CFX manager 3.1 software.

In general, Tribbles mRNA levels were higher in melanoma cell lines compared to non-melanoma cell lines U2OS, and HEK293T (figure 3.1). TRIB2 mRNA levels (figure 3.1 A) were higher in melanoma cell lines, (except for A375 cell line) than in non-melanoma cells. TRIB1 (figure 3.1 B) mRNA levels were higher in melanoma cell lines (except in A375 cells), and in HEK293T cells which in turn was slightly higher than in A375 cell line. TRIB3 (Figure 3.1 C) mRNA levels were higher in melanoma cell lines compared to U2OS cell line. HEK293T cell line had the higher TRIB3 mRNA levels.

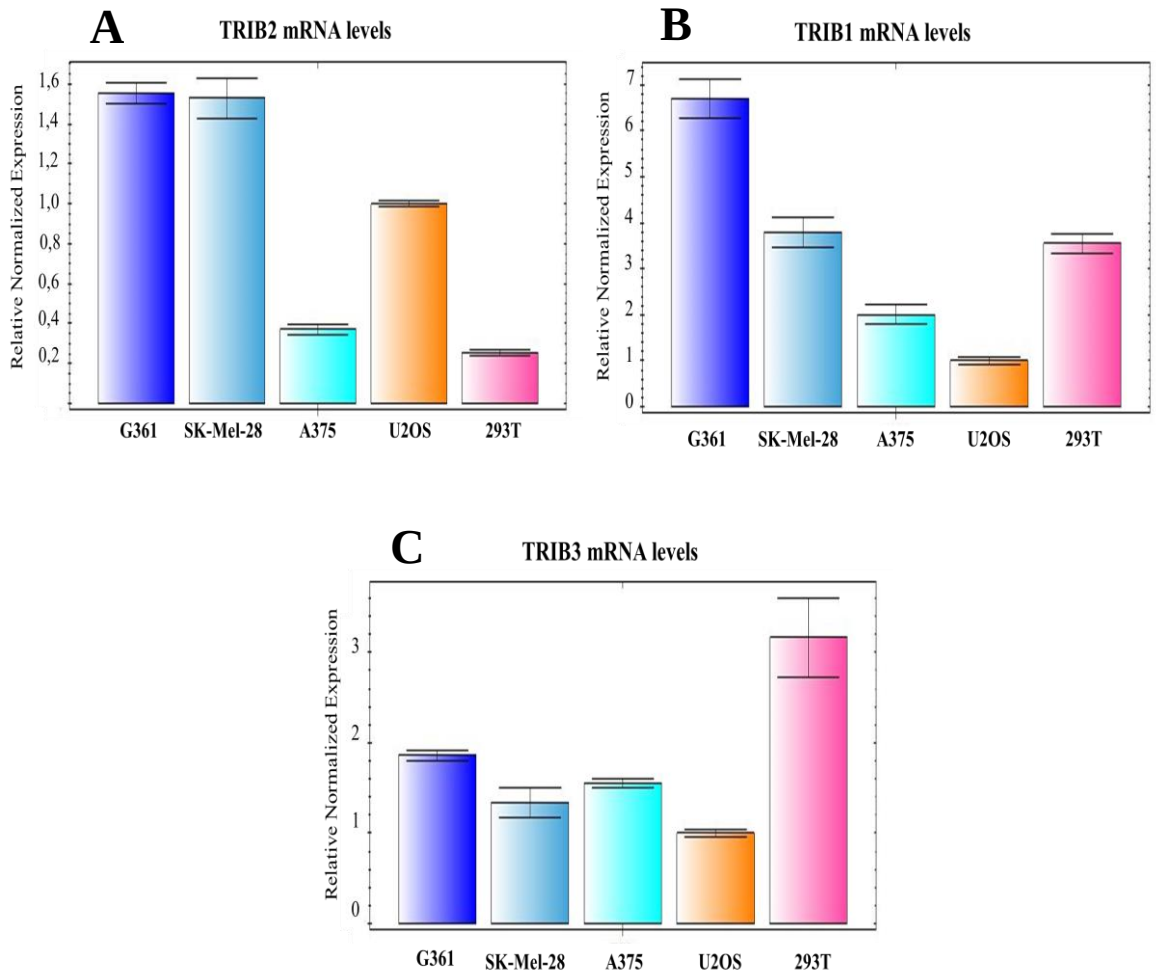

Figure 3.1. Tribbles mRNA levels of a panel of melanoma and non-melanoma cell lines. Melanoma cell lines are represented in blue (G361, SK-Mel-28 and A375), U2OS (osteosarcoma cell line) is represented in orange and HEK293T (human embryonic kidney cell line) is represented in pink. mRNA expression levels were evaluated using RT-PCR and data was analyzed using Bio-Rad CFX manager 3.1 software. Y axis represents the fold change relative to U2OS cell line. (A) TRIB2 mRNA levels; (B) TRIB1 mRNA levels;) (C) TRIB3 mRNA levels. Three technical replicates. GAPDH- housekeeping gene. One experiment has been performed.

3.1.2. Tribbles protein levels are higher in melanoma cell lines.

Transcript levels do not always correspond to protein levels. We wondered whether Tribbles mRNA levels correlated with protein levels in the panel of cell lines that we used (section 2.2). To investigate this, we evaluated the protein expression by western blot using specific antibodies (see annex C). Figure 3.2 shows that the expression of all Tribble proteins was higher in melanoma cell lines compared to U2OS and HEK293T cell lines. In non-melanoma cell lines, the expression of TRIB2 was undetectable, the expression of TRIB1 was similar between HEK293T and U2OS cell lines. Interestingly, G361 cell line showed increased TRIB3 expression in comparison with the remaining melanoma cell lines. Our results indicate that TRIB1 and TRIB2 protein expression correlate with mRNA levels. TRIB3 protein levels are in fact higher in the panel of melanoma cell lines compared to the non-melanoma cells correlating with the transcript levels obtained by RT-PCR. Intriguingly, TRIB3 band in HEK293T cell line is very faint compared to the rest of the cell lines, indicative of low expression, but the mRNA levels were the highest.

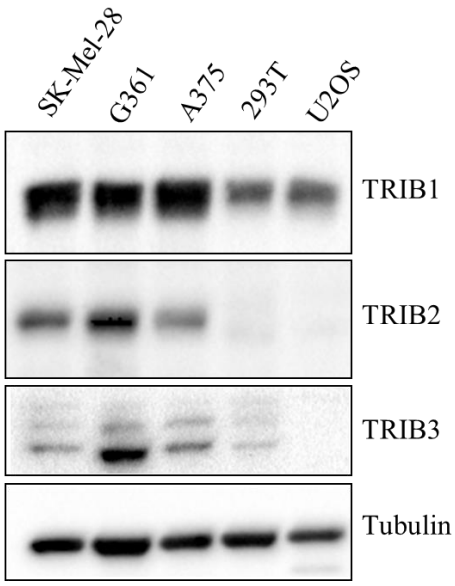

Figure 3.2. Tribble protein levels in melanoma and non-melanoma cell lines. The first three lanes correspond to melanoma cell lines and the two last lanes correspond to HEK293T and U2OS cell lines respectively. Protein levels were assessed with Tribble specific antibodies by western blot technique. Tubulin was used as a loading control. 20µg total protein loaded per lane and separated by 10% SDS-PAGE. One experiment has been performed.

3.2 Optimizing Experimental Conditions

To test the effect of TRIB2 on MEK resistance we have decided to assess cell death induced by the MEK inhibitor (Refametinib) with different approaches. For that reason, we primarily optimized different variables that will influence the success of the following experiments.

3.2.1. 100nM of Refametinib is sufficient to inhibit MAPK pathway.

We determined the optimal concentration of Refametinib to use in the different melanoma cell lines. We used two different concentrations 100nM and 1µM (based in previous studies in our lab) during drug exposure for 2, 4, 8, and 24 hours (figure 3.3). To confirm the efficacy of MEK inhibition, we performed a western blot and analyzed the phosphorylation status of ERK protein using a phospho specific antibody against ERK in SK-MEK-28 cell line. ERK is a downstream effector of MEK and it is directly phosphorylated by MEK (201, 202). Two hours after treatment the MAPK pathway was already inhibited as it can be seen in figure 3.3 by the absence of p-ERK signal (figure 3.3). This effect is phosphorylation specific and not due to alterations on total protein levels since total ERK levels are maintained. Additionally, 100nM of Refametinib was sufficient to inhibit the MAPK pathway. Here we demonstrate that Refametinib successfully inhibits MEK1/2 in our melanoma cell lines and that the pathway is inhibited as soon as two hours and as long as 24 hours after treatment.

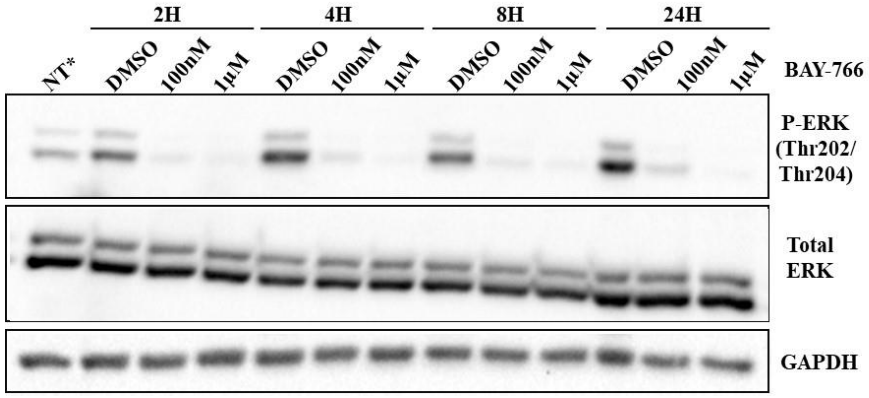

Figure 3.3. Effect of Refametinib treatment on MAPK pathway in SK-Mel-28 cell line. SK-Mel-28 cell line was treated with Refametinib (BAY766), a selective MEK inhibitor for 2, 4, 8 and 24 hours using two different concentrations 100nM and 1µM. *NT-Non-treated cells. MAPK pathway activation status was evaluated using a phosphor-specific antibody against ERK. GAPDH was used as a loading control. 20µg total protein loaded per lane and separated by 10% SDS-PAGE. One experiment has been performed.

3.2.2. Refametinib treatment for 72hours induces cell death.

Our main goal was to study the role of TRIB2 in resistance to MEK inhibition by analyzing the effect on cell death. In order to allow cell death to occur and detect it, we decided to test longer drug incubation time-points. To this end, we repeated the experiment performed in the previous section (3.2.1) but included an additional time point of 72 hours.

After 72 hours of Refametinib treatment, we documented the overall cells phenotype with bright light pictures. Figure 3.4 shows that treatment with the MEK inhibitor reduced cell density when compared to DMSO treatment. Cell death is also notably higher in both concentrations, compared to the control.

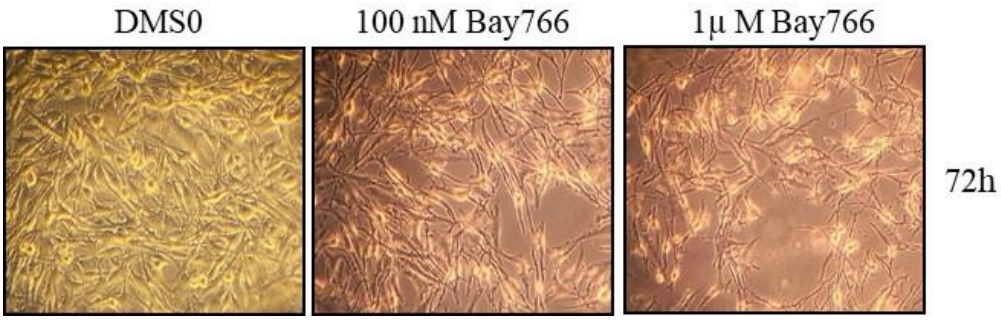

Figure 3.4. SK-Mel-28 cell line treated with Refametinib for 72hours. SK-Mel-28 cell line density and appearance after 72hours of treatment with 100nM or 1µM Refametinib. Amplification 100x. Images are representative of three independent experiments.

In order to analyze cell death, we performed Annexin V/PI protocol that allows the detection of apoptotic cells using flow cytometry. Annexin V/ PI protocol is used to identify apoptotic cells population through differences in plasma membrane integrity and permeability. Etoposide is known to induce DNA double strand breaks (ds-breaks) resulting in cell death (203, 204) and it is commonly used as a positive control in apoptosis induction experiments. Upon 16 hours treatment, Etoposide lead to 12,60% of apoptotic cell death. Refametinib treatment induced cell death at both concentrations, being higher with increasing concentration. At 100nM concentration, Refametinib induced 13,10%, similar to what we obtained with Etoposide (12,60%). The concentration of 1µM of Refametinib treatment for 72hours induced 30,90% of cell death (figure 3.5). These results are preliminary data obtained from one experiment that have to be confirmed by additional experiments.

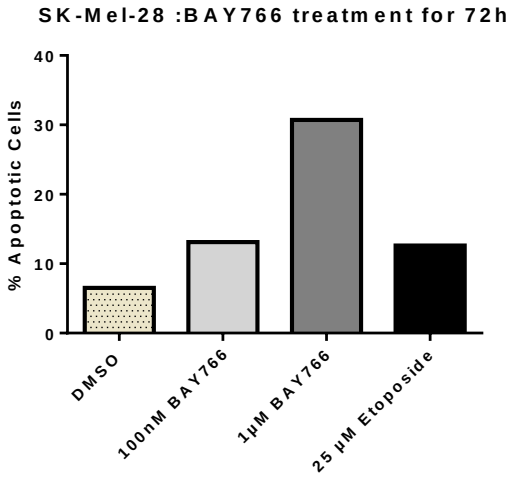

Figure 3.5. Effect of Refametinib treatment on apoptotic cell death in SK-Mel-28 cell line. SK-MEL28 cell line was cultured for 72 hours with Refametinib inhibitor and cell death was assessed with AnnexinV/PI. The data was obtained with Facs-Calibur using CellQuestPro software and analyzed with GraphPad prism6 (one experiment). The Y axis represents the percentage of apoptotic cells. The X axis shows the different treatments: DMSO (vehicle), different concentrations of Refametinib and Etoposide. One experiment has been performed.

We verified the MAPK pathway status in this experiment to confirm the efficacy of the inhibitor Refametinib after 72 hours of incubation. We showed that even 72 hours after treatment the MAPK pathway is still turn-off as it can be observed by the lack of p-ERK signal seen in figure 3.6.

Since the pathway was still inhibited after 72h of Refametinib treatment, and we were able to detect cell death after this period with Annexin V/ PI, we opted for this time-point. Exposure to 100nM and 1µM Refametinib potently inhibited the MAPK pathway. Since we were testing our hypothesis in several melanoma cell lines with different sensitivities, we decided to use both concentrations in future experiments.

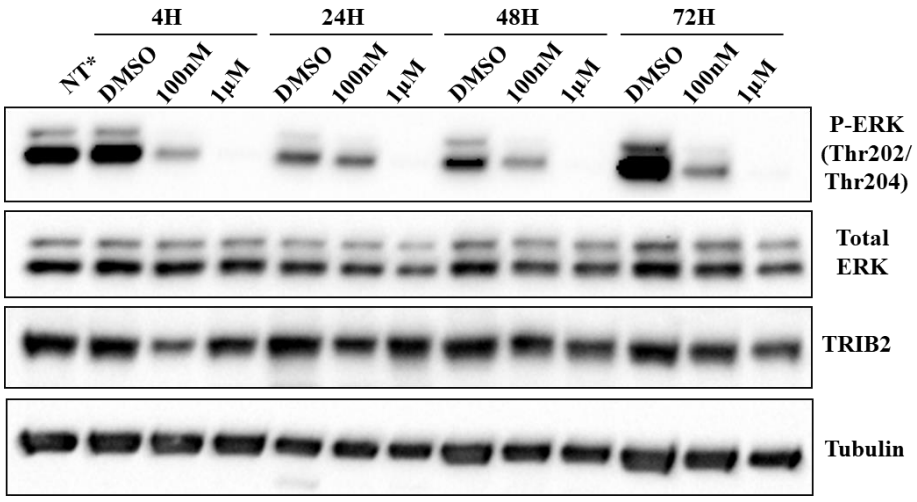

Figure 3.6. Effect of Refametinib treatment on MAPK pathway in SK-Mel-28 cell line. SK-Mel-28 cell line was treated with Refametinib, a selective MEK inhibitor for 4, 24, 48 and 72 hours using two different concentrations 100nM and 1μM. *NT-Non-treated cells. MAPK pathway activation status was evaluated using a phospho-specific antibody against ERK. Tubulin was used as a loading control. 20μg total protein loaded per lane and separated by 10% SDS-PAGE. One experiment has been performed.

3.3. Generation of cell lines with different TRIB2 status

We hypothesized that TRIB2 confers resistance to MEK inhibition. To test our hypothesis, we needed a system in which we would have different amounts of TRIB2. To generate such a cell system, we decided to abrogate TRIB2 expression using CRISPR-Cas9 technique and reduce TRIB2 expression levels using short hairpin RNAs (shRNA) against TRIB2. Both techniques were performed in three melanoma cell lines: G61, SK-Mel-28 and A375. We plated the cells the day before transfection and transfected different shTRIB2 to obtain TRIB2 knockdowns. To generate the TRIB2 knockout we transfected a plasmid coding simultaneously for single guide RNA (sgRNA) and Cas9. Clones were selected and validated by western blot using a specific antibody against TRIB2.

3.3.1. A375

3.3.1.1. A375: TRIB2 Knockdown

We transfected A375 cell line with five different short hairpins against TRIB2 previously used in our lab (144). All five short hairpins reduced TRIB2 expression as shown in figure 3.7. The negative control (shGFP) also seemed to have an effect on TRIB2 expression. For this reason, we also included the parental A375 cell line as a control.

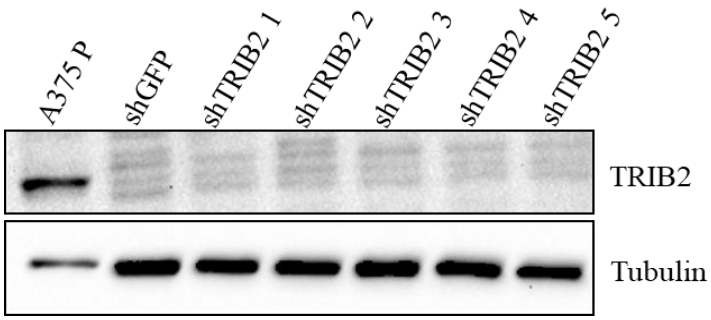

Figure 3.7. TRIB2 Knockdown in A375 cell line. A375 was transfected with five different short hairpins against TRIB2. A375 P represents the parental cell line. Short hairpin against GFP refers to the negative control. Protein expression levels were analyzed by western blot with a specific TRIB2 antibody. Tubulin was used as a loading control. 20µg total protein loaded per lane and separated by 10% SDS-PAGE. Images are representative of two independent experiments.

3.3.1.2. Refametinib treatment caused increased cell death in A375 TRIB2 knockdown.

Considering that our negative control (shGFP) interfered with TRIB2 expression (figure 3.7), we used the parental cell line as a control. A375 cells were treated with 100 nM Refametinib for 72 hours and this treatment induced 20% of cell death in the knockdown cell line (shTRIB2 #1) compared to 13,8% of cell death in the parental cell line (figure 3.8). Using a higher concentration (1µM) of Refametinib caused 48,2% of cell death in the knockdown cell line compared to 26,7% in the parental cell line (figure 3.8). This data suggests that TRIB2 confers resistance to MEK inhibition. However, as shGFP caused reduced expression of TRIB2 through an unknown mechanism we decided to use additional cell lines to confirm the result.

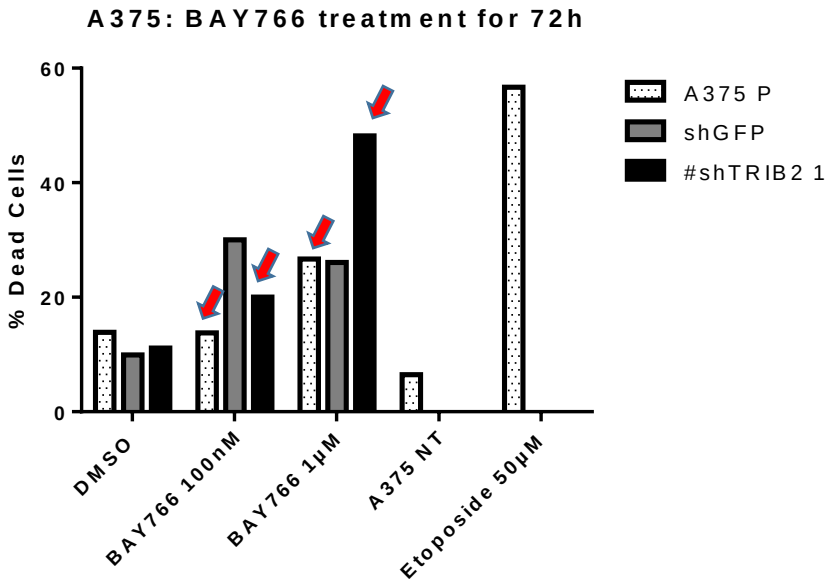

Figure 3.8. Cell death analysis of Refametinib treatment in A375 TRIB2 Knockdown cell line. The different cell lines are represented in different shades of blue: white corresponds to A375 parental cell line (A375P), grey to the control transfected with shRNA against GFP (shGFP) and the black to the A375 TRIB2 knockdown (shTRIB2 #1). Red arrows sign the percentage of cell death in A375 P and the TRIB2 knockdown (#shTRIB2 1) cell line under Refametinib (BAY766) treatment. Etoposide was used at 50 µM for 48 hours. The Y axis shows the percentage of dead cells and in X axis the different treatments. Cell death was analyzed with trypan blue cell death counting. Results were analyzed with GraphPad prism6. NT- non-treated cells. Graph represents one experiment.

3.3.2. G361

3.3.2.1 G361: TRIB2 knockdown

We tested two different shRNA against TRIB2 in G361 cell line. The shTRIB2 #2 showed to be more efficient downregulating TRIB2 expression when compared to shTRIB2 #1 (figure 3.9). In this cell line the shGFP did not interfere with TRIB2 expression. The following experiments were performed using shTRIB2 #2.

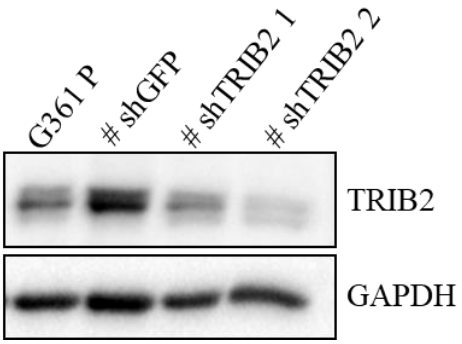

Figure 3.9. TRIB2 Knockdown in G361 cell line. G361 cell line was transfected with two different shRNA against TRIB2 (shTRIB2 #1 and shTRIB2 #2). Negative control refers to short hairpin against GFP (shGFP) and parental cell line is represented by G361P. Western blot using an antibody specific to TRIB2; GAPDH was used as a loading control. 20µg total protein loaded per lane and separated by 10% SDS-PAGE. Images are representative of two independent experiments.

3.3.2.2. Refametinib caused increased cell death in G361 TRIB2 knockdown.

We next tested the effect of TRIB2 upon Refametinib treatment. To this end we used G361 shTRIB2 #2 cell line (figure 3.9) and analyzed cell death with trypan blue cell death counting (as mentioned in section 2.1) and also with PI staining.

G361 shTRIB2 #2 knockdown treated with 100nM of Refametinib for 72 hours induced a modest increase in cell death (29%) compared to the control (shGFP) (21,7% of cell death) (figure 3.10). At 1µM concentration cell death was high in both cell lines suggesting that this concentration was cytotoxic for G361 cell line causing unspecific cell death.

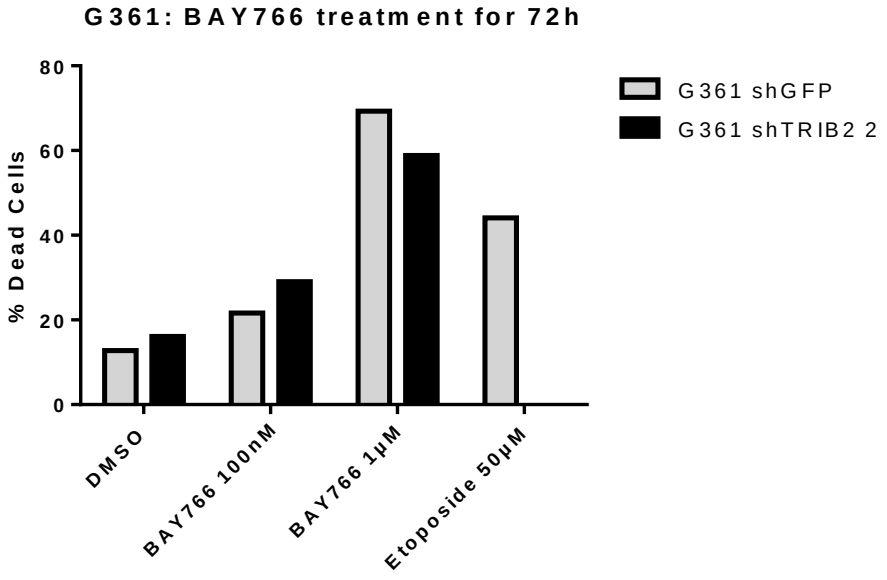

Figure 3.10. Cell death analysis of Refametinib treatment in TRIB2 knockdown. G361 shGFP (in grey) and G361 shTRIB2 #2 (in black) were treated with Refametinib for 72 hours. Cell death was assessed by trypan blue exclusion test. Etoposide was used at 50 µM for 48 hours as a positive control. Y axis shows the percentage of dead cells and X axis the different treatments. Results were analyzed with GraphPad prism6. Graph represents one experiment.

During cell death, cells undergo plasma membrane changes, allowing the PI, fluorochrome, to pass thought it and bind to DNA, displaying fluorescence. We analyzed the percentage of SubG1 cells as an indicator of cell death in FACs Calibur using CellQuestPro software after staining with PI.

This analysis revealed a significant difference in cell death between the G361 shTRIB2 #2 (586%) and the control shGFP (26,7%) upon treatment with 100nM of Refametinib (figure 3.11). This difference was also evident with a higher concentration of MEK inhibitor, although the difference was only 10%. In fact, using 1µM Refametinib cell death in G361 shGFP caused 48% of cell death. These observations may indicate that 1µM is cytotoxic for G361 cell lines.

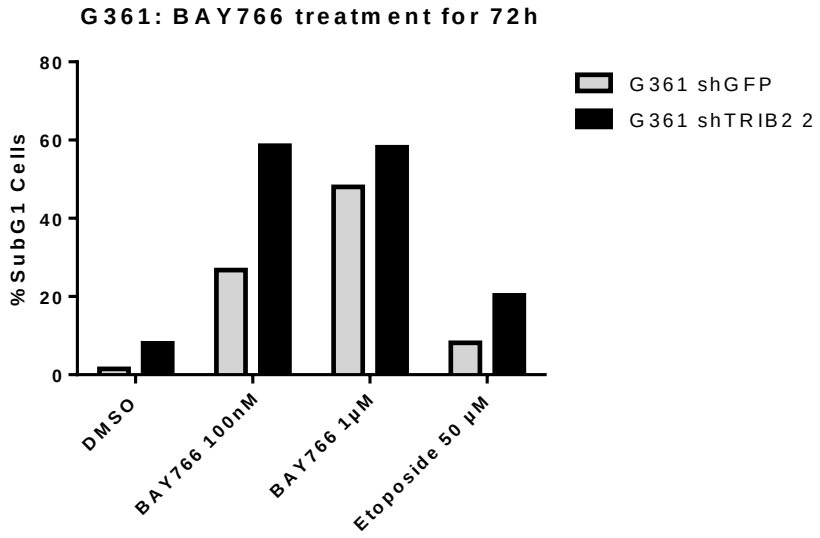

Figure 3.11. PI staining of G361 cell line upon Refametinib treatment. G361 shGFP (in grey) and G361 shTRIB2 #2 (in black) were treated with Refametinib for 72 hours. Percentage of SubG1 cells was obtained after PI staining and analyzed with BD FACs Calibur and CellQuest software. Etoposide was used at 50 µM for 48 hours. Y axis shows the percentage of SubG1 cells and the X axis the different treatments. Results were analyzed with GraphPad prism6. Graph represents one experiment

3.3.2.3. G361: TRIB2 Knockout

We screened thirteen G361 clones for TRIB2 knockout. Clones were tested assessing protein levels with a specific TRIB2 antibody by western blot. Figure 3.12 shows five clones including. Clone #14 which was positive for TRIB2 knockout.

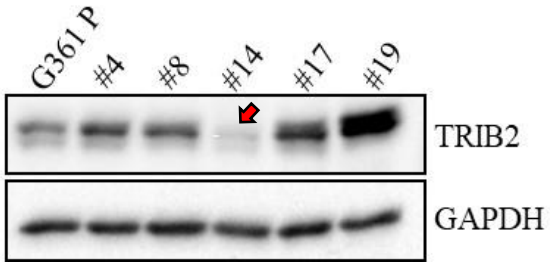

Figure 3.12. TRIB2 Knockout (KO) in G361 cell line. The first lane shows G361 parental cell line followed by different G361 clones for TRIB2 KO. Clone #14 was a positive KO for TRIB2 Protein levels were evaluated by western blot using a specific antibody against TRIB2. GAPDH was used as a loading control. 20µg total protein loaded per lane and separated by 10% SDS-PAGE. One experiment has been performed.

3.3.2.4. Refametinib caused increased cell death in G361 TRIB2 knockout.

We used G361 #14, a KO for TRIB2 (figure 3.12) and the parental cell line G361 to quantify cell death using trypan blue exclusion test. Results from this experiment were very similar to the ones obtained using G361 TRIB2 knockdown (figure 3.11). Refametinib treatment at 100nM caused 33% of cell death in the knockout cell line and 22% in the parental cell line (figure 3.13). As in the previous experiment with G361 TRIB2 knockdown, the difference in cell death between parental cell line and the cell line with TRIB2 depletion, was not detected at 1µM Refametinib concentration: cell death was high in both cell lines (59,5% in the knockout and 66,3% in the parental cell line) which may suggest that this concentration is cytotoxic for G361 cell line causing unspecific cell death.

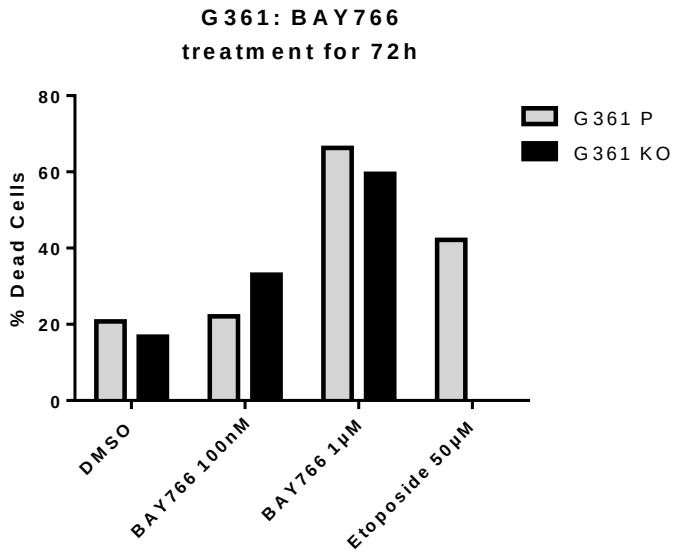

Figure 3.13. Influence of Refametinib treatment in cell death using G361 TRIB2 knockout cells. G361 P (in grey) and G361 KO (in black) were treated with Refametinib for 72 hours. Cell death was assessed by trypan blue exclusion test. Etoposide was used at 50 µM for 48 hours as a positive control. Y axis shows the percentage of dead cells and X axis the different treatments. Results were analyzed with GraphPad prism6. Graph represents one experiment.

3.3.3. SK-Mel-28 cell line

3.3.3.1. SK-Mel-28: TRIB2 Knockout

In SK-Mel-28 we screened 15 different clones for TRIB2 knockouts. Clones were tested through the analysis of protein expression by Western Blot technique. In this cell line we obtained several TRIB2- knockouts: #5A, #40, #1, #6 and #8 with complete TRIB2 abrogation (figure 3.14). We selected a positive TRIB2 knockout clone: SK-Mel-28 #8 to be used in the following experiments.

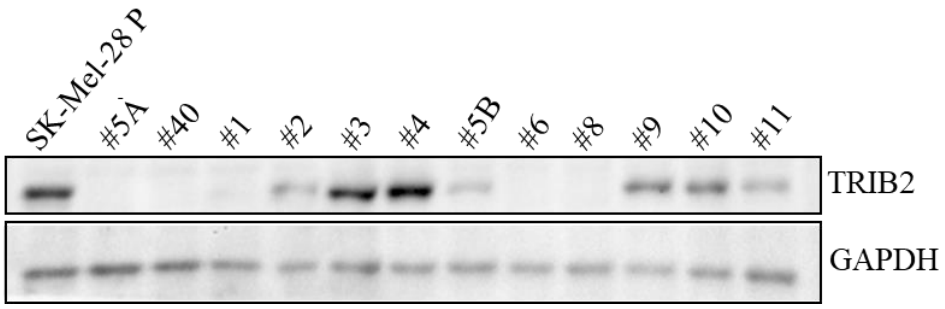

Figure 3.14. TRIB2 Knockout (KO) in SK-Mel-28 cell line. The first lane shows SK-Mel-28 parental cell line TRIB2 followed by different SK-Mel-28 clones for TRIB2 KO. Protein levels were evaluated by western blot using a specific antibody against TRIB2. GAPDH was used as a loading control. 20µg total protein loaded per lane and separated by 10% SDS-PAGE. One experiment has been performed.

3.3.3.2. Refametinib treatment in SK-Mel-28 with different levels of TRIB2 shows that cell death correlates with TRIB2.

To test the effect of TRIB2 expression after MEK inhibition we used SK-Mel-28 #8 TRIB2 KO cell line and analyzed the cell death percentage upon 72 hours of Refametinib treatment Results were analyzed by trypan blue cell death counting and PI staining.

In order to determine the effect of the vecle on cell viability we treated the cells with DMSO and observed that, cell death was similar between parental cell line (9,11%) and the knockout cell line (11,56%) (figure 3.15). Etoposide induced 40% of cell death in the parental cell line. In the parental cell line, the difference in cell death between the higher and the lower concentration of Refametinib treatment was 23,4% and was statistically significant, (*$p \leq 0.05$). Comparing both cell lines, 1 µM of Refametinib treatment induced a higher percentage of cell death in the SK-Mel-28 TRIB2 knockout, statistically significant(*$p \leq 0.05$). In the presence of

TRIB2 (parental cell line), 1µM of Refametinib caused cell death in 30,2% of cells while the cell line where TRIB2 has been depleted Refametinib caused death in 76,9% of the cells, a 2.5 fold increase c. (figure 3.15). These results strongly suggest that TRIB2 is conferring resistance to MEK inhibition.

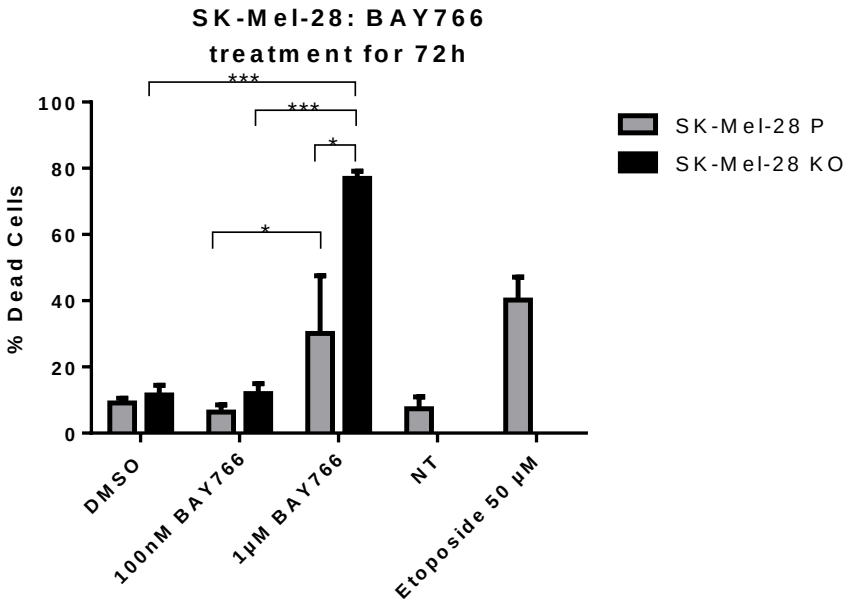

Figure 3.15. Cell death analysis of Refametinib treatment in TRIB2 knockout. SK-Mel-28 P (in grey) and SK-Mel-28 KO (in black) were treated with Refametinib for 72 hours. Cell death was assessed by trypan blue exclusion test. Etoposide was used at 50 µM for 48 hours as a positive control. Y axis shows the percentage of dead cells and X axis the different treatments. Results were analyzed with GraphPad prism6. Standard Deviation (SD) is present in the graph. Results were analyzed with two-way anova (ANOVA) and Bonferroni correction in GraphPad prism6. *$p \leq 0.05$; **$p \leq 0.01$; ***$p \leq 0.001$. NT=non-treated cells. Graph represents two independent experiments.

The difference in cell death between both cell lines was also detected with PI staining. Results show that, under the same conditions, Refametinib treatment for 72 hours caused more cell death in cells with TRIB2 depletion. Comparing both cell lines, using 100nM Refametinib, the percentage of SubG1 cells in parental cell line was only 5,9% compared to 22% in the knockout cell line (3.7 times more cell death in the TRIB2 knockout cell line). This difference was also detected using a high concentration of our drug (1µM) causing 22% cell death in parental cell line compared to 47% in the knockout (figure 3.16).

In our negative control, DMSO treatment, cell death was also higher in the TRIB2 knockout cell line (7%) compared to the parental cell line (0,5%) which may indicate that DMSO can be more toxic to this cell line. However, this difference is not high. Also the positive control, caused 15,6% of cell death in the TRIB2 knockout cell line, and 12,2% in the parental cell line, also a minimal difference. The difference in cell death due to Refametinib treatment was more than the double comparing both cell lines. Refametinib Results from SK-Mel-28 TRIB2 knockout cell line demonstrated that TRIB2 presence correlated with cell death Yet, this experiment should be repeated.

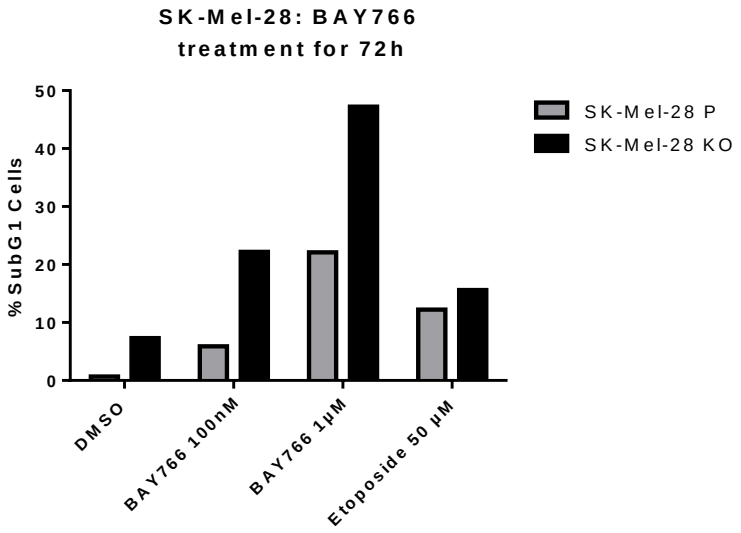

Figure 3.16. Cell death analysis after 72hours of Refametinib treatment in SK-Mel-28 TRIB2 KO cell line. The different cell lines are represented in different colors: grey corresponds to SK-Mel-28 parental cell line, represented by SK-Mel-28P and black to the SK-Mel-28 TRIB2 knockout cell line, represented by SK-Mel-28 KO. The positive control for cell death was 50 µM Etoposide for 48 hours. Y axis shows the percentage of SubG1 cells and in X axis the different treatments applied in these cell lines. % of SubG1 cell line was achieved using BD FACs Calibur and CellQuest software. Results were analyzed with GraphPad prism6. Graph represents one experiment.

3.3.3.3.SK-Mel-28: TRIB2 Knock-In

The fact that we have data that strongly indicates that TRIB2 confers resistance to MEK inhibition, MEK inhibition prompts us to study the underlying molecular mechanism. In order to perform experiments like Co-Immunoprecipitation to test protein-protein interaction or protein localization assays upon MEK inhibitor treatment using the endogenous TRIB2 protein, we seek to generate TRIB2-FLAG Knock-In (KI) using the CRISPR-Cas9 system. Similar to the knockout, a knock-in can be obtained with the introduction of the same tools into the cell, a sgRNA and a Cas9 protein, plus an oligo, a DNA sequence to serve as a template to the Homology Direct repair mediated by the CAS9 (187). FLAG is a tag used for the study of structural and functional protein properties (205).

We screened 63 clones for A375 cell line, 23 clones for SK-Mel-28 cell line and clones for G361 cell line are yet to be tested. We obtained positive TRIB2-FLAG knock-in for SK-Mel-28 cell line (figure 3.17). In figure 3.17 we show some of the clones tested for TRIB2-FLAG knock-in. Clone #13 was a positive knock-in that expresses both TRIB2 and FLAG. The other two clones #12 and #15 have a less strong expression of TRIB2 and FLAG.

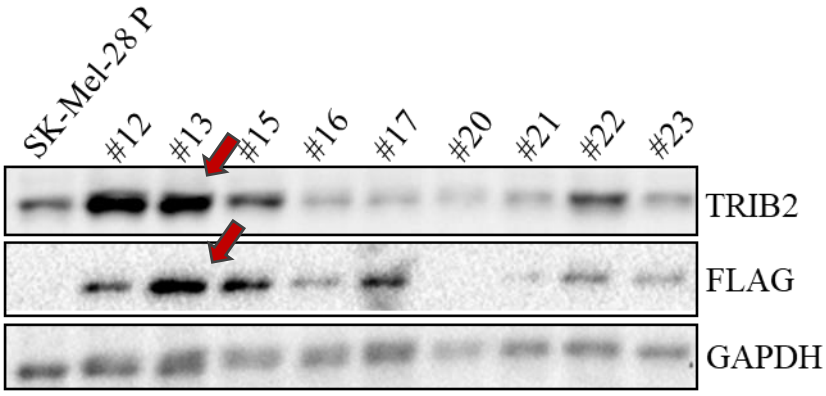

Figure 3.17. TRIB2-FLAG Knock-In (KI) in SK-Mel-28 cell line. The first lane shows SK-Mel-28 parental cell line (SK-Mel-28 P) followed by different SK-Mel-28 clones marked by # and its number for TRIB2 KI. Red arrows show a positive Knock-In for TRIB2-FLAG. Protein levels were evaluated by western blot using specific antibodies against TRIB2 and FLAG. GAPDH was used as a loading control. 20µg total protein loaded per lane and separated by 10% SDS-PAGE. One experiment has been performed.

4. Discussion

Melanoma is one of the deadliest cancers mainly due to its highly metastatic propensity, frequent relapses and its high resistance to therapy (22, 24). Melanomas are highly resistant to therapies, and despite all the scientific advances this is still a major concern in public health. The clinical benefit from current therapies applied in Melanoma is quite limited (73, 103) and understanding the resistance mechanisms, is crucial to improve therapies and the outcome of melanoma patients. Here we provide evidences that TRIB2 confers resistance to MEK inhibition in melanoma. Based on the fact that (a) TRIB2 has a MEK1 binding site; (b) TRIB2 is overexpressed in melanoma (144) and (c) TRIB2 confers resistance to some PI3K and mTOR inhibitors (143) we hypothesized that **TRIB2 confers resistance to MEK inhibitors.**

We first analyzed Tribbles expression on a panel of melanoma and non-melanoma cell lines and decided which cell system would be a better option to test our hypothesis. Tribbles mRNA levels are higher in melanoma cell lines compared to non-melanoma cell lines (U2OS and HEK293T). Studies demonstrate that Tribbles are highly conserved and display also a high degree of similarity between the human Tribbles amino acid sequences being TRIB1/TRIB2 71,3%, TRIB1/TRIB3 53,3% and TRIB2/TRIB3 53,7% conserved (158, 206). It has been reported that the expression of both TRIB1 and TRIB2 induces AML in mice (164). This similarity between TRIB1/TRIB2 and their oncogenic activities in AML suggest redundant functions, but a formal proof for this hypothesis remains to be established.

Protein levels of the three tribbles members were higher in melanoma cell lines compared to the non-melanoma cell lines U2OS and HEK293T that, overall, correlates with our RT-PCR data. Surprisingly, the band for TRIB3 protein levels in HEK293T cell line was very faint comparing to the TRIB3 mRNA expression data. TRIB3 is mostly regulated at the transcriptional level (207) which may explain the difference between mRNA and protein levels in HEK293T cell line. The levels of mRNA not always correlate with the protein levels possibly due to post-transcriptional mechanisms, such as transcript turnover and the action of micro RNAs (miRNAs), and the fact that proteins can have different half-lives (208). Also, the absence of correlation can be due to errors and noise from both experiments to detect mRNA and protein expression (208). According to previous studies, TRIB2 protein levels were low in U2OS cells (143) , consistent with our data. Soubeyrand *et al.*, presented evidences that TRIB1

may be post-translationally regulated. Nonetheless, the authors did not detect TRIB1 protein expression in HEK293T cell line as in our data (209).

Overall, in our cell line panel **mRNA levels correlated with protein levels**. Okamoto H. *et al.*, showed that Tribbles members are differentially expressed in different tissues (210) and that the expression of TRIB1 and TRIB2 did not change in mice with TRIB3 depletion, indicating the absence of a compensatory mechanism(210). This initial data shows that **different melanoma cell lines have high endogenous TRIB2 levels**. For this reason, we decided to downregulate and abrogate TRIB2 expression in this melanoma cell line panel, creating two different cell systems with the same genetic background and different levels of TRIB2. These tools were fundamental to test the effect of TRIB2 mediated resistance to MEK inhibitors. To this end, we used Refametinib, a non-ATP competitive MEK1/2 inhibitor that showed to reduce proliferation in some cell lines, including SK-Mel-28 and A375 (211, 212).

Refametinib successfully inhibited MAPK pathway and induced cell death. In our experimental conditions, the MAPK pathway was inhibited after Refametinib treatment since we did not detect p-ERK upon MEK inhibition. This inhibitory effect is specific and not due to changes on total ERK levels. Moreover, we can conclude that the lowest concentration of Refametinib was enough to inhibit MAPK pathway. In fact, also the lowest concentration of Refametinib was enough to induce cell death in melanoma cell line. After 72hours of Refametinib treatment, the percentage of cell death was similar to the one generated by Etoposide (positive cell death control) treatment. The MAPK pathway was still inhibited after 72 hours of Refametinib treatment. The half maximal inhibitory concentration (IC50) , measured by the incorporation of radioactive phosphate from ATP into ERK as substrate, for Refametinib is between 19nM (MEK1) and 47 nM (MEK2) (211). In Hepatocellular carcinoma cell lines Refametinib had an half-maximum inhibitory concentration values between 33nM to 762nM (213) Here, we demonstrated that 100nM Refametinib inhibited MAPK signaling in melanoma cell lines.

TRIB2 downregulation was successful in G361 melanoma cell line, using shTRIB2 #2. TRIB2 knockdown was performed in all three melanoma cell lines, since they have high endogenous TRIB2 levels. We successfully downregulated TRIB2 expression in A375 cell line. However, the negative control shRNA against GFP also interfered with TRIB2 expression. The RNAi mediated silencing is time consuming and associated with off-target effects (183). Many studies have shown a RNAi can silence several transcripts (214, 215) due to partial complementarity between RNAi and the unintended target (215). Here, probably the shGFP

had some homology to TRIB2 mRNA promoting its degradation. To guarantee that our negative control would not interfere with our protein of interest, we should have used an empty vector instead (183).

Refametinib treatment caused increased cell death in TRIB2 knockdown cell lines. Using the TRIB2 knockdowns cell lines, our preliminary data shows that TRIB2 may be in fact conferring resistance to MEK inhibitors. Refametinib treatment induced an increase in cell death in the A375 TRIB2 knockdown cell line, comparing to the parental cell line. This difference was attenuated when we used lower Refametinib concentrations. This is probably due to the fact that there might be residual TRIB2 expression levels that can impact the effect of cell death at lower drug concentrations. Iverson C *et al*., demonstrated that the inhibition of A375 cells proliferation, by Refametinib was preferentially by cell cycle arrest rather that apoptosis because membrane integrity was maintained in the presence of Refametinib and also SubG1 population was very low (211). This might suggest that 100nM Refametinib induced cell cycle arrest rather than cell death explaining the fact that under the lower concentration, the difference in cell death between both cell lines was lower. G361 TRIB2 knockdown cells showed higher cell death levels compared to control cells only at 100nM concentration. In fact, treatment of A375 cells with 1µM of Refametinib induced the same amount of cell death than the exposure of G361 cells to 100Nm Refametinib. This observation indicates that G361cells are more sensitive to MEK inhibition than A375 cells. This was not completely unexpected since different cell lines have different tolerance to different drugs. Importantly, PI staining showed a higher difference in cell death between the TRIB2 knockdown and the isogenic control cells. Using flow cytometry, apoptotic cells stained with PI are hypodiploid (result from DNA fragmentation, a characteristic of apoptosis) and detected as a subG1 peak, while normal cells are diploid (216, 217). Trypan blue cell death counting is performed manually with a Neubauer chamber, which makes this technique more prone to human error. Another factor is the time that live cells are in contact with trypan blue that is highly toxic causing increase cell death (218, 219) and masking the differences between cell lines with and without TRIB2. This problem is overcome with PI staining since cells are fixed immediately after collection.

Refametinib treatment caused increased cell death in TRIB2 knock-out cell lines. In the TRIB2 downregulation system we reduced TRIB2 expression while in the knockout we abrogated TRIB2 expression. Results from TRIB2 knockout cells provided further evidence that TRIB2 is conferring resistance to Refametinib treatment. In G361 and SK-Mel-28 melanoma cell we successfully obtained TRIB2 knockouts using the CRISPR Cas9 system.

Results obtained from G361 TRIB2 knockouts were quite similar to the ones obtained with G361 TRIB2 knockdown: cell death was higher in cells with TRIB2 depletion using 100nM Refametinib compared to the control. This difference is higher in the TRIB2 knockout G361 cell line compared to the G361 TRIB2 knockdown.

Importantly, SK-Mel-28 TRIB2 knockout cells are more sensitive to the treatment with 100nM and 1Mm of Refametinib than the parental cell line, strongly suggesting that TRIB2 mediates resistance to MEK inhibitors. Results from SK-MEL-28 cell line reinforced the hypothesis that TRIB2 may be conferring resistance to MEK inhibitors.

TRIB2-FLAG knock-in was successful in SK-Mel-28 cell line.

We also wanted to characterize the underlying mechanism through how TRIB2 might be conferring resistance to MEK inhibition with the analysis of protein-protein interaction and protein-localization assays. Having this in mind we tried to generate FLAG-TRIB2 knock-in (KI) also using CRISPR-Cas9 system in the same panel of melanoma cell lines. We tested several clones and obtained positive FLAG-TRIB2 KI in SK-MeL-28. Consistent with other studies (220, 221), we also noted that a gene knock-in using CRISPR-Cas9 was low efficiency 10-20%. For that reason, we tested several clones from each cell line. Some clones had a weaker expression of TRIB2 and FLAG compared to other clones. This can be due to mutations (indels) generated during the knock-in process that affects protein expression. Shin SE *et al*., reported that CRISPR-Cas9 knock-in also generates mutations through NHEJ (222). Recent studies shows that Homology Direct Repair (HDR) can be favored by the inhibition of NHEJ, improving the efficiency of gene editing tools (223).

The mechanism by which TRIB2 confers resistance to MEK inhibitors remains yet to be established. Possible hypothesis are: (a) by direct interaction with MEK, (b) by regulating downstream pro or anti-apoptotic proteins, (c) by the regulation of other subfamilies of MAPK (p38 and JNK) or (d) through a similar mechanism described by Hill *et al*. (143). A good hypothesis would be that, under MEK inhibition, TRIB2 could increase the activation of AKT, resulting in PI3K pathway activation. This is a possibility considering that several studies points to crosstalk as one of the main causes of treatment resistance because they can counterbalance treatment effects (64, 137, 138, 224). Inhibiting one pathway (in this case MAPK) TRIB2 could compensate this and activate PI3K pathway with consequent tumor progression. In fact, Jae-Kyung Won *et al.*, showed that BRAF V600E mutated cells in the presence of a MEK inhibitor showed high levels of phosphorylated AKT, while levels of phosphorylated ERK were down

suggesting that bypassing ERK signaling to the activation of PI3K pathway leads to resistance to the MEK inhibitors (225). Another plausible mechanism would be a direct interaction between TRIB2 and MEK1 since TRIB2 has a MEK1 binding domain (177). Also, there are several studies showing that TRIB2 regulates MAPKs activity (194), so it is possible that TRIB2 might be involved in MEK inhibition-mediated resistance. In addition, it is also possible that TRIB2 may confer resistance to MEK inhibitors through the regulation of the other MAPK. So far, three main subgroups of MAPK have been identified: ERKS, JNKs and p38-MAPKs (annex G). ERKs are essentially involved in cell survival while JNKs and p-38 mediates cell stress responses and apoptosis (226-228). JNK and p-38 regulates BCL-2 proteins, including BAX, which was already associated with radio resistance (228, 229). Also TRIB2 overexpression was associated with low levels of *BAX* in radioresistant cells (229). Another interesting fact, is that TRIB2 was found to modulate JNK and p-38 but not ERK1/2 in inflammatory bowel disease (197). Moreover, p-38 is activated by MAP kinase kinase (MKK) 3/6 and JNK by MKK 4/7 while ERK is activated by MEK 1/2. (230-232). p-38 has a dual role in apoptosis: promote apoptosis or anti-apoptotic and proliferative effects, demonstrated in cancer cells. p-38 increases the malignant potential of cancer cells by increasing proliferation and inhibiting apoptosis in prostate cancer (233), breast cancer (234), liver cancer (235), lung cancer (236), colon cancer (237) and bladder (238). In some cancers, p38 can play a tumor suppressor role (239, 240). Some studies start to demonstrate the role of p38 in melanoma tumorigenesis. A study with 8 melanoma cell lines revealed that 7 had both p-ERK and p-38 activated (241). The same study shows a positive feedback-loop between this 2 pathways showing that are both activated in melanoma. Apparently, in melanoma p-38 is required for cell migration and proliferation. This means that future treatment should target both pathways (241). The inhibition of MAPK pathway by MEK inhibitor can somehow increase p-38 promoting cell survival. This hypothesis that TRIB2 may modulate p38 in melanoma promoting resistance should be further investigated.

Here, we show data supports the idea that TRIB2 may be conferring resistance to MEK inhibitors: TRIB2 levels correlated with cell death, making it an important therapeutic target in melanoma therapy. Understanding the resistance mechanisms to the therapeutic agents can improve the outcomes of current therapies and contribute to the development of new therapeutic approaches.

5. Conclusion and Future Perspectives

Melanoma is the deadliest form of skin cancer, being responsible for 80% of skin cancer deaths. Chemoresistance and the high rate of metastasis are the main reasons for treatment failure (15-17, 21). The identification and characterization of resistance mechanisms to therapies is crucial to develop new improved therapies. In the last decade two new therapeutic strategies revolutionized the standard care for melanoma patients: immunotherapies based on immunocheckpoint inhibitors and targeted therapies including BRAF and MEK inhibitors (17, 64). Only 30% of the melanoma patients can benefit from immunotherapy because most of the patients are intrinsically resistant (17, 64). The development of BRAF inhibitors, such as Vemurafenib, improved survival of melanoma patients. Yet, most of the patients who initially respond, eventually acquire resistance to this compound (92). A promising strategy is the development of new inhibitors for downstream effectors of BRAF, such as MEK. The first MEK inhibitor approved for clinical use by the FDA was Trametinib that was proven to be clinically effective in the presence of BRAF and NRAS mutations (104, 105). Resistance is a major concern in melanoma treatment. The understanding of resistance mechanism should be a major concern in cancer treatment. The concept of personalized medicine emerged some years ago: a medicine / treatment based on the person's unique clinical, genetic and environmental conditions. In practical terms, means that if we can prove that a given protein is conferring resistance to a certain therapy, we can divide population and only administrate the therapy to the ones who we predict favorable responses (80, 242). The Link lab has discovered a novel resistance mechanism to PI3K and mTOR inhibitors mediated by TRIB2 (143). TRIB2 was found to be overexpressed in melanoma and has a MEK binding site in its structure (156, 159). Our data provides evidences that TRIB2 is conferring resistance to the MEK inhibitor Refametinib, similar to trametinib, making TRIB2 an important target in melanoma therapy. Further studies are needed to understand the mechanism by which TRIB2 promotes resistance to this drug. A reasonable hypothesis is a similar mechanism to the one described in the PI3K pathway (143). Alternatively, the modulation of p38 (the crosstalk between p-ERK and p-38 promotes cell proliferation and migration in melanoma (241)) and JNK signaling or by direct interaction with MEK (197, 241) are also possible mechanisms that can explain this effect.

In summary, despite the advances in the field of melanoma treatment in the past few years, there are still significant obstacles to be overcome that should be treated as a priority in melanoma treatment. Understanding the resistance mechanisms to therapeutic agents can

certainly improve the outcome of current therapies and contribute to the development of new therapeutic approaches. TRIB2 is presented here as potential candidate for MEK inhibition mediated resistance, representing an attractive therapeutic target to the development of future inhibitors in melanoma. TRIB2 was already suggested as a biomarker that predicts clinical responses to melanoma therapy (14). Here, we show further evidences that TRIB2 might be useful to predict which patients may benefit from therapy: Patients with TRIB2 overexpression may not clinically benefit from PI3K and mTOR inhibitors, MEK inhibitors and possibly to other therapies including imunnocheckpoint inhibitors. Future research may be focused on improving the risk-benefit of targeted therapies and immunotherapies by understanding the resistance mechanisms to these therapies and establishing biomarkers in order to provide information about the patient response to the treatment. Hopefully, the ability to distinguish patients that may benefit from these treatments may improve the clinical outcome of melanoma patients (243).

6. Bibliographic References

1. Global Burden of Disease Cancer C. THe global burden of cancer 2013. JAMA Oncology. 2015;1(4):505-27.
2. Ferlay J, Steliarova-Foucher E, Lortet-Tieulent J, Rosso S, Coebergh JW, Comber H, et al. Cancer incidence and mortality patterns in Europe: estimates for 40 countries in 2012. Eur J Cancer. 2013;49(6):1374-403.
3. Jemal A, Center MM, DeSantis C, Ward EM. Global patterns of cancer incidence and mortality rates and trends. Cancer Epidemiol Biomarkers Prev. 2010;19(8):1893-907.
4. Martin AM, Weber BL. Genetic and hormonal risk factors in breast cancer. J Natl Cancer Inst. 2000;92(14):1126-35.
5. Anand P, Kunnumakara AB, Sundaram C, Harikumar KB, Tharakan ST, Lai OS, et al. Cancer is a Preventable Disease that Requires Major Lifestyle Changes. Pharmaceutical Research. 2008;25(9):2097-116.
6. Blanpain C. Tracing the cellular origin of cancer. Nat Cell Biol. 2013;15(2):126-34.
7. Watson IR, Takahashi K, Futreal PA, Chin L. Emerging patterns of somatic mutations in cancer. Nat Rev Genet. 2013;14(10):703-18.
8. Vogelstein B, Papadopoulos N, Velculescu VE, Zhou S, Diaz LA, Kinzler KW. Cancer Genome Landscapes. Science (New York, NY). 2013;339(6127):1546-58.
9. Zhu K, Liu Q, Zhou Y, Tao C, Zhao Z, Sun J, et al. Oncogenes and tumor suppressor genes: comparative genomics and network perspectives. BMC Genomics. 2015;16 Suppl 7:S8.
10. Lahtz C, Pfeifer GP. Epigenetic changes of DNA repair genes in cancer. Journal of Molecular Cell Biology. 2011;3(1):51-8.
11. You JS, Jones PA. Cancer Genetics and Epigenetics: Two Sides of the Same Coin? Cancer Cell. 2012;22(1):9-20.
12. Hanahan D, Weinberg RA. The hallmarks of cancer. Cell. 2000;100(1):57-70.
13. Hanahan D, Weinberg RA. Hallmarks of cancer: the next generation. Cell. 2011;144(5):646-74.
14. Hill R, Kalathur RK, Colaco L, Brandao R, Ugurel S, Futschik M, et al. TRIB2 as a biomarker for diagnosis and progression of melanoma. Carcinogenesis. 2015;36(4):469-77.
15. Gray-Schopfer V, Wellbrock C, Marais R. Melanoma biology and new targeted therapy. Nature. 2007;445(7130):851-7.
16. Cummins DL, Cummins JM, Pantle H, Silverman MA, Leonard AL, Chanmugam A. Cutaneous malignant melanoma. Mayo Clin Proc. 2006;81(4):500-7.
17. Winder M, Viros A. Mechanisms of Drug Resistance in Melanoma. Handb Exp Pharmacol. 2017.
18. Lo JA, Fisher DE. The melanoma revolution: from UV carcinogenesis to a new era in therapeutics. Science (New York, NY). 2014;346(6212):945-9.
19. Hirobe T. Keratinocytes regulate the function of melanocytes. Dermatologica Sinica. 2014;32(4):200-4.
20. Cichorek M, Wachulska M, Stasiewicz A, Tymińska A. Skin melanocytes: biology and development. Advances in Dermatology and Allergology/Postępy Dermatologii I Alergologii. 2013;30(1):30-41.
21. Soengas MS, Lowe SW. Apoptosis and melanoma chemoresistance. Oncogene. 2003;22(20):3138-51.
22. Kulesa PM, Morrison JA, Bailey CM. The Neural Crest and Cancer: A Developmental Spin on Melanoma. Cells, tissues, organs. 2013;198(1):10.1159/000348418.

23. Chung C-Y, Madhunapantula SV, Desai D, Amin S, Robertson GP. Melanoma Prevention Using Topical PBISe. Cancer prevention research (Philadelphia, Pa). 2011;4(6):935-48.
24. Sun C, Wang L, Huang S, Heynen GJ, Prahallad A, Robert C, et al. Reversible and adaptive resistance to BRAF(V600E) inhibition in melanoma. Nature. 2014;508(7494):118-22.
25. Zbytek B, Carlson JA, Granese J, Ross J, Mihm MC, Slominski A. Current concepts of metastasis in melanoma. Expert review of dermatology. 2008;3(5):569-85.
26. Chudnovsky Y, Khavari PA, Adams AE. Melanoma genetics and the development of rational therapeutics. Journal of Clinical Investigation. 2005;115(4):813-24.
27. Greenwald HS, Friedman EB, Osman I. Superficial spreading and nodular melanoma are distinct biological entities: a challenge to the linear progression model. Melanoma Research. 2012;22(1):1-8.
28. McClain SE, Mayo KB, Shada AL, Smolkin ME, Patterson JW, Slingluff CL. Amelanotic Melanomas Presenting as Red Skin Lesions: A Diagnostic Challenge with Potentially Lethal Consequences. International journal of dermatology. 2012;51(4):420-6.
29. Kaliki S, Shields CL, Shields JA. Uveal melanoma: Estimating prognosis. Indian Journal of Ophthalmology. 2015;63(2):93-102.
30. Dhillon AS, Hagan S, Rath O, Kolch W. MAP kinase signalling pathways in cancer. Oncogene. 2007;26(22):3279-90.
31. Roberts PJ, Der CJ. Targeting the Raf-MEK-ERK mitogen-activated protein kinase cascade for the treatment of cancer. Oncogene. 2007;26(22):3291-310.
32. Inamdar GS, Madhunapantula SV, Robertson GP. Targeting the MAPK pathway in melanoma: why some approaches succeed and other fail. Biochem Pharmacol. 2010;80(5):624-37.
33. Weinberg R. The Biology of Cancer, Second Edition: Taylor & Francis Group; 2013.
34. Whitmarsh AJ. Regulation of gene transcription by mitogen-activated protein kinase signaling pathways. Biochim Biophys Acta. 2007;1773(8):1285-98.
35. Santarpia L, Lippman SM, El-Naggar AK. Targeting the MAPK-RAS-RAF signaling pathway in cancer therapy. Expert Opin Ther Targets. 2012;16(1):103-19.
36. Gomes AR, Zhao F, Lam EWF. Role and regulation of the forkhead transcription factors FOXO3a and FOXM1 in carcinogenesis and drug resistance. Chinese Journal of Cancer. 2013;32(7):365-70.
37. Roy SK, Srivastava RK, Shankar S. Inhibition of PI3K/AKT and MAPK/ERK pathways causes activation of FOXO transcription factor, leading to cell cycle arrest and apoptosis in pancreatic cancer. J Mol Signal. 2010;5:10.
38. McCain J. The MAPK (ERK) Pathway: Investigational Combinations for the Treatment Of BRAF-Mutated Metastatic Melanoma. Pharmacy and Therapeutics. 2013;38(2):96-108.
39. Gorden A, Osman I, Gai W, He D, Huang W, Davidson A, et al. Analysis of BRAF and N-RAS mutations in metastatic melanoma tissues. Cancer Res. 2003;63(14):3955-7.
40. Davies H, Bignell GR, Cox C, Stephens P, Edkins S, Clegg S, et al. Mutations of the BRAF gene in human cancer. Nature. 2002;417(6892):949-54.
41. Celebi JT, Shendrik I, Silvers D, Peacocke M. Identification of PTEN mutations in metastatic melanoma specimens. Journal of Medical Genetics. 2000;37(9):653-7.
42. Jakob JA, Bassett RL, Jr., Ng CS, Curry JL, Joseph RW, Alvarado GC, et al. NRAS mutation status is an independent prognostic factor in metastatic melanoma. Cancer. 2012;118(16):4014-23.
43. Stahl JM, Sharma A, Cheung M, Zimmerman M, Cheng JQ, Bosenberg MW, et al. Deregulated Akt3 activity promotes development of malignant melanoma. Cancer Res. 2004;64(19):7002-10.

44. Balch CM, Gershenwald JE, Soong S-j, Thompson JF, Atkins MB, Byrd DR, et al. Final Version of 2009 AJCC Melanoma Staging and Classification. Journal of Clinical Oncology. 2009;27(36):6199-206.
45. Sullivan RJ, LoRusso PM, Flaherty KT. The Intersection of Immune-Directed and Molecularly Targeted Therapy in Advanced Melanoma: Where We Have Been, Are, and Will Be. Clinical Cancer Research. 2013;19(19):5283.
46. Raigani S, Cohen S, Boland GM. The Role of Surgery for Melanoma in an Era of Effective Systemic Therapy. Curr Oncol Rep. 2017;19(3):17.
47. Phan GQ, Messina JL, Sondak VK, Zager JS. Sentinel lymph node biopsy for melanoma: indications and rationale. Cancer Control. 2009;16(3):234-9.
48. Morton DL, Thompson JF, Cochran AJ, Mozzillo N, Nieweg OE, Roses DF, et al. Final Trial Report of Sentinel-Node Biopsy versus Nodal Observation in Melanoma. The New England journal of medicine. 2014;370(7):599-609.
49. Perez-Herrero E, Fernandez-Medarde A. Advanced targeted therapies in cancer: Drug nanocarriers, the future of chemotherapy. Eur J Pharm Biopharm. 2015;93:52-79.
50. Baudino TA. Targeted Cancer Therapy: The Next Generation of Cancer Treatment. Curr Drug Discov Technol. 2015;12(1):3-20.
51. Mouawad R, Sebert M, Michels J, Bloch J, Spano JP, Khayat D. Treatment for metastatic malignant melanoma: old drugs and new strategies. Crit Rev Oncol Hematol. 2010;74(1):27-39.
52. Bhatia S, Tykodi SS, Thompson JA. Treatment of Metastatic Melanoma: An Overview. Oncology (Williston Park, NY). 2009;23(6):488-96.
53. Sanada M, Takagi Y, Ito R, Sekiguchi M. Killing and mutagenic actions of dacarbazine, a chemotherapeutic alkylating agent, on human and mouse cells: effects of Mgmt and Mlh1 mutations. DNA Repair (Amst). 2004;3(4):413-20.
54. Damia G, D'Incalci M. Mechanisms of resistance to alkylating agents. Cytotechnology. 1998;27(1-3):165-73.
55. Yang AS, Chapman PB. The history and future of chemotherapy for melanoma. Hematol Oncol Clin North Am. 2009;23(3):583-97, x.
56. Agarwala SS, Kirkwood JM. Temozolomide, a novel alkylating agent with activity in the central nervous system, may improve the treatment of advanced metastatic melanoma. Oncologist. 2000;5(2):144-51.
57. Quereux G, Dreno B. Fotemustine for the treatment of melanoma. Expert Opin Pharmacother. 2011;12(18):2891-904.
58. Kondo N, Takahashi A, Ono K, Ohnishi T. DNA damage induced by alkylating agents and repair pathways. J Nucleic Acids. 2010;2010:543531.
59. Hall AG, Tilby MJ. Mechanisms of action of, and modes of resistance to, alkylating agents used in the treatment of haematological malignancies. Blood Rev. 1992;6(3):163-73.
60. Grady WM, Ulrich CM. DNA alkylation and DNA methylation: cooperating mechanisms driving the formation of colorectal adenomas and adenocarcinomas? Gut. 2007;56(3):318-20.
61. Fu D, Calvo JA, Samson LD. Balancing repair and tolerance of DNA damage caused by alkylating agents. Nat Rev Cancer. 2012;12(2):104-20.
62. Strebhardt K, Ullrich A. Paul Ehrlich's magic bullet concept: 100 years of progress. Nat Rev Cancer. 2008;8(6):473-80.
63. Luke JJ, Schwartz GK. Chemotherapy in the Management of Advanced Cutaneous Malignant Melanoma. Clinics in dermatology. 2013;31(3):290-7.
64. Meierjohann S. Crosstalk signaling in targeted melanoma therapy. Cancer Metastasis Rev. 2017;36(1):23-33.

65. Redman JM, Gibney GT, Atkins MB. Advances in immunotherapy for melanoma. BMC Med. 2016;14:20.
66. Johnson DB, Peng C, Sosman JA. Nivolumab in melanoma: latest evidence and clinical potential. Therapeutic Advances in Medical Oncology. 2015;7(2):97-106.
67. Schumacher TN, Schreiber RD. Neoantigens in cancer immunotherapy. Science. 2015;348(6230):69.
68. Wang R-F, Wang HY. Immune targets and neoantigens for cancer immunotherapy and precision medicine. Cell Res. 2017;27(1):11-37.
69. Verdegaal EM, de Miranda NF, Visser M, Harryvan T, van Buuren MM, Andersen RS, et al. Neoantigen landscape dynamics during human melanoma-T cell interactions. Nature. 2016;536(7614):91-5.
70. Haanen JBAG. Immunotherapy of melanoma. EJC Supplements. 2013;11(2):97-105.
71. Osborn JL, Greer SF. Metastatic Melanoma Cells Evade Immune Detection by Silencing STAT1. International Journal of Molecular Sciences. 2015;16(2):4343-61.
72. Blankenstein T, Coulie PG, Gilboa E, Jaffee EM. The determinants of tumour immunogenicity. Nat Rev Cancer. 2012;12(4):307-13.
73. Fisher R, Larkin J. Vemurafenib: a new treatment for BRAF-V600 mutated advanced melanoma. Cancer Management and Research. 2012;4:243-52.
74. Baluna R, Vitetta ES. Vascular leak syndrome: a side effect of immunotherapy. Immunopharmacology. 1997;37(2-3):117-32.
75. Drake CG, Lipson EJ, Brahmer JR. Breathing new life into immunotherapy: review of melanoma, lung and kidney cancer. Nat Rev Clin Oncol. 2014;11(1):24-37.
76. Tarhini A, Lo E, Minor DR. Releasing the Brake on the Immune System: Ipilimumab in Melanoma and Other Tumors. Cancer Biotherapy & Radiopharmaceuticals. 2010;25(6):601-13.
77. Raedler LA. Opdivo (Nivolumab): Second PD-1 Inhibitor Receives FDA Approval for Unresectable or Metastatic Melanoma. American Health & Drug Benefits. 2015;8(Spec Feature):180-3.
78. Britten CD. PI3K and MEK inhibitor combinations: examining the evidence in selected tumor types. Cancer Chemother Pharmacol. 2013;71(6):1395-409.
79. Atefi M, Avramis E, Lassen A, Wong D, Robert L, Foulad D, et al. Effects of MAPK and PI3K Pathways on PD-L1 Expression in Melanoma. Clinical cancer research : an official journal of the American Association for Cancer Research. 2014;20(13):3446-57.
80. Ferreira BI, Hill R, Link W. Special Review: Caught in the Crosshairs: Targeted Drugs and Personalized Medicine. Cancer J. 2015;21(6):441-7.
81. Johnson DB, Puzanov I. Treatment of NRAS-Mutant Melanoma. Current treatment options in oncology. 2015;16(4):15-.
82. Baines AT, Xu D, Der CJ. Inhibition of Ras for cancer treatment: the search continues. Future Medicinal Chemistry. 2011;3(14):1787-808.
83. Goldinger SM, Murer C, Stieger P, Dummer R. Targeted therapy in melanoma – the role of BRAF, RAS and KIT mutations. EJC Supplements. 2013;11(2):92-6.
84. Gençler B, Gönül M. Cutaneous Side Effects of BRAF Inhibitors in Advanced Melanoma: Review of the Literature. Dermatology Research and Practice. 2016;2016:5361569.
85. Eisen T, Ahmad T, Flaherty KT, Gore M, Kaye S, Marais R, et al. Sorafenib in advanced melanoma: a Phase II randomised discontinuation trial analysis. Br J Cancer. 2006;95(5):581-6.
86. Azijli K, Stelloo E, Peters GJ, AJ VDE. New developments in the treatment of metastatic melanoma: immune checkpoint inhibitors and targeted therapies. Anticancer Res. 2014;34(4):1493-505.

87. Eisen T, Marais R, Affolter A, Lorigan P, Robert C, Corrie P, et al. Sorafenib and dacarbazine as first-line therapy for advanced melanoma: phase I and open-label phase II studies. Br J Cancer. 2011;105(3):353-9.
88. Flaherty KT, Lee SJ, Zhao F, Schuchter LM, Flaherty L, Kefford R, et al. Phase III trial of carboplatin and paclitaxel with or without sorafenib in metastatic melanoma. J Clin Oncol. 2013;31(3):373-9.
89. Sharma A, Shah SR, Illum H, Dowell J. Vemurafenib: targeted inhibition of mutated BRAF for treatment of advanced melanoma and its potential in other malignancies. Drugs. 2012;72(17):2207-22.
90. Santarpia L, Lippman SL, El-Naggar AK. Targeting the Mitogen-Activated Protein Kinase RAS-RAF Signaling Pathway in Cancer Therapy. Expert opinion on therapeutic targets. 2012;16(1):103-19.
91. Lacouture ME, O'Reilly K, Rosen N, Solit DB. Induction of cutaneous squamous cell carcinomas by RAF inhibitors: cause for concern? J Clin Oncol. 2012;30(3):329-30.
92. Aplin AE, Kaplan FM, Shao Y. Mechanisms of resistance to RAF inhibitors in melanoma. J Invest Dermatol. 2011;131(9):1817-20.
93. Montagut C, Sharma SV, Shioda T, McDermott U, Ulman M, Ulkus LE, et al. Elevated CRAF as a potential mechanism of acquired resistance to BRAF inhibition in melanoma. Cancer Res. 2008;68(12):4853-61.
94. Goetz EM, Ghandi M, Treacy DJ, Wagle N, Garraway LA. ERK Mutations Confer Resistance to Mitogen-Activated Protein Kinase Pathway Inhibitors. Cancer research. 2014;74(23):7079-89.
95. Tsao H, Zhang X, Benoit E, Haluska FG. Identification of PTEN/MMAC1 alterations in uncultured melanomas and melanoma cell lines. Oncogene. 1998;16(26):3397-402.
96. Deichmann M, Thome M, Benner A, Egner U, Hartschuh W, Näher H. PTEN/MMAC1 expression in melanoma resection specimens. British Journal of Cancer. 2002;87(12):1431-6.
97. Teng DH, Hu R, Lin H, Davis T, Iliev D, Frye C, et al. MMAC1/PTEN mutations in primary tumor specimens and tumor cell lines. Cancer Res. 1997;57(23):5221-5.
98. Wilson TR, Fridlyand J, Yan Y, Penuel E, Burton L, Chan E, et al. Widespread potential for growth-factor-driven resistance to anticancer kinase inhibitors. Nature. 2012;487(7408):505-9.
99. Manzano JL, Layos L, Bugés C, de los Llanos Gil M, Vila L, Martínez-Balibrea E, et al. Resistant mechanisms to BRAF inhibitors in melanoma. Annals of Translational Medicine. 2016;4(12):237.
100. King JW, Nathan PD. Role of the MEK inhibitor trametinib in the treatment of metastatic melanoma. Future Oncol. 2014;10(9):1559-70.
101. Nazarian R, Shi H, Wang Q, Kong X, Koya RC, Lee H, et al. Melanomas acquire resistance to B-RAF(V600E) inhibition by RTK or N-RAS upregulation. Nature. 2010;468(7326):973-7.
102. Wagle N, Emery C, Berger MF, Davis MJ, Sawyer A, Pochanard P, et al. Dissecting therapeutic resistance to RAF inhibition in melanoma by tumor genomic profiling. J Clin Oncol. 2011;29(22):3085-96.
103. Poulikakos PI, Persaud Y, Janakiraman M, Kong X, Ng C, Moriceau G, et al. RAF inhibitor resistance is mediated by dimerization of aberrantly spliced BRAF(V600E). Nature. 2011;480(7377):387-90.
104. Grimaldi AM, Simeone E, Ascierto PA. The role of MEK inhibitors in the treatment of metastatic melanoma. Curr Opin Oncol. 2014;26(2):196-203.
105. Tsai J, Lee JT, Wang W, Zhang J, Cho H, Mamo S, et al. Discovery of a selective inhibitor of oncogenic B-Raf kinase with potent antimelanoma activity. Proc Natl Acad Sci U S A. 2008;105(8):3041-6.

106. Arcaro A, Guerreiro AS. The Phosphoinositide 3-Kinase Pathway in Human Cancer: Genetic Alterations and Therapeutic Implications. Current Genomics. 2007;8(5):271-306.
107. Favata MF, Horiuchi KY, Manos EJ, Daulerio AJ, Stradley DA, Feeser WS, et al. Identification of a novel inhibitor of mitogen-activated protein kinase kinase. J Biol Chem. 1998;273(29):18623-32.
108. Akinleye A, Furqan M, Mukhi N, Ravella P, Liu D. MEK and the inhibitors: from bench to bedside. Journal of Hematology & Oncology. 2013;6:27-.
109. Narita Y, Okamoto K, Kawada MI, Takase K, Minoshima Y, Kodama K, et al. Novel ATP-competitive MEK inhibitor E6201 is effective against vemurafenib-resistant melanoma harboring the MEK1-C121S mutation in a preclinical model. Mol Cancer Ther. 2014;13(4):823-32.
110. Byron SA, Loch DC, Wellens CL, Wortmann A, Wu J, Wang J, et al. Sensitivity to the MEK inhibitor E6201 in melanoma cells is associated with mutant BRAF and wildtype PTEN status. Mol Cancer. 2012;11:75.
111. Johnson D. Cell Death Signaling in Cancer Biology and Treatment: Springer New York; 2012.
112. Lugowska I, Koseła-Paterczyk H, Kozak K, Rutkowski P. Trametinib: a MEK inhibitor for management of metastatic melanoma. OncoTargets and therapy. 2015;8:2251-9.
113. Hatzivassiliou G, Haling JR, Chen H, Song K, Price S, Heald R, et al. Mechanism of MEK inhibition determines efficacy in mutant KRAS- versus BRAF-driven cancers. Nature. 2013;501(7466):232-6.
114. Tran KA, Cheng MY, Mitra A, Ogawa H, Shi VY, Olney LP, et al. MEK inhibitors and their potential in the treatment of advanced melanoma: the advantages of combination therapy. Drug Design, Development and Therapy. 2016;10:43-52.
115. Carlino MS, Fung C, Shahheydari H, Todd JR, Boyd SC, Irvine M, et al. Preexisting MEK1P124 mutations diminish response to BRAF inhibitors in metastatic melanoma patients. Clin Cancer Res. 2015;21(1):98-105.
116. Poulikakos PI, Solit DB. Resistance to MEK inhibitors: should we co-target upstream? Sci Signal. 2011;4(166):pe16.
117. Caunt CJ, Sale MJ, Smith PD, Cook SJ. MEK1 and MEK2 inhibitors and cancer therapy: the long and winding road. Nat Rev Cancer. 2015;15(10):577-92.
118. Kodaki T, Woscholski R, Hallberg B, Rodriguez-Viciana P, Downward J, Parker PJ. The activation of phosphatidylinositol 3-kinase by Ras. Curr Biol. 1994;4(9):798-806.
119. Mendoza MC, Er EE, Blenis J. The Ras-ERK and PI3K-mTOR Pathways: Cross-talk and Compensation. Trends in biochemical sciences. 2011;36(6):320-8.
120. Lippert TH, Ruoff HJ, Volm M. Intrinsic and acquired drug resistance in malignant tumors. The main reason for therapeutic failure. Arzneimittelforschung. 2008;58(6):261-4.
121. Holohan C, Van Schaeybroeck S, Longley DB, Johnston PG. Cancer drug resistance: an evolving paradigm. Nat Rev Cancer. 2013;13(10):714-26.
122. Housman G, Byler S, Heerboth S, Lapinska K, Longacre M, Snyder N, et al. Drug Resistance in Cancer: An Overview. Cancers. 2014;6(3):1769-92.
123. Townsend DM, Tew KD. The role of glutathione-S-transferase in anti-cancer drug resistance. Oncogene. 0000;22(47):7369-75.
124. Sheehan D, Meade G, Foley VM, Dowd CA. Structure, function and evolution of glutathione transferases: implications for classification of non-mammalian members of an ancient enzyme superfamily. Biochemical Journal. 2001;360(Pt 1):1-16.
125. Tew KD, Monks A, Barone L, Rosser D, Akerman G, Montali JA, et al. Glutathione-associated enzymes in the human cell lines of the National Cancer Institute Drug Screening Program. Mol Pharmacol. 1996;50(1):149-59.

126. Grossman D, Altieri DC. Drug resistance in melanoma: mechanisms, apoptosis, and new potential therapeutic targets. Cancer Metastasis Rev. 2001;20(1-2):3-11.
127. Anasagasti MJ, Martin JJ, Mendoza L, Obrador E, Estrela JM, McCuskey RS, et al. Glutathione protects metastatic melanoma cells against oxidative stress in the murine hepatic microvasculature. Hepatology. 1998;27(5):1249-56.
128. Hande KR. Topoisomerase II inhibitors. Update on Cancer Therapeutics. 2008;3(1):13-26.
129. Nitiss JL. Targeting DNA topoisomerase II in cancer chemotherapy. Nature reviews Cancer. 2009;9(5):338-50.
130. Lage H, Helmbach H, Dietel M, Schadendorf D. Modulation of DNA topoisomerase II activity and expression in melanoma cells with acquired drug resistance. Br J Cancer. 2000;82(2):488-91.
131. Helmbach H, Rossmann E, Kern MA, Schadendorf D. Drug-resistance in human melanoma. Int J Cancer. 2001;93(5):617-22.
132. Fukunaga-Kalabis M, Herlyn M. Beyond ABC: another mechanism of drug resistance in melanoma side population. The Journal of investigative dermatology. 2012;132(10):2317-9.
133. van der Pol MA, Broxterman HJ, Pater JM, Feller N, van der Maas M, Weijers GW, et al. Function of the ABC transporters, P-glycoprotein, multidrug resistance protein and breast cancer resistance protein, in minimal residual disease in acute myeloid leukemia. Haematologica. 2003;88(2):134-47.
134. Schadendorf D, Makki A, Stahr C, van Dyck A, Wanner R, Scheffer GL, et al. Membrane transport proteins associated with drug resistance expressed in human melanoma. Am J Pathol. 1995;147(6):1545-52.
135. Runger TM, Emmert S, Schadendorf D, Diem C, Epe B, Hellfritsch D. Alterations of DNA repair in melanoma cell lines resistant to cisplatin, fotemustine, or etoposide. J Invest Dermatol. 2000;114(1):34-9.
136. Pepponi R, Marra G, Fuggetta MP, Falcinelli S, Pagani E, Bonmassar E, et al. The effect of O6-alkylguanine-DNA alkyltransferase and mismatch repair activities on the sensitivity of human melanoma cells to temozolomide, 1,3-bis(2-chloroethyl)1-nitrosourea, and cisplatin. J Pharmacol Exp Ther. 2003;304(2):661-8.
137. Sun X, Bao J, You Z, Chen X, Cui J. Modeling of signaling crosstalk-mediated drug resistance and its implications on drug combination. Oncotarget. 2016;7(39):63995-4006.
138. Prahallad A, Bernards R. Opportunities and challenges provided by crosstalk between signalling pathways in cancer. Oncogene. 2016;35(9):1073-9.
139. Elmore S. Apoptosis: A Review of Programmed Cell Death. Toxicologic pathology. 2007;35(4):495-516.
140. Helmbach H, Sinha P, Schadendorf D. Human melanoma: drug resistance. Recent Results Cancer Res. 2003;161:93-110.
141. Marusyk A, Polyak K. Tumor heterogeneity: causes and consequences. Biochimica et biophysica acta. 2010;1805(1):105.
142. Somasundaram R, Villanueva J, Herlyn M. Intratumoral Heterogeneity as a Therapy Resistance Mechanism: Role of Melanoma Subpopulations. Advances in pharmacology (San Diego, Calif). 2012;65:335-59.
143. Hill R, Madureira PA, Ferreira B, Baptista I, Machado S, Colaço L, et al. TRIB2 confers resistance to anti-cancer therapy by activating the serine/threonine protein kinase AKT. Nature Communications. 2017;8:14687.
144. Zanella F, Renner O, Garcia B, Callejas S, Dopazo A, Peregrina S, et al. Human TRIB2 is a repressor of FOXO that contributes to the malignant phenotype of melanoma cells. Oncogene. 2010;29(20):2973-82.

145. Yang JY, Zong CS, Xia W, Yamaguchi H, Ding Q, Xie X, et al. ERK promotes tumorigenesis by inhibiting FOXO3a via MDM2-mediated degradation. Nat Cell Biol. 2008;10(2):138-48.
146. Yang J-Y, Zong CS, Xia W, Yamaguchi H, Ding Q, Xie X, et al. ERK promotes tumorigenesis by inhibiting FOXO3a via MDM2-mediated degradation. Nature cell biology. 2008;10(2):138-48.
147. Daitoku H, Sakamaki J-i, Fukamizu A. Regulation of FoxO transcription factors by acetylation and protein–protein interactions. Biochimica et Biophysica Acta (BBA) - Molecular Cell Research. 2011;1813(11):1954-60.
148. Martins R, Lithgow GJ, Link W. Long live FOXO: unraveling the role of FOXO proteins in aging and longevity. Aging Cell. 2016;15(2):196-207.
149. Calnan DR, Brunet A. The FoxO code. Oncogene. 0000;27(16):2276-88.
150. Zhang X, Tang N, Hadden TJ, Rishi AK. Akt, FoxO and regulation of apoptosis. Biochim Biophys Acta. 2011;1813(11):1978-86.
151. Jagani Z, Singh A, Khosravi-Far R. FoxO Tumor Suppressors and BCR-ABL-Induced Leukemia: A Matter of Evasion of Apoptosis. Biochimica et biophysica acta. 2008;1785(1):63-84.
152. Trotman LC, Alimonti A, Scaglioni PP, Koutcher JA, Cordon-Cardo C, Pandolfi PP. Identification of a tumour suppressor network opposing nuclear Akt function. Nature. 2006;441(7092):523-7.
153. Kikuno N, Shiina H, Urakami S, Kawamoto K, Hirata H, Tanaka Y, et al. Knockdown of astrocyte-elevated gene-1 inhibits prostate cancer progression through upregulation of FOXO3a activity. Oncogene. 2007;26(55):7647-55.
154. Cornforth AN, Davis JS, Khanifar E, Nastiuk KL, Krolewski JJ. FOXO3a mediates the androgen-dependent regulation of FLIP and contributes to TRAIL-induced apoptosis of LNCaP cells. Oncogene. 2008;27(32):4422-33.
155. Brunet A, Bonni A, Zigmond MJ, Lin MZ, Juo P, Hu LS, et al. Akt promotes cell survival by phosphorylating and inhibiting a Forkhead transcription factor. Cell. 1999;96(6):857-68.
156. Dobens LL, Jr., Bouyain S. Developmental roles of tribbles protein family members. Dev Dyn. 2012;241(8):1239-48.
157. Eyers PA, Keeshan K, Kannan N. Tribbles in the 21st Century: The Evolving Roles of Tribbles Pseudokinases in Biology and Disease. Trends Cell Biol. 2016.
158. Cunard R. Mammalian tribbles homologs at the crossroads of endoplasmic reticulum stress and Mammalian target of rapamycin pathways. Scientifica (Cairo). 2013;2013:750871.
159. Sakai S, Miyajima C, Uchida C, Itoh Y, Hayashi H, Inoue Y. Tribbles-Related Protein Family Members as Regulators or Substrates of the Ubiquitin-Proteasome System in Cancer Development. Curr Cancer Drug Targets. 2016;16(2):147-56.
160. Bailey FP, Byrne DP, Oruganty K, Eyers CE, Novotny CJ, Shokat KM, et al. The Tribbles 2 (TRB2) pseudokinase binds to ATP and autophosphorylates in a metal-independent manner. The Biochemical journal. 2015;467(1):47-62.
161. Guan H, Shuaib A, Leon DDD, Angyal A, Salazar M, Velasco G, et al. Competition between members of the tribbles pseudokinase protein family shapes their interactions with mitogen activated protein kinase pathways. Scientific Reports. 2016;6:32667.
162. Salazar M, Lorente M, García-Taboada E, Pérez Gómez E, Dávila D, Zúñiga-García P, et al. Loss of Tribbles pseudokinase-3 promotes Akt-driven tumorigenesis via FOXO inactivation. Cell Death and Differentiation. 2015;22(1):131-44.
163. Stein Sarah J, Mack Ethan A, Rome Kelly S, Pear Warren S. Tribbles in normal and malignant haematopoiesis. Biochemical Society Transactions. 2015;43(5):1112-5.

164. Dedhia PH, Keeshan K, Uljon S, Xu L, Vega ME, Shestova O, et al. Differential ability of Tribbles family members to promote degradation of C/EBPalpha and induce acute myelogenous leukemia. Blood. 2010;116(8):1321-8.
165. Keeshan K, Bailis W, Dedhia PH, Vega ME, Shestova O, Xu L, et al. Transformation by Tribbles homolog 2 (Trib2) requires both the Trib2 kinase domain and COP1 binding. Blood. 2010;116(23):4948-57.
166. Salazar M, Lorente M, Garcia-Taboada E, Perez Gomez E, Davila D, Zuniga-Garcia P, et al. Loss of Tribbles pseudokinase-3 promotes Akt-driven tumorigenesis via FOXO inactivation. Cell Death Differ. 2015;22(1):131-44.
167. Lourenco AR, Coffer PJ. A tumor suppressor role for C/EBPalpha in solid tumors: more than fat and blood. Oncogene. 2017.
168. Ramji DP, Foka P. CCAAT/enhancer-binding proteins: structure, function and regulation. Biochemical Journal. 2002;365(Pt 3):561-75.
169. Strimbu K, Tavel JA. What are Biomarkers? Current opinion in HIV and AIDS. 2010;5(6):463-6.
170. Mayeux R. Biomarkers: Potential Uses and Limitations. NeuroRx. 2004;1(2):182-8.
171. Goossens N, Nakagawa S, Sun X, Hoshida Y. Cancer biomarker discovery and validation. Translational cancer research. 2015;4(3):256-69.
172. Ballman KV. Biomarker: Predictive or Prognostic? Journal of Clinical Oncology. 2015;33(33):3968-71.
173. Freedman DA, Wu L, Levine AJ. Functions of the MDM2 oncoprotein. Cell Mol Life Sci. 1999;55(1):96-107.
174. Oliner JD, Pietenpol JA, Thiagalingam S, Gyuris J, Kinzler KW, Vogelstein B. Oncoprotein MDM2 conceals the activation domain of tumour suppressor p53. Nature. 1993;362(6423):857-60.
175. Haupt Y, Maya R, Kazaz A, Oren M. Mdm2 promotes the rapid degradation of p53. Nature. 1997;387(6630):296-9.
176. Kubbutat MH, Vousden KH. Proteolytic cleavage of human p53 by calpain: a potential regulator of protein stability. Mol Cell Biol. 1997;17(1):460-8.
177. Foulkes DM, Byrne DP, Bailey FP, Eyers PA. Tribbles pseudokinases: novel targets for chemical biology and drug discovery? Biochem Soc Trans. 2015;43(5):1095-103.
178. Deepak SA, Kottapalli KR, Rakwal R, Oros G, Rangappa KS, Iwahashi H, et al. Real-Time PCR: Revolutionizing Detection and Expression Analysis of Genes. Current Genomics. 2007;8(4):234-51.
179. Garibyan L, Avashia N. Research Techniques Made Simple: Polymerase Chain Reaction (PCR). The Journal of investigative dermatology. 2013;133(3):e6-e.
180. Mahmood T, Yang P-C. Western Blot: Technique, Theory, and Trouble Shooting. North American Journal of Medical Sciences. 2012;4(9):429-34.
181. Ernst O, Zor T. Linearization of the Bradford Protein Assay. Journal of Visualized Experiments : JoVE. 2010(38):1918.
182. Carlsson N, Borde A, Wolfel S, Kerman B, Larsson A. Quantification of protein concentration by the Bradford method in the presence of pharmaceutical polymers. Anal Biochem. 2011;411(1):116-21.
183. Moore CB, Guthrie EH, Huang MT-H, Taxman DJ. Short Hairpin RNA (shRNA): Design, Delivery, and Assessment of Gene Knockdown. Methods in molecular biology (Clifton, NJ). 2010;629:141-58.
184. Paddison PJ, Caudy AA, Bernstein E, Hannon GJ, Conklin DS. Short hairpin RNAs (shRNAs) induce sequence-specific silencing in mammalian cells. Genes Dev. 2002;16(8):948-58.

185. Ran FA, Hsu PD, Wright J, Agarwala V, Scott DA, Zhang F. Genome engineering using the CRISPR-Cas9 system. Nat Protoc. 2013;8(11):2281-308.
186. Chen S, Sun H, Miao K, Deng C-X. CRISPR-Cas9: from Genome Editing to Cancer Research. International Journal of Biological Sciences. 2016;12(12):1427-36.
187. He X, Tan C, Wang F, Wang Y, Zhou R, Cui D, et al. Knock-in of large reporter genes in human cells via CRISPR/Cas9-induced homology-dependent and independent DNA repair. Nucleic Acids Res. 2016;44(9):e85.
188. Hopp TP, Prickett KS, Price VL, Libby RT, March CJ, Pat Cerretti D, et al. A Short Polypeptide Marker Sequence Useful for Recombinant Protein Identification and Purification. Nat Biotech. 1988;6(10):1204-10.
189. Lobbestael E, Reumers V, Ibrahimi A, Paesen K, Thiry I, Gijsbers R, et al. Immunohistochemical detection of transgene expression in the brain using small epitope tags. BMC Biotechnology. 2010;10:16-.
190. Vermes I, Haanen C, Steffens-Nakken H, Reutelingsperger C. A novel assay for apoptosis. Flow cytometric detection of phosphatidylserine expression on early apoptotic cells using fluorescein labelled Annexin V. J Immunol Methods. 1995;184(1):39-51.
191. Vermes I, Haanen C, Reutelingsperger C. Flow cytometry of apoptotic cell death. J Immunol Methods. 2000;243(1-2):167-90.
192. Rieger AM, Nelson KL, Konowalchuk JD, Barreda DR. Modified annexin V/propidium iodide apoptosis assay for accurate assessment of cell death. J Vis Exp. 2011(50).
193. Fadok VA, Bratton DL, Frasch SC, Warner ML, Henson PM. The role of phosphatidylserine in recognition of apoptotic cells by phagocytes. Cell Death Differ. 1998;5(7):551-62.
194. Kiss-Toth E, Bagstaff SM, Sung HY, Jozsa V, Dempsey C, Caunt JC, et al. Human tribbles, a protein family controlling mitogen-activated protein kinase cascades. J Biol Chem. 2004;279(41):42703-8.
195. Liang KL, Paredes R, Carmody R, Eyers PA, Meyer S, McCarthy TV, et al. Human TRIB2 Oscillates during the Cell Cycle and Promotes Ubiquitination and Degradation of CDC25C. Int J Mol Sci. 2016;17(9).
196. Keeshan K, He Y, Wouters BJ, Shestova O, Xu L, Sai H, et al. Tribbles homolog 2 (Trib2) inactivates C/EBPalpha and causes acute myelogenous leukemia. Cancer cell. 2006;10(5):401-11.
197. Wei SC, Rosenberg IM, Cao Z, Huett AS, Xavier RJ, Podolsky DK. Tribbles 2 (Trib2) is a novel regulator of toll-like receptor 5 signaling. Inflamm Bowel Dis. 2012;18(5):877-88.
198. Wang J, Park JS, Wei Y, Rajurkar M, Cotton JL, Fan Q, et al. TRIB2 acts downstream of Wnt/TCF in liver cancer cells to regulate YAP and C/EBPalpha function. Mol Cell. 2013;51(2):211-25.
199. Yokoyama T, Kanno Y, Yamazaki Y, Takahara T, Miyata S, Nakamura T. Trib1 links the MEK1/ERK pathway in myeloid leukemogenesis. Blood. 2010;116(15):2768-75.
200. Guan H, Shuaib A, Leon DD, Angyal A, Salazar M, Velasco G, et al. Competition between members of the tribbles pseudokinase protein family shapes their interactions with mitogen activated protein kinase pathways. Sci Rep. 2016;6:32667.
201. Seger R, Ahn NG, Posada J, Munar ES, Jensen AM, Cooper JA, et al. Purification and characterization of mitogen-activated protein kinase activator(s) from epidermal growth factor-stimulated A431 cells. J Biol Chem. 1992;267(20):14373-81.
202. Yoon S, Seger R. The extracellular signal-regulated kinase: multiple substrates regulate diverse cellular functions. Growth Factors. 2006;24(1):21-44.
203. Schonn I, Hennesen J, Dartsch DC. Cellular responses to etoposide: cell death despite cell cycle arrest and repair of DNA damage. Apoptosis. 2010;15(2):162-72.

204. Jamil S, Lam I, Majd M, Tsai S-H, Duronio V. Etoposide induces cell death via mitochondrial-dependent actions of p53. Cancer Cell International. 2015;15:79.
205. Einhauer A, Jungbauer A. The FLAG peptide, a versatile fusion tag for the purification of recombinant proteins. J Biochem Biophys Methods. 2001;49(1-3):455-65.
206. Yokoyama T, Nakamura T. Tribbles in disease: Signaling pathways important for cellular function and neoplastic transformation. Cancer Sci. 2011;102(6):1115-22.
207. Ohoka N, Yoshii S, Hattori T, Onozaki K, Hayashi H. TRB3, a novel ER stress-inducible gene, is induced via ATF4–CHOP pathway and is involved in cell death. The EMBO Journal. 2005;24(6):1243-55.
208. Greenbaum D, Colangelo C, Williams K, Gerstein M. Comparing protein abundance and mRNA expression levels on a genomic scale. Genome Biol. 2003;4(9):117.
209. Soubeyrand S, Martinuk A, Lau P, McPherson R. TRIB1 Is Regulated Post-Transcriptionally by Proteasomal and Non-Proteasomal Pathways. PLoS ONE. 2016;11(3):e0152346.
210. Okamoto H, Latres E, Liu R, Thabet K, Murphy A, Valenzeula D, et al. Genetic deletion of Trb3, the mammalian Drosophila tribbles homolog, displays normal hepatic insulin signaling and glucose homeostasis. Diabetes. 2007;56(5):1350-6.
211. Iverson C, Larson G, Lai C, Yeh LT, Dadson C, Weingarten P, et al. RDEA119/BAY 869766: a potent, selective, allosteric inhibitor of MEK1/2 for the treatment of cancer. Cancer Res. 2009;69(17):6839-47.
212. Chang Q, Chapman MS, Miner JN, Hedley DW. Antitumour activity of a potent MEK inhibitor RDEA119/BAY 869766 combined with rapamycin in human orthotopic primary pancreatic cancer xenografts. BMC Cancer. 2010;10(1):515.
213. Schmieder R, Puehler F, Neuhaus R, Kissel M, Adjei AA, Miner JN, et al. Allosteric MEK1/2 Inhibitor Refametinib (BAY 86-9766) in Combination with Sorafenib Exhibits Antitumor Activity in Preclinical Murine and Rat Models of Hepatocellular Carcinoma. Neoplasia (New York, NY). 2013;15(10):1161-71.
214. Jackson AL, Bartz SR, Schelter J, Kobayashi SV, Burchard J, Mao M, et al. Expression profiling reveals off-target gene regulation by RNAi. Nat Biotechnol. 2003;21(6):635-7.
215. Scacheri PC, Rozenblatt-Rosen O, Caplen NJ, Wolfsberg TG, Umayam L, Lee JC, et al. Short interfering RNAs can induce unexpected and divergent changes in the levels of untargeted proteins in mammalian cells. Proc Natl Acad Sci U S A. 2004;101(7):1892-7.
216. Riccardi C, Nicoletti I. Analysis of apoptosis by propidium iodide staining and flow cytometry. Nat Protocols. 2006;1(3):1458-61.
217. Kajstura M, Halicka HD, Pryjma J, Darzynkiewicz Z. Discontinuous fragmentation of nuclear DNA during apoptosis revealed by discrete "sub-G1" peaks on DNA content histograms. Cytometry A. 2007;71(3):125-31.
218. Tsaousis KT, Kopsachilis N, Tsinopoulos IT, Dimitrakos SA, Kruse FE, Welge-Luessen U. Time-dependent morphological alterations and viability of cultured human trabecular cells after exposure to Trypan blue. Clin Exp Ophthalmol. 2013;41(5):484-90.
219. Chan LL-Y, Kuksin D, Laverty DJ, Saldi S, Qiu J. Morphological observation and analysis using automated image cytometry for the comparison of trypan blue and fluorescence-based viability detection method. Cytotechnology. 2015;67(3):461-73.
220. Chu VT, Weber T, Graf R, Sommermann T, Petsch K, Sack U, et al. Efficient generation of Rosa26 knock-in mice using CRISPR/Cas9 in C57BL/6 zygotes. BMC Biotechnology. 2016;16:4.
221. Nakao H, Harada T, Nakao K, Kiyonari H, Inoue K, Furuta Y, et al. A possible aid in targeted insertion of large DNA elements by CRISPR/Cas in mouse zygotes. Genesis. 2016;54(2):65-77.

222. Shin S-E, Lim J-M, Koh HG, Kim EK, Kang NK, Jeon S, et al. CRISPR/Cas9-induced knockout and knock-in mutations in Chlamydomonas reinhardtii. Scientific Reports. 2016;6:27810.
223. Maruyama T, Dougan SK, Truttmann MC, Bilate AM, Ingram JR, Ploegh HL. Increasing the efficiency of precise genome editing with CRISPR-Cas9 by inhibition of nonhomologous end joining. Nat Biotech. 2015;33(5):538-42.
224. Tsao H, Goel V, Wu H, Yang G, Haluska FG. Genetic Interaction Between NRAS and BRAF Mutations and PTEN/MMAC1 Inactivation in Melanoma. The Journal of investigative dermatology. 2004;122(2):337-41.
225. Won J-K, Yang HW, Shin S-Y, Lee JH, Heo WD, Cho K-H. The crossregulation between ERK and PI3K signaling pathways determines the tumoricidal efficacy of MEK inhibitor. Journal of Molecular Cell Biology. 2012;4(3):153-63.
226. Balmanno K, Cook SJ. Tumour cell survival signalling by the ERK1/2 pathway. Cell Death Differ. 2009;16(3):368-77.
227. Wada T, Penninger JM. Mitogen-activated protein kinases in apoptosis regulation. Oncogene. 2004;23(16):2838-49.
228. Cai B, Chang SH, Becker EB, Bonni A, Xia Z. p38 MAP kinase mediates apoptosis through phosphorylation of BimEL at Ser-65. J Biol Chem. 2006;281(35):25215-22.
229. Zhang HH, Pang M, Dong W, Xin JX, Li YJ, Zhang ZC, et al. miR-511 induces the apoptosis of radioresistant lung adenocarcinoma cells by triggering BAX. Oncol Rep. 2014;31(3):1473-9.
230. Raingeaud J, Whitmarsh AJ, Barrett T, Dérijard B, Davis RJ. MKK3- and MKK6-regulated gene expression is mediated by the p38 mitogen-activated protein kinase signal transduction pathway. Molecular and Cellular Biology. 1996;16(3):1247-55.
231. Tournier C, Dong C, Turner TK, Jones SN, Flavell RA, Davis RJ. MKK7 is an essential component of the JNK signal transduction pathway activated by proinflammatory cytokines. Genes & Development. 2001;15(11):1419-26.
232. Zhang Z, Zhou X, Shen H, Wang D, Wang Y. Phosphorylated ERK is a potential predictor of sensitivity to sorafenib when treating hepatocellular carcinoma: evidence from an in vitro study. BMC Medicine. 2009;7:41-.
233. Browne AJ, Göbel A, Thiele S, Hofbauer LC, Rauner M, Rachner TD. p38 MAPK regulates the Wnt inhibitor Dickkopf-1 in osteotropic prostate cancer cells. Cell Death & Disease. 2016;7(2):e2119.
234. Donnelly SM, Paplomata E, Peake BM, Sanabria E, Chen Z, Nahta R. P38 MAPK contributes to resistance and invasiveness of HER2-overexpressing breast cancer. Current medicinal chemistry. 2014;21(4):501-10.
235. Hui L, Bakiri L, Mairhorfer A, Schweifer N, Haslinger C, Kenner L, et al. p38alpha suppresses normal and cancer cell proliferation by antagonizing the JNK-c-Jun pathway. Nat Genet. 2007;39(6):741-9.
236. Ventura JJ, Tenbaum S, Perdiguero E, Huth M, Guerra C, Barbacid M, et al. p38alpha MAP kinase is essential in lung stem and progenitor cell proliferation and differentiation. Nat Genet. 2007;39(6):750-8.
237. Gupta J, del Barco Barrantes I, Igea A, Sakellariou S, Pateras IS, Gorgoulis VG, et al. Dual function of p38alpha MAPK in colon cancer: suppression of colitis-associated tumor initiation but requirement for cancer cell survival. Cancer Cell. 2014;25(4):484-500.
238. Kumar B, Koul S, Petersen J, Khandrika L, Hwa JS, Meacham RB, et al. p38 mitogen-activated protein kinase-driven MAPKAPK2 regulates invasion of bladder cancer by modulation of MMP-2 and MMP-9 activity. Cancer Res. 2010;70(2):832-41.

239. Yoshizuka N, Chen RM, Xu Z, Liao R, Hong L, Hu W-Y, et al. A Novel Function of p38-Regulated/Activated Kinase in Endothelial Cell Migration and Tumor Angiogenesis. Molecular and Cellular Biology. 2012;32(3):606-18.
240. Bulavin DV, Fornace AJ, Jr. p38 MAP kinase's emerging role as a tumor suppressor. Adv Cancer Res. 2004;92:95-118.
241. Estrada Y, Dong J, Ossowski L. Positive crosstalk between ERK and p38 in melanoma stimulates migration and in vivo proliferation. Pigment Cell Melanoma Res. 2009;22(1):66-76.
242. Offit K. Personalized medicine: new genomics, old lessons. Human Genetics. 2011;130(1):3-14.
243. Khattak M, Fisher R, Turajlic S, Larkin J. Targeted therapy and immunotherapy in advanced melanoma: an evolving paradigm. Therapeutic Advances in Medical Oncology. 2013;5(2):105-18.

ANNEXES

ANNEX A- E.Z.N.A Total RNA Kit (Omega) Protocol

Principle

The E.Z.N.A.® Total RNA Kits utilized the reversible binding properties of HiBind® matrix, a new silica-based material, combined with the speed of mini-column spin technology to provide a fast and easy way for isolating total cellular RNA from cultured cells or animal tissues. A specifically formulated high salt buffer system allows more than 100 µg of RNA molecules greater than 200 bases to bind to the matrix. Cells or tissues are first lysed and homogenized under denaturing conditions that practically inactivate RNases. After adjust the binding condition by add ethanol, samples are then applied to the HiBind® spin columns to which total RNA binds, while cellular debris and other contaminants are effectively washed away. High quality RNA is finally eluted in DEPC-treated sterile water.

Procedure:

1. Lyse cells or tissues with 350µl of TRK Lysis Buffer. Remember to add 20µl of 2-mercaptoethanol per 1 ml of TRK Lysis Buffer before use.

350µl of TRK Lysis Buffer is sufficient for# 5 x 106 cells or approximately 20 mg disrupted tissue (~3 mm cube). For difficult tissues, more than 5 x 106 cells, or greater than 20 mg tissue, use 700 µl of TRK Lysis Buffer. However, use no more than 30 mg tissue.

For tissue culture cells grown in monolayer (fibroblasts, endothelial cells, etc.), lyse the cells directly in the culture vessel as follows. Aspirate culture medium completely and add TRK Lysis Buffer directly to the cells. Use 700µl for T35 flasks or 10 cm dishes, and 350µl for smaller vessels. Pipette buffer over entire surface of vessel to ensure complete lysis. Transfer lysate to a clean 1.5 ml microfuge tube and proceed to step 2 below. (This method is preferable to trypsinization followed by washing because it minimizes RNA degradation by nuclease contamination.)

For cells grown in suspension cultures, pellet cells at no greater than 1,500 rpm (400 x g) for 5 min. Discard supernatant, add TRK Lysis Buffer, lyse by vortex or pipetting up and down, and transfer to a clean 1.5 ml microfuge tube. Proceed to step 2.

For tissue samples, homogenize using one of the methods discussed on page 4. For fatty tissues such as brain or adipose tissues, please use E.Z.N.A.® Total RNA Kit II (Product # R6934). For fibrous sample such as sample for muscle or heart, use protocol B in this user manual. Also OBI offers special designed kit for fibrous tissues (Product # R6688). Unless using liquid

nitrogen, homogenize samples directly in TRK Lysis Buffer/2-mercaptoethanol and proceed to step 2.

2. Add an equal volume (350 µl or 700 µl) 70% Ethanol to the lysate and mix thoroughly by vortexing.

3. Apply sample onto HiBind® RNA spin column. The maximum capacity of the spin cartridge is 750 ml. (Larger volumes can be loaded successively.) A precipitate may form on addition of ethanol in step 2. Vortex and add the entire mixture to the column. With the spin column inside a 2ml collecting tube (supplied with kit), centrifuge at 10,000 x g for 15 seconds at room temperature. Discard flowthrough and collection tube.

4. Place column in a clean 2ml collection tube, and add 300 µl RNA Wash Buffer I. Centrifuge and discard flow-through. Reuse the collection tube in step 6. If on-membrane DNase I digestion is desired, proceed step 5, otherwise go to step 6.

5. DNase digestion (Optional) Since HiBind® RNA resin and spin-column technology actually removes most of DNA without the DNase treatment, it is not necessary to do DNase digestion for most downstream applications. However, certain sensitive RNA applications might require further DNA removal. Following steps provide on-membrane DNase I digestion:(see DNase I cat.# E1091for detail information)

a. For each HiBind® RNA column, prepare the DNase I digestion reaction mix as follows:

OBI DNase I Digestion Buffer	73.5 µl
RNase-free DNase I (20 Kunitz units/µl)	1.5 µl
Total volume	75 µl

Note:

1. **DNase I is very sensitive for physical denaturaion, so do not vortex this DNase I mixture. Mix gently by inverting the tube. Prepare the fresh DNase I digestion mixture before RNA isolation.**
2. **OBI DNase I digestion buffer is supplied with OBI RNase-free DNase set.**
3. **Standard DNase buffers are not compatible with on-membrane DNase digestion.**

b. Pipet 75 µl of the DNase I digestion reaction mix directly onto the surface of HiBind® RNA resin in each column. Make sure to pipet the DNase I digestion reaction mixture directly onto

the membrane. DNase I digestion will not be completed if some of the mix stick to the wall or the O-ring of the HiBind® RNA column.

c. Incubate at room temperature(25-30NC) for 15 minutes

6. Place column in a 2ml collection tube, and add 500 µl RNA Wash Buffer I. (If on-membrane DNase digestion was performed in the previous step, wait at least 5 minutes before proceeding). Centrifuge and discard flow-through.

7. Place column in the same 2ml collection tube, and add 500 µl RNA Wash Buffer II diluted with ethanol. Centrifuge and discard flow-through. Reuse the collection tube in step 8.

Note: Wash Buffer II Concentrate must be diluted with absolute ethanol before use. Refer to label on bottle for instruction.

8. Wash column with a second 500 µl of Wash Buffer II as in step 7. Centrifuge and discard flow-through. Then with the collection tube empty, centrifuge the spin cartridge for 1 min at full speed to completely dry the HiBind® matrix.

9. Elution of RNA. Transfer the column to a clean 1.5 ml microfuge tube (not supplied with kit) and elute the RNA with 50-100 µl of DEPC-treated water (supplied with kit). Make sure to add water directly onto column matrix. Centrifuge 1 min at maximum speed. A second elution may be necessary if the expected yield of RNA >50 µg. Alternatively, RNA may be eluted with a greater volume of water. While additional elutions increase total RNA yield, the concentration will be lowered since more than 80% of RNA is recovered with the first elution. Pre-heating the water to 70oC before adding to column and incubating column 5 min at room temperature before centrifugation may increase yields.

ANNEX B- NZY First Strand CDNA Synthesis Kit

Description

The NZY First-Strand cDNA Synthesis Kit is a system that includes all the necessary components to synthesize firststrand cDNA, except template RNA.

The resulting single-stranded cDNA is suitable for use in realtime quantitative Reverse Transcription PCR (RT-qPCR). NZY First-Strand cDNA Synthesis Kit is formulated to provide high yields of full-length cDNA products and to increase sensitivity in RT-qPCR.

System Components

Component	MB12501 (50 reactions)	MB12502 (250 reactions)
NZYRT Enzyme Mix (1)	100 µL	5 × 100 µL
NZYRT 2× Master Mix (2)	500 µL	5 × 500 µL
NZY RNase H (*E. coli*)	50 µL	5 × 50 µL
DEPC-treated H_2O	1 mL	2 × 1 mL

(1) Includes NZY Reverse Transcriptase and NZY Ribonuclease Inhibitor
(2) Includes oligo$(dT)_{18}$, random hexamers, $MgCl_2$ and dNTPs

Protocol

1. On ice, add the following reaction components into a sterile, nuclease-free microcentrifuge tube (for multiple reactions, a master mix without RNA may be prepared):

NZYRT 2× Master Mix	10 µL
NZYRT Enzyme Mix	2 µL
RNA (up to 5 µg)	× µL
DEPC-treated H_2O	up to 20 µL

2. Mix gently and incubate at 25 °C for 10 min.

3. Incubate at 50 °C for 30 min.

4. Inactivate the reaction by heating at 85 °C for 5 min, and then chill on ice.

5. Add 1 µL of NZY RNase H (*E.coli*) and incubate at 37 °C for 20 min.

6. Use the cDNA product directly in PCR or qPCR diluted in TE buffer or undiluted; or store at -20 °C until required.

Important notes

 High quality intact RNA, free of residual genomic DNA and RNases is essential for full-length, high quality cDNA synthesis and accurate RNA quantification. For this reason, special precautions should be taken when working with RNA:

o Aseptic conditions should be maintained: always wear gloves; change gloves whenever you suspect

that they are contaminated; use RNase-free tubes and pipet tips; designate a special area and equipment for RNA work only. o DNase I (not provided) may be used to eliminate genomic DNA contamination from the starting total RNA. o The template RNA should be stored at -70 °C. Avoid multiple freeze/thaw cycles of RNA.

 This kit does not include control RNA.

 Keep all reagents of the kit on ice while setting up the reactions.

 When performing RT-qPCR using the synthesized cDNA as template, no more than 1/10 of the final PCR volume should be derived from the reverse-transcription product. For instance, use up to 5 µL of cDNA obtained in the firststrand synthesis in a 50 µL PCR reaction.

ANNEX C- Antibodies list

Protein	Primary Antibody	Dilution	Company	Secondary Antibody	Dilution	Company
p-ERK	Anti- p-ERK #2370 (Rabbit)	1:1000 in BSA (5% azide)	Cell Signaling Technology	Goat Anti-rabbit SC F2215	1:30000 in 5% milk	Santa Cruz Biotechnology
Total ERK	Anti- total ERK sc-94 (Rabbit)	1:300 in BSA (5% azide)	Santa Cruz Biotechnology			
TRIB2	Anti-TRIB2 home made 2B407 (Rabbit)	1:2000 in BSA (5% azide)				
	Anti-TRIB2 home made 2B406 (Rabbit)	1:2000 in BSA (5% azide)				
TRIB1	Anti-TRIB1 09- 126 (Rabbit)	1:2000 in BSA (5% azide)	Millipore			
TRIB3	Anti-TRIB3 75846 (Rabbit)	1:500 in BSA (5% azide)	Abcam			
GAPDH	Anti- GAPDH SC 25778 (Rabbit)	1:5000 in BSA (5% azide)	Santa Cruz Biotechnology	Donkey Anti-Mouse sc-2314	1:5000 in 5% milk	Santa Cruz Biotechnology
FLAG	Anti-Flag F7425 (Rabbit)	1:1000 in 5% milk	Sigma Aldrich			
	Anti- Flag M2 F1904 mouse	1:1000 in 5% milk	Sigma Aldrich			
TUBULIN	Anti- α Tubulin 5168 mouse	1:2000 in BSA (5% azide)	Sigma Aldrich			

ANNEX D- Plasmids used in shRNA technique

D.1- shGFP

Plasmid pRS GFP shRNA	Code #916
Insert GFP shRNA	
Origin OriGene	
Kind of Plasmid	
Bacteria DH5alpha	
Bacterial Selection Amp	Cell Selection Puro
Localisation	

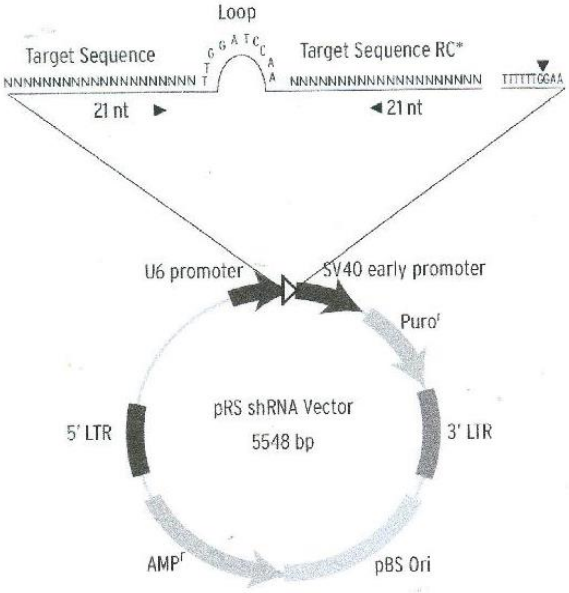

Features for pRS vector:

Start	End	Description
8	59	Gene specific shRNA coding sequence
60	69	RNA polymerase III termination site
72	422	SV40 early promoter
435	1034	Puromycin-N-acetyl transferase sequence
1133	1726	Moloney murine leukemia virus (MMLV) 3' LTR
1666	2735	pBS origin of replication
2486	3724	beta-lactamase for ampicillin resistance
3872	4332	Moloney murine leukemia virus (MMLV) 5' LTR
5214	5545	U6 promoter

*RC: reverse component

pRS-GFP-v1
(GFP shRNA Expression Plasmid)
Catalog # TR20001
Lot # H03

Product Description: Transfection grade of purified mammalian expression plasmid carrying GFP sequence that when transfected into mammalian cells, expresses a short-hairpin RNA (shRNA) from U6 promoter, resulting in the inhibition of the target gene.

Target Gene Information: Enhanced green fluorescent protein (EGFP), GenBank Accession Number U55761.

ORIGENE TECHNOLOGIES INC

Content: 10 ug of purified plasmid DNA in 20 ul 10 mM This-HCl, pH 7.5, 1 mM EDTA. Final concentration of DNA is 500 ng/ul.

Species of Target Gene: Aequorea Victoria

Storage and Stability: The plasmid is stable for at least 1 yr at –20°C from the date of shipment.

Guarantee: This product is guaranteed to inhibit the expression of intended target gene by at least 70% when co-transfected with the target into HEK293 cells following the protocols provided.

Related Products: EGFP expression vector available from Clontech.

D.2- shTRIB2 1

Plasmid pRS TRB2 shRNA (1)	Code #917
Insert TI200873 TRB2 shRNA	
Origin OriGene	
Kind of Plasmid	
Bacteria DH5alpha	
Bacterial Selection Amp	Cell Selection Puro
Localisation	

CCAGGACGAGATCCAGTTCTC	TI200873	H
CCTGCCGACCGAGGACCCCCG	TI200874	H
TAAAATCAGTGGCACCGAGGC	TI200875	H
CTCCCTCTTCAGCAAGATCCG	TI200877	H
CCCAGGAGTGAGCGAGGGCAG	TI200878	H
AGCGAGATATGGGAGATCGCG	TI200876	H,M

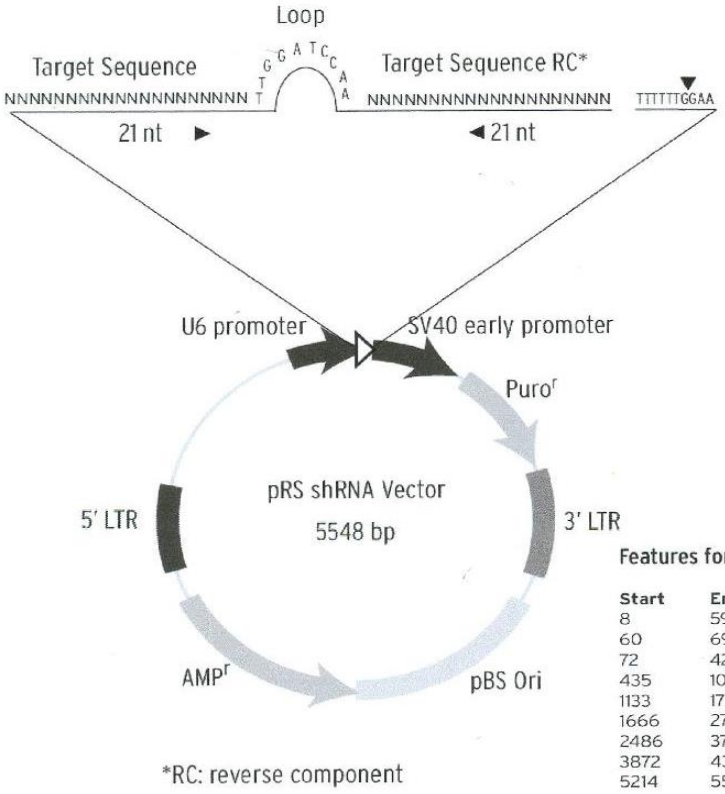

Features for pRS vector:

Start	End	Description
8	59	Gene specific shRNA coding sequence
60	69	RNA polymerase III termination site
72	422	SV40 early promoter
435	1034	Puromycin-N-acetyl transferase sequence
1133	1726	Moloney murine leukemia virus (MMLV) 3'
1666	2735	pBS origin of replication
2486	3724	beta-lactamase for ampicillin resistance
3872	4332	Moloney murine leukemia virus (MMLV) 5'
5214	5545	U6 promoter

D.3- shTRIB2 2

Plasmid pRS TRB2 shRNA (2)	Code #918
Insert TI200874 TRB2 shRNA	
Origin OriGene	
Kind of Plasmid	
Bacteria DH5alpha	
Bacterial Selection Amp	Cell Selection Puro
Localisation	

CCAGGACGAGATCCAGTTCTC	TI200873	H
CCTGCCGACCGAGGACCCCCG	TI200874	H
TAAAATCAGTGGCACCGAGGC	TI200875	H
CTCCCTCTTCAGCAAGATCCG	TI200877	H
CCCAGGAGTGAGCGAGGGCAG	TI200878	H
AGCGAGATATGGGAGATCGCG	TI200876	H,M

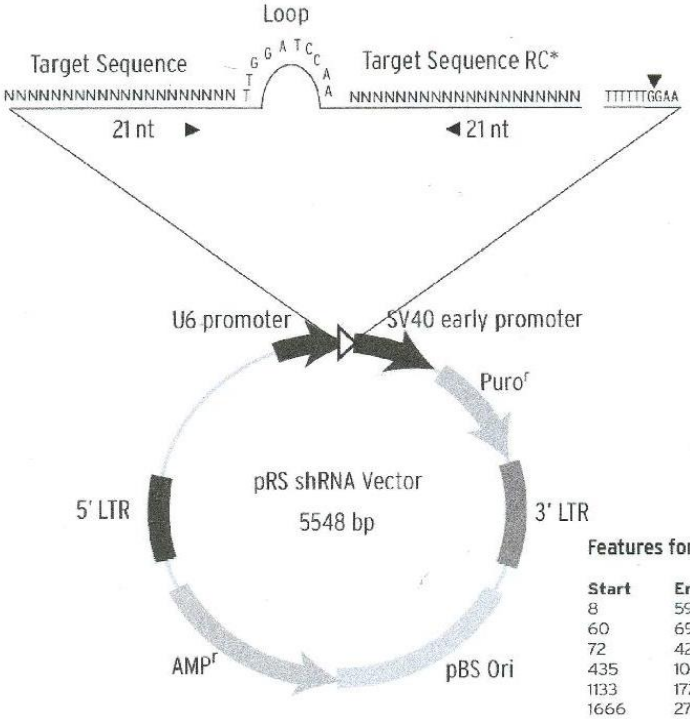

*RC: reverse component

Features for pRS vector:

Start	End	Description
8	59	Gene specific shRNA coding sequence
60	69	RNA polymerase III termination site
72	422	SV40 early promoter
435	1034	Puromycin-N-acetyl transferase sequence
1133	1726	Moloney murine leukemia virus (MMLV) 3' LT
1666	2735	pBS origin of replication
2486	3724	beta-lactamase for ampicillin resistance
3872	4332	Moloney murine leukemia virus (MMLV) 5' LT
5214	5545	U6 promoter

D.4- shTRIB2 3

Plasmid pRS TRB2 shRNA (3)	Code #919
Insert TI200875 TRB2 shRNA	
Origin OriGene	
Kind of Plasmid	
Bacteria DH5alpha	
Bacterial Selection Amp	Cell Selection Puro
Localisation	

CCAGGACGAGATCCAGTTCTC	TI200873	H
CCTGCCGACCGAGGACCCCCG	TI200874	H
TAAAATCAGTGGCACCGAGGC	TI200875	H
CTCCCTCTTCAGCAAGATCCG	TI200877	H
CCCAGGAGTGAGCGAGGGCAG	TI200878	H
AGCGAGATATGGGAGATCGCG	TI200876	H,M

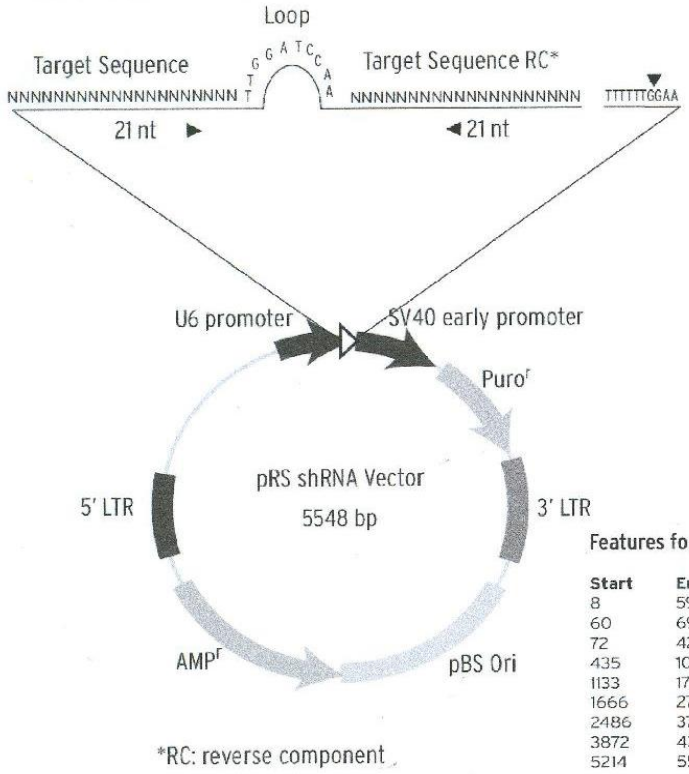

Features for pRS vector:

Start	End	Description
8	59	Gene specific shRNA coding sequence
60	69	RNA polymerase III termination site
72	422	SV40 early promoter
435	1034	Puromycin-N-acetyl transferase sequence
1133	1726	Moloney murine leukemia virus (MMLV) 3' LTR
1666	2735	pBS origin of replication
2486	3724	beta-lactamase for ampicillin resistance
3872	4332	Moloney murine leukemia virus (MMLV) 5' LTR
5214	5545	U6 promoter

D.5- shTRIB2 4

Plasmid pRS TRB2 shRNA (4)	Code #920
Insert TI200877 TRB2 shRNA	
Origin OriGene	
Kind of Plasmid	
Bacteria DH5alpha	
Bacterial Selection Amp	Cell Selection Puro
Localisation	

CCAGGACGAGATCCAGTTCTC	TI200873	H
CCTGCCGACCGAGGACCCCCG	TI200874	H
TAAAATCAGTGGCACCGAGGC	TI200875	H
CTCCCTCTTCAGCAAGATCCG	TI200877	H
CCCAGGAGTGAGCGAGGGCAG	TI200878	H
AGCGAGATATGGGAGATCGCG	TI200876	H,M

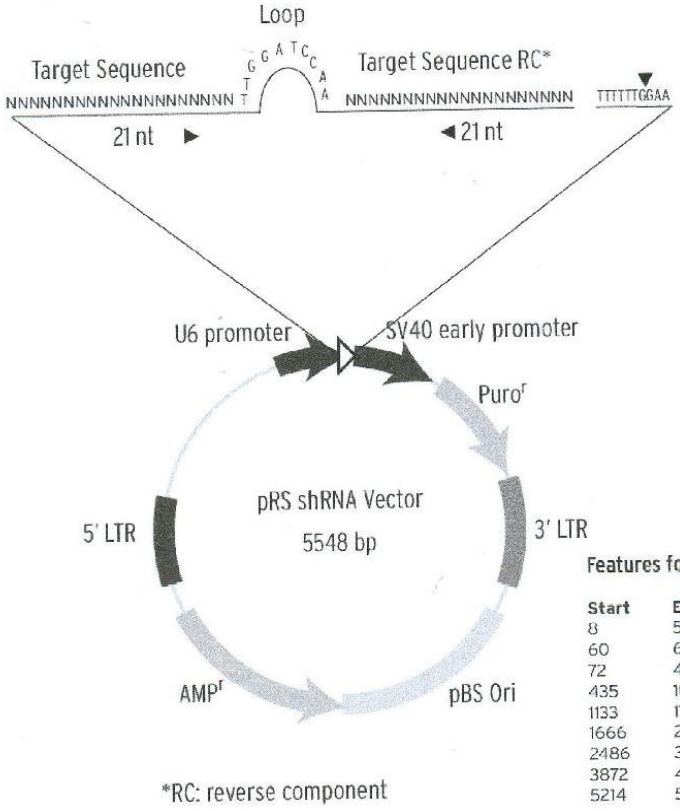

Features for pRS vector:

Start	End	Description
8	59	Gene specific shRNA coding sequence
60	69	RNA polymerase III termination site
72	422	SV40 early promoter
435	1034	Puromycin-N-acetyl transferase sequence
1133	1726	Moloney murine leukemia virus (MMLV) 3' LTR
1666	2735	pBS origin of replication
2486	3724	beta-lactamase for ampicillin resistance
3872	4332	Moloney murine leukemia virus (MMLV) 5' LTR
5214	5545	U6 promoter

D.6- shTRIB2 5

Plasmid pRS TRB2 shRNA (5)	Code #921
Insert TI200878 TRB2 shRNA	
Origin OriGene	
Kind of Plasmid	
Bacteria DH5alpha	
Bacterial Selection Amp	Cell Selection Puro
Localisation	

CCAGGACGAGATCCAGTTCTC	TI200873	H
CCTGCCGACCGAGGACCCCCG	TI200874	H
TAAAATCAGTGGCACCGAGGC	TI200875	H
CTCCCTCTTCAGCAAGATCCG	TI200877	H
CCCAGGAGTGAGCGAGGGCAG	TI200878	H
AGCGAGATATGGGAGATCGCG	TI200876	H,M

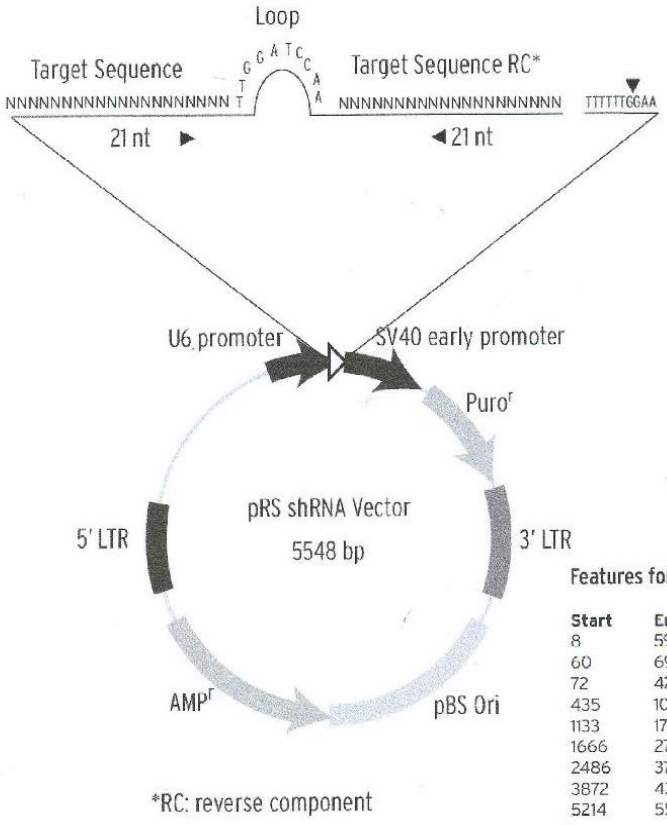

*RC: reverse component

Features for pRS vector:

Start	End	Description
8	59	Gene specific shRNA coding sequence
60	69	RNA polymerase III termination site
72	422	SV40 early promoter
435	1034	Puromycin-N-acetyl transferase sequence
1133	1726	Moloney murine leukemia virus (MMLV) 3' LTR
1666	2735	pBS origin of replication
2486	3724	beta-lactamase for ampicillin resistance
3872	4332	Moloney murine leukemia virus (MMLV) 5' LTR
5214	5545	U6 promoter

ANNEX E- Annexin V/ PI Apoptosis Detection Kit: SC-4252 AK

The AnnexinV apoptosis detection kit includes the reagents required for identifying a population of cells that have initiated apoptosis using a simple staining procedure and analysis by fluorescence microscopy or flow cytometry.

Analysis of samples can be done on live cells and does not require cell fixation. Normal viable cells in culture will stain negative for Annexin V FITC and negative for PI. Cells that are induced to undergo apoptosis will stain positive for Annexin V FITC and negative for PI as early as 1 hour after stimulation. Both cells in later stages of apoptosis and necrotic cells will stain positive for Annexin V FITC and PI.

PRODUCT

The Annexin V apoptosis detection kit (sc-4252 AK) contains 50 µg of Annexin V FITC in 250 µl buffer, 5 ml of 10x Assay Buffer and 2 ml of Propidium Iodide at 50 µg/ml in PBS. Sufficient reagent for 100 tests, assuming 0.5 µg of Annexin V FITC is used per sample.

PREPARATION OF SOLUTIONS

- 1x Assay Buffer: dilute 1 part 10x Assay Buffer in 9 parts distilled H_2O. Store at 4° C.
- 1x Phosphate Buffered Saline: 9.1 mM dibasic sodium phosphate, 1.7 mM monobasic sodium phosphate and 150 mM NaCl. Adjust to pH 7.4 with NaOH. Sterile filter and store at 4–22° C.

Protocol:

1. Induce apoptosis according to the desired method.
2. Collect supernatant. Wash with PBS 1X, collect supernatant. Trypsinize cells and transfer cells to a 15mL conical tube. Pellet cells by low speed centrifugation at 1500 rpm for 5 minutes. Wash cells once with PBS and ressuspend pellet in 500 µL 1X Assay Buffer.
3. Transfer 100µL aliquot of cells 1 x 10^5 cells to a 5mL flow cytometry tube.
4. To cell samples add 1µL of Annexin V FITC and 10µL of Propidium Iodite (PI) per 100µL cell samples.
5. Vortex samples gently and incubate 15 minutes at room temperature, in the dark.
6. Add 400 µL of 1X Assay Buffer to each tube.
7. Analyze samples using a single laser emitting light at 488 nm for FITC.

Reccomended Negative Controls:

a. No Annexin V / No PI
b. Annexin V alone
c. PI alone

ANNEX E- PI Protocol

ANNEX F- Propidium Iodide Protocol

1. Harvest cells in the appropriate manner, and wash in PBS 1X.
2. Fix in cold 70% Etanol (EtOH). Add dropwise to the cell pellet while vortexing to minimize clumpling.
3. Let the cells fix at least for 30minutes at 4ºC (Samples can be left at this stage for several weeks).
4. To make sure that only DNA is stained, treat samples with Ribonuclease (50µL of 100µg/mL RNAse).
5. Add 200 µL of PI (50µg/mL).
6. Analyze samples by flow cytometry (PI is excited at 488nm laser and emission of fluorescence is collected above 580nm.

Note: Phosphate Buffer is composed of 192 parts of 0.2M Na_2HPO_4 and 8 parts of 0.1M citric acid (pH 7.8)

ANNEX G: MAPK Pathways

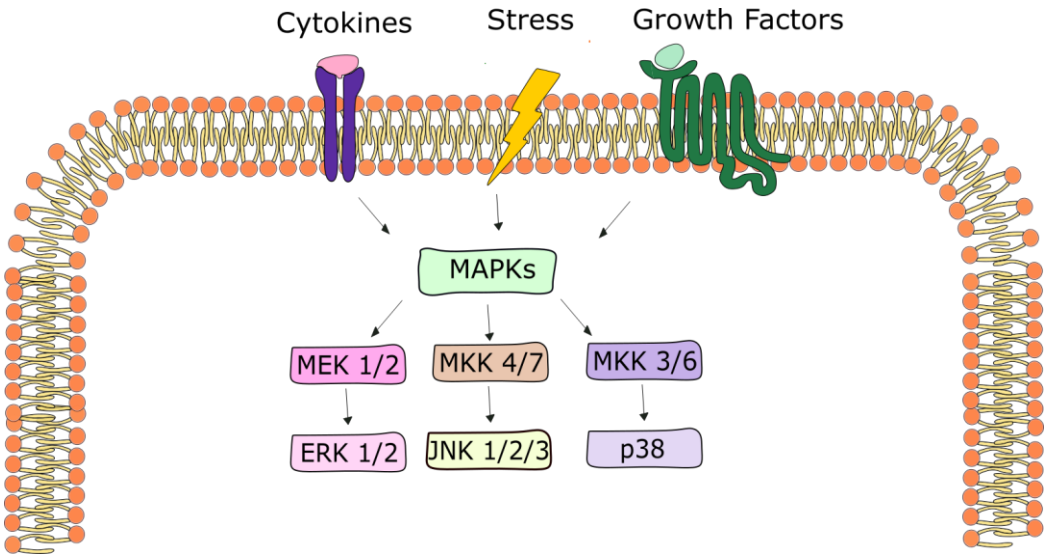

Figure G1. The three main subgroups of MAPK ERKS, JNKs and p38-MAPKs.